

Petroleum geochemical analysis of oil and oil seepage samples from the Salin Basin, Central Burma Depression, Myanmar

Jørgen A. Bojesen-Koefoed, Michael B. W. Fyhn, Lars Henrik Nielsen,
Hans Peter Nytoft & Ioannis Abatzis

GEOLOGICAL SURVEY OF DENMARK AND GREENLAND
DANISH MINISTRY OF ENERGY, UTILITIES AND CLIMATE

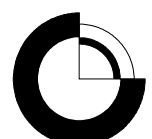


**Petroleum geochemical analysis of oil and oil seepage
samples from the Salin Basin,
Central Burma Depression,
Myanmar**

Jørgen A. Bojesen-Koefoed, Michael B. W. Fyhn, Lars Henrik Nielsen,
Hans Peter Nytoft & Ioannis Abatzis

Petroleum geochemical analysis of oil and oil seepage samples from the Salin Basin, Central Burma Depression, Myanmar

Jørgen A. Bojesen-Koefoed, Michael B. W. Fyhn, Lars Henrik Nielsen,
Hans Peter Nytoft & Ioannis Abatzis



Contents

1. Introduction	2
2. Samples and Methods.....	5
3. Results.....	6
3.1 Group type fractionation	6
3.2 Gas chromatography.....	7
3.3 Biological markers.....	8
3.3.1. Thermal maturity	9
3.3.2. Biological marker fingerprinting and source correlation.....	11
4. Discussion.....	24
5. Conclusions	26
6. References	27
Appendix 1: Separation, n-alkane and acyclic isoprenoid data	28
Appendix 2: Tri- and tetracyclic terpanes	46
Appendix 3: Hopanes	64
Appendix 4: Isohopanes.....	82
Appendix 5: Steranes	91
Appendix 6: Bicadinanes	102

1. Introduction

The present report summarizes petroleum geochemical analyses carried out of a set of oil samples collected from producing fields or oil seepages in the Central Burma Depression of Myanmar.

The petroleum geology of onshore Myanmar is excellently summarised by Ridd & Racey (2015), to which paper reference is made for further information. All samples were collected from oil-wells or seepages in the Salin Basin, which is one of at least seven subbasins found within the large (approximately 2000 km long) downwarp known as the Central Burma Depression, developed along the Indo-Burman ranges that border the depression to the west. (fig. 1.).

The Central Burma Depression hosts an up to 15 kilometres thick succession of Albian to recent sediments, including both marine and terrestrial deposits. Within the Central Burma Depression, extensive folding and faulting is common, giving rise to a variety of structural traps that in several subbasins hold petroleum accumulations. Among the petroliferous basins, the Salin Basin is the more important, with an exploration history extending approximately 130 years back in time.

The thick sedimentary succession can be studied along the margins of the depression, first and foremost to the West (generally known as “The Western Outcrops”), but to the North, in the Chindwin Basin, outcrops are accessible on both sides of the depression. Data from outcrops combined with well-information make it clear that a large number of both potential reservoir units and source units are present within the depression (Fig. 2).

Compositional data on oils and source rocks of Myanmar are very sparse, but an important study was published by Curiale et al. (1994), who investigated a series of oils (31 samples) from the Salin Basin plus two rock samples (a “resin” accumulation embedded in shale and an Eocene age coal). The study is highly commendable. It is comprehensive and thorough and constitute unrivalled the most important source of information pertaining to petroleum composition in Myanmar/Burma. The overall petroleum composition is generally very uniform, pointing to a predominantly terrestrial source, and the authors conclude that all oils belong to a single family, where the differences observed may essentially be attributed to differences in the level of biodegradation. Moreover, the authors suggest a deep Palaeogene (presumably Eocene) terrestrial source for the oils, and propose an exploration model where deeper and older traps were filled first with shallower and younger traps being filled later by more mature charges bypassing previously filled deeper/older traps, causing shallower/younger traps to host oils showing higher maturity than deeper/older traps.

The investigations and analyses, carried out at GEUS in Denmark, aim to demonstrate if further detail can be added to the conclusions made by Curiale et al. (1994) by analysing samples from the same study area by present day techniques.

Pending a positive outcome and procurement of necessary funding, it is the intention of GEUS, in collaboration with the M.O.G.E. to expand the study to cover larger parts of Myanmar by analysing samples from other petroliferous basins, as well as from areas outside the Central Burma Depression, as for instance seepage areas in the Rakhine Province along the western coast of Myanmar, offshore which petroleum exploration is presently taking place.

A comprehensive and integrated overview of petroleum and source rock characteristics in Myanmar will be of great value to both the national petroleum administration for better understanding the hydrocarbon potential of the country and to the industry responsible for carrying out active exploration.

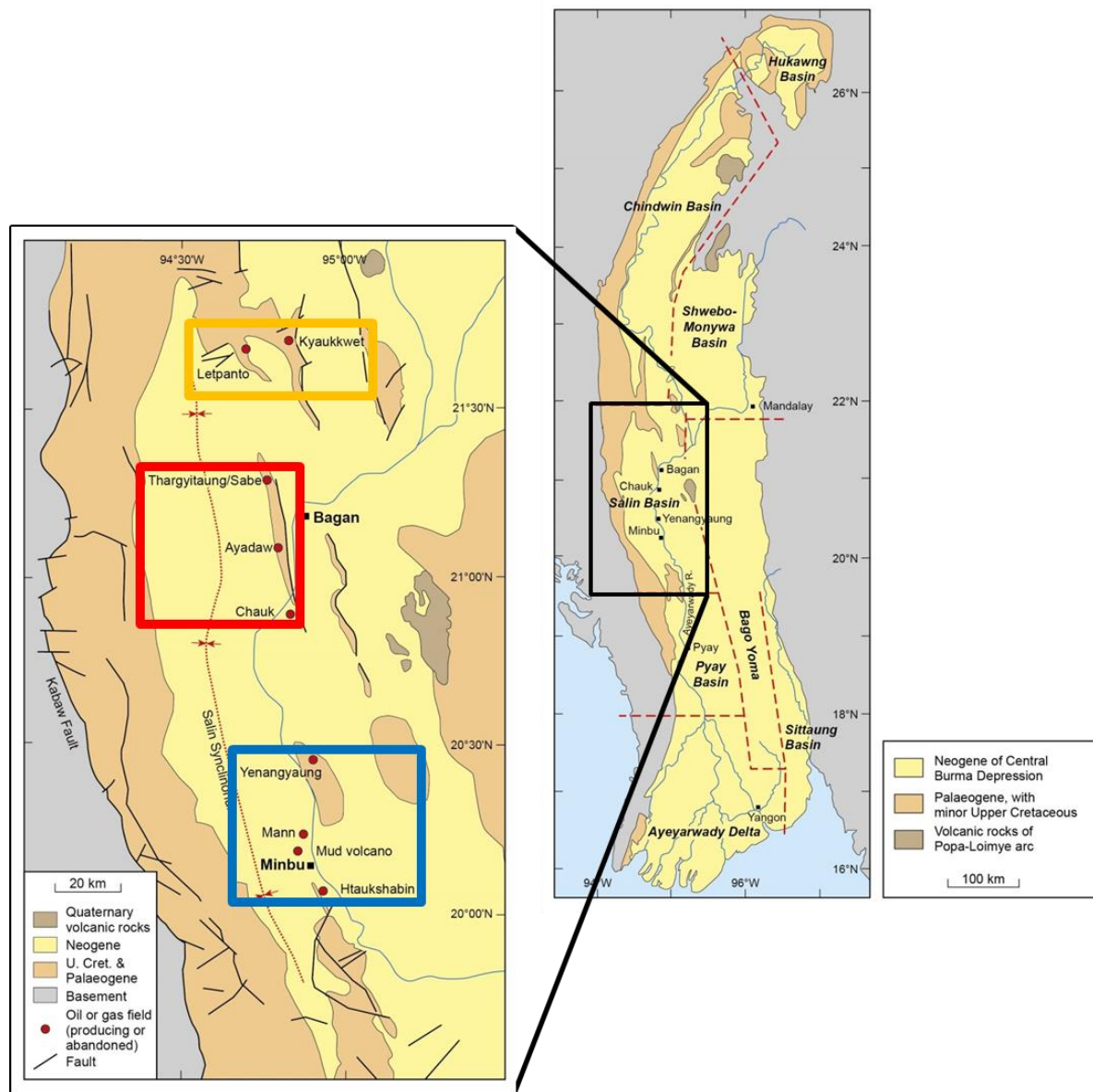


Fig. 1. Location map. Samples were collected from three general areas: the northern area marked in orange, the central area marked in red and the southern area marked in blue. Sampling sites marked with red dots. See "Samples and Methods" for further explanation. Maps modified from Ridd & Racey (2015).

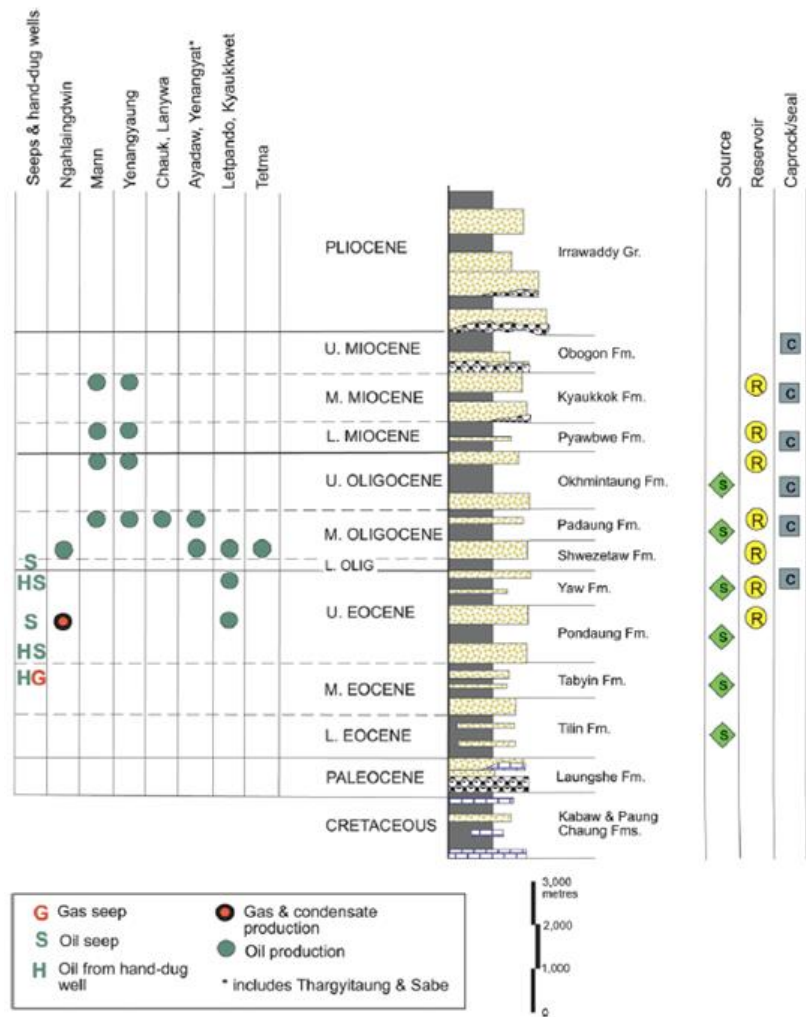


Fig. 2. Summary of the occurrence of petroleum/gas seepages, petroleum source rocks, reservoir rocks and caprocks within the Salin Basin. From Ridd & Racey (2015).

2. Samples and Methods

The sample set comprises a total of 15 produced oils or oils from seepages, including petroleum extracted from water retrieved from a mud volcano. Samples were either collected on site or supplied by the MOGE. Samples are listed in table 1 below. The samples have been grouped and colour-coded according to geographical origin as follows (see map, fig. 1):

- 1. Northern Area:** Kyaukkwet and Letpanto fields, colour-code **ORANGE**
- 2. Central Area:** Chauk and Thargyitaung fields and a hand-dug well near the Aydaw field, colour-code **RED**
- 3. Southern Area:** Yenangyaung, Mann and Htaukshabin field plus the Mimbu mud volcano, colour-code **BLUE**

This colour-coding will be recurring in figures etc. throughout the present report.

Lab. #	Alt. Lab. #	Sample type	Field/Discovery	Lat/Long.	Well	Depth (feet)	Reservoir Fm.	Reservoir age	Comment
20150028-26919	548601	Oil		N21°08,07'/E94°47,58'	Hand-dug well near Aydaw (gas) field	~1500		Probably Oligocene	
20150028-26920	548602	Seepage oil from mud volcano		N20°09,67'/E94°52,45'		0			Mimbu mud volcano
20150028-26921	548603	Oil	Mann	Few km south of N20°09,67'/E94°52,45'				Oligocene-Miocene	
20150028-26922	548604	Oil	Yenangyaung	N20°28,30'/E94°53,47'	Well 3211		Pyawpwe Fm.	Lower Miocene	
20150028-26923	548605	Oil seepage		N20°28,30'/E94°53,47'		0	Kyaukkok Fm.	Upper Miocene	Oil seepage from within the Yenangyaung oil field
20150028-26924	548606	Oil seepage		N20°28,30'/E94°53,47'		0	Kyaukkok Fm.	Upper Miocene	Oil seepage from within the Yenangyaung oil field
20150028-26925	548607	Oil	Yenangyaung	Few km from N20°28,30'/E94°53,47'	Well 3242		Pyawpwe Fm.	Lower Miocene	
20150028-26926	548608	Oil	Yenangyaung	Few km from N20°28,30'/E94°53,47'	Well 3248		Pyawpwe Fm.	Lower Miocene	
20150028-26927	548609	Oil	Chauk	N20°55,30'/E94°49,97'	Well 950			Oligocene	
20150028-26953	CHK # 1101	Oil	Chauk			2000		Oligocene	
20150028-26954	KKT	Oil	Kyaukkwet			3000		Oligocene	
20150028-26955	Yng # 3241	Oil	Yenangyaung			1500		Oligocene	
20150028-26956	L # 110	Letpanto				3000		Oligocene	
20150028-26957	TSB-DT-1	Oil	Htaukshabin			5000		Oligocene	New discovery SE of mud volcano at Mann
20150028-26958	TGT # 9	Oil	Thargyitaung			4000		Oligocene	
<hr/>									
Northern area									
Central area									
Southern area									

Table 1. Sample data

Aliquots of all samples were left overnight at room temperature to attain stable weights. Asphaltenes were precipitated by addition of 40-fold excess n-pentane. Asphaltenes were recovered by centrifugation and rinsed through several stages with n-pentane. Maltene (i.e. asphaltene-free) fractions were separated in saturated, hydrocarbon, aromatic hydrocarbon and polar fractions by MPLC, using a procedure modified from Radke et al. (1980).

Saturated fractions were analysed by GC_{FID} using a Shimadzu gas chromatograph, furnished with a 30m WCOT ZB-1 capillary column.

Biomarker analysis were carried out using an Agilent 6890N gas chromatograph, fitted with a 30m WCOT ZB-5 capillary column, coupled to a Waters (Micromass) Quattro Micro GC tandem quadropole-hexapole-quadropole mass spectrometer. The instrument was run in both GCMS_{SIM}

mode and GCMS-MS parent-daughter mode, and all samples were run several times using methods designed to optimize the representation of various compounds.

3. Results

The aims of the analyses reported here are in the present case threefold: (1.) to assess the level of thermal maturity of the source of various oil samples analysed; (2.) to assess if the various samples can be grouped and discriminated; (3.) to assess the nature of the source depositional environment.

3.1 Group type fractionation

Group-type separation data are tabulated in Appendix 1. Asphaltene contents are strongly variable, from close to zero to nearly 40% by weight with no unambiguous relation to the level of biodegradation as assessed from gas chromatography data (see below). The compositions of the maltene fractions are variable, but with rather clear relationships to the level of biodegradation as assessed from gas chromatography data (see below). The proportion of saturated hydrocarbons varies from app. 20% to app. 65%, with the lower values yielded by biodegraded samples (fig. 3). Aromatic hydrocarbons constitute between app. 20% and app. 50% with biodegraded samples showing the higher values. Polar (heteroatomic, NSO) compounds constitute app. 35% to app. 55% of the maltene fractions.

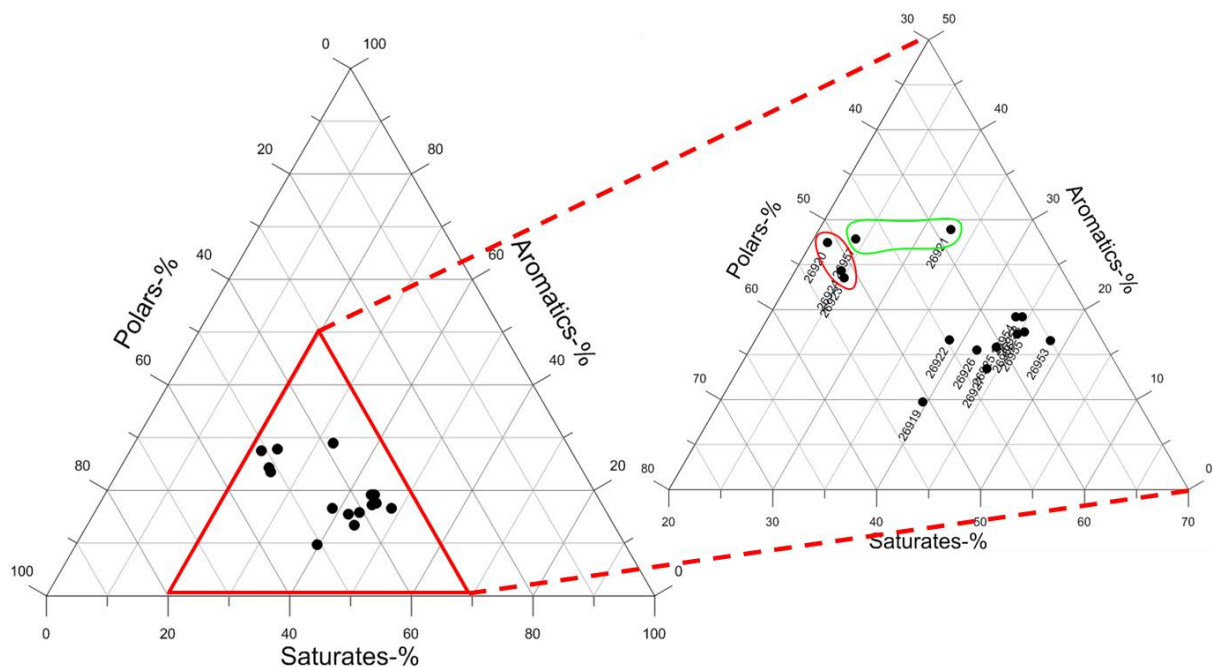


Fig. 3. Group type fractionation data, detail on the right includes sample laboratory-number (suffix only). Samples encircled by a red marking are biodegraded with n-alkanes being more or less eliminated, samples encircled by a green marking are less biodegraded with some n-alkanes preserved, see gas chromatography data below.

3.2 Gas chromatography

Original gas chromatograms are reproduced in Appendix 1 together with tabulated key parameters derived from gas chromatographic data.

Ignoring the adulteration of a number of samples caused by biodegradation, it is clear that all samples show an overall similarity by showing broad n-alkane distributions with a strong preponderance of C₂₂₊ waxy compounds extending often to C₄₀₊, CPI slightly >1, and high or even very high pristane/phytane ratios, varying from a little less than 3 for one single outlying sample collected from the Mimbu mud-volcano to values in the overall range 5 – 8, for the remainder of the samples (fig. 4).

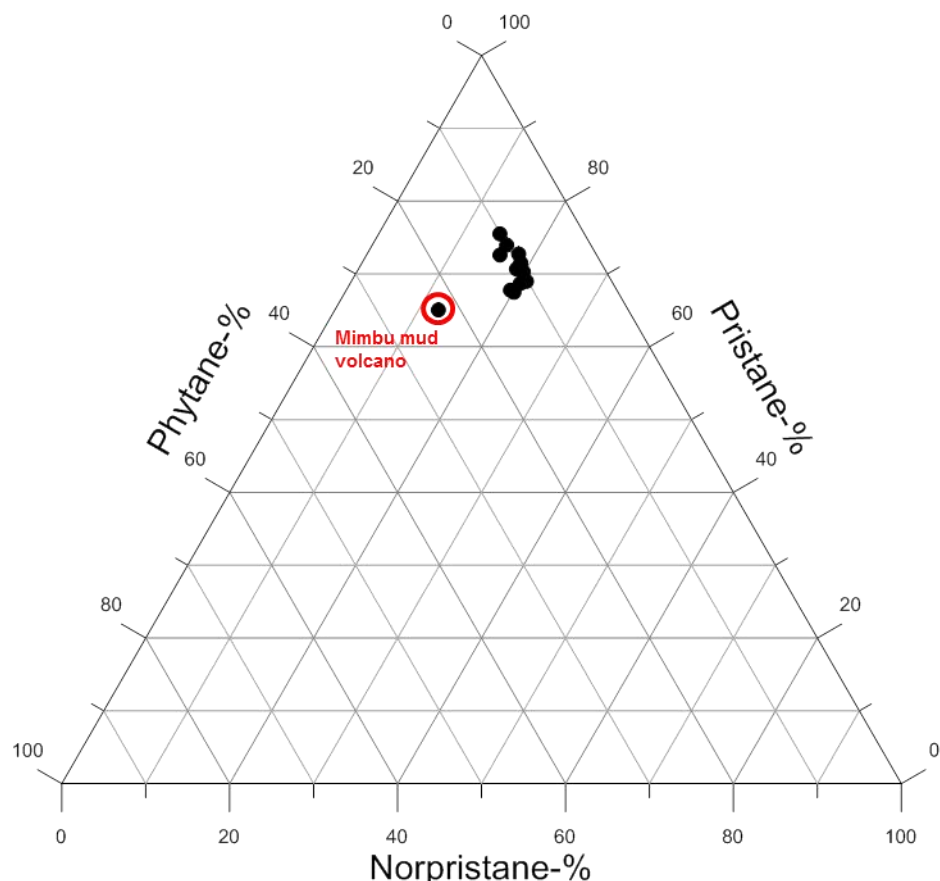


Fig. 4. Normalised distribution of acyclic isoprenoids norpristane, pristane and phytane. Note large similarity except for a single outlying sample collected from the seepage at the Mimbu mud volcano.

Within the dataset some grouping of samples can be established (fig. 5): The northern area, hosting the Letpanto and Kyaukkwet fields (samples -26954, -26956), show very similar characteristics including bimodal n-alkane distributions and CPI clearly >1. Somewhat similar but less pronounced characteristics are found in samples from the central area. In the southern area, surface seep and mud-volcano samples have suffered severe depletion in n-alkanes, leading to near-total elimination in two samples (-26923, 26924). Moreover, the Mann and Htaukshabin fields (samples -26921 & -26957), both situated in rather close geographical proximity in the southern part of the southern area show fairly similar characteristics, featuring partial depletion of n-alkanes. Besides this, the

remaining samples, all collected from the Yenangyaung field show rather similar characteristics, featuring broad, somewhat light-end skewed n-alkane distributions without any clear signs of n-alkane depletion.

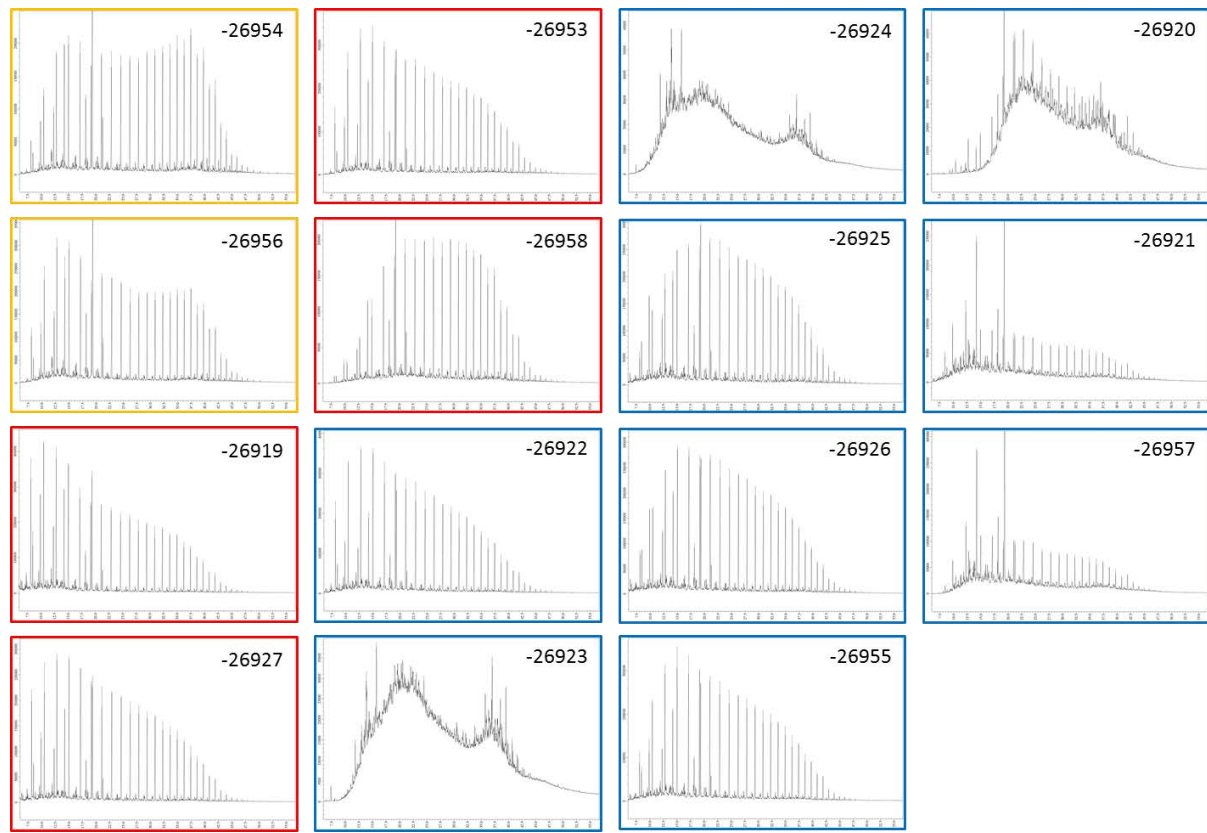


Fig. 5 Gas chromatograms arranged according to geographical area and colour-coded: orange = northern area; red = central area; blue = southern area. Sample laboratory-numbers (suffix only) are shown to allow identification of samples, cfr. Table 1.

3.3 Biological markers

Tricyclic and tetracyclic compounds were monitored by the m/z 191 ion fragmentogram using GCMS_{SIM} technique. Original data are reproduced in Appendix 2 together with a tabulation of calculated parameters and a compound identification key.

Hopanes and other pentacyclic triterpanes were monitored using GCMSMS_{parent-daughter} technique. Original data are reproduced in Appendix 3 together with a tabulation of calculated parameters and a compound identification key.

Isohopanes were monitored using GCMSMS_{parent-daughter} technique. Original data are reproduced in Appendix 4 together with a tabulation of calculated parameters and a compound identification key.

C_{26} – C_{30} steranes were monitored using GCMSMS_{parent-daughter} technique. Original data are reproduced in Appendix 5 together with a tabulation of calculated parameters and a compound identification key.

Bicadinanes were monitored using GCMSMS_{parent-daughter} technique. Original data are reproduced in Appendix 6 together with a tabulation of calculated parameters and a compound identification key.

3.3.1. Thermal maturity

Homohopane S/R-isomerisation has attained equilibrium in all samples and does not carry any further useful information pertaining to the level of thermal maturity. Despite its sensitivity to facies variations, the overall similarity of the samples it seems to justify the use of the $T_s/(T_s+T_m)$ -parameter, which shows notable variation, for maturity assessment. Moreover, C_{29} -regular sterane isomerisation ratios show notable variation, both with respect to the $20S/(20S+20R)$ ratio and the $\alpha\beta\beta/(\alpha\beta\beta+\alpha\alpha\alpha)$ ratios. Combined these parameters consistently show the presence of maturity variations among the different sampling areas and an increasing level in overall maturity of the samples from the North to the South across the Salin Basin (Fig. 6a & 6b). Conversely, the “bicadinane maturity index”, “BMI1”, devised by Murray et al. (1994) does not seem to work well.

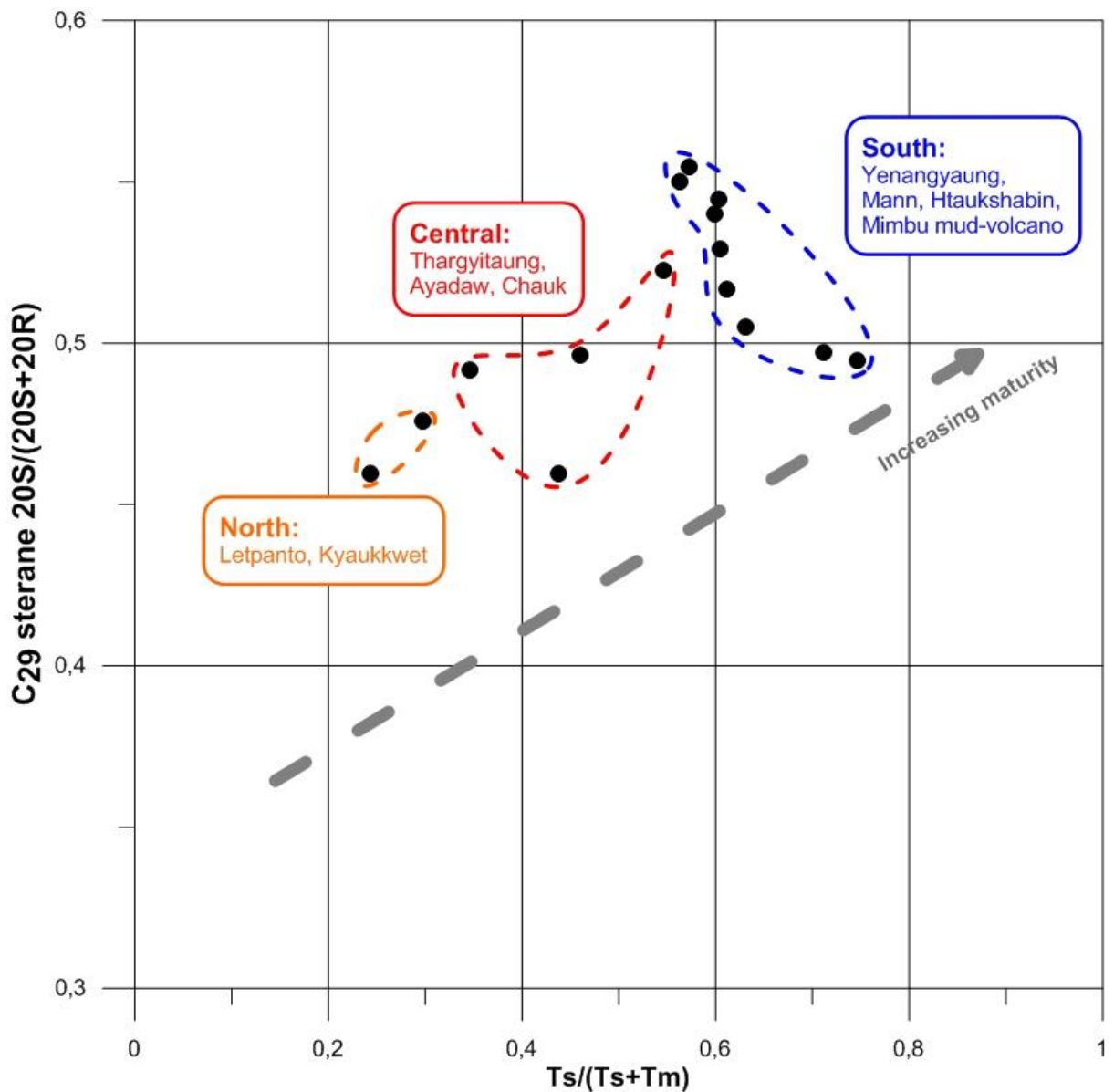


Fig. 6a. $Ts/(Ts+Tm)$ versus C_{29} Sterane $20S/(20S+20R)$ isomerisation ratio. The three sampling areas are clearly distinguished, suggesting a regional increase in the level of thermal maturity from the North to the South across the Salin Basin.

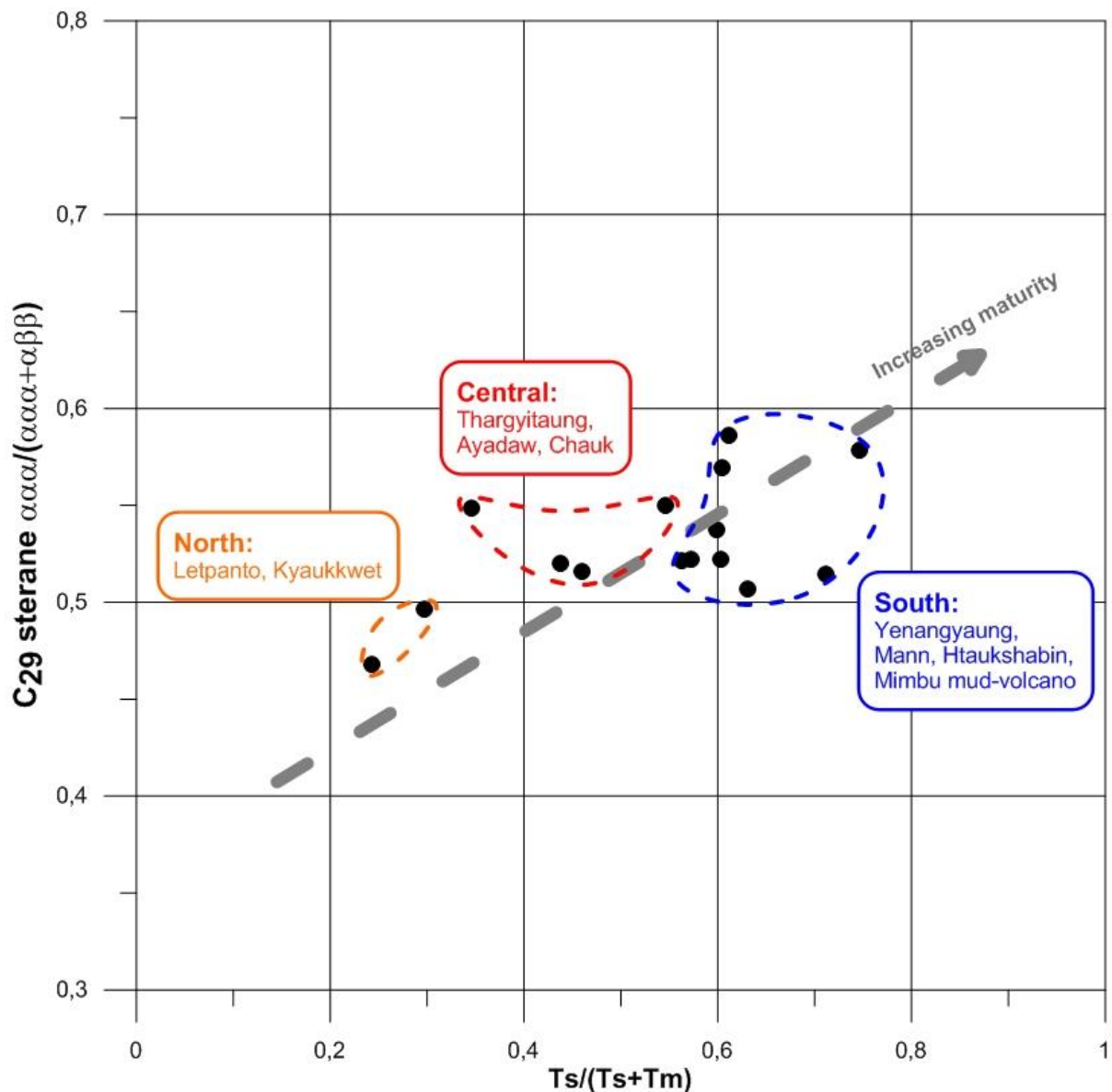


Fig. 6b. $Ts/(Ts+Tm)$ versus C_{29} Sterane $\alpha\alpha\alpha/(\alpha\alpha\alpha+\beta\beta\beta)$ epimer ratio. The three sampling areas are clearly distinguished, suggesting a regional increase in the level of thermal maturity from the North to the South across the Salin Basin.

3.3.2. Biological marker fingerprinting and source correlation

Tricyclic compounds of the cheilanthane series are generally very sparse but in combination with other parameters, they may still yield useful information – see below. An example of the compounds to be observed is shown in fig. 7. Often their recognition is rendered difficult by the presence of partially coeluting substances, and in some cases by n-alkanes, which when present in high concentrations may be visible even in the m/z 191 fragmentogram. Other compounds include a series of somewhat poorly known tricyclic and tetracyclic compounds, probably derived from the well-known angiosperm higher landplant marker oleanane, described by Samuel et al. (2010). Six different compounds described by Samuel et al. (2010) have been included here: Compound X (2 stereoisomers), compounds Y & Y1, and compounds Z & Z1. Samuel et al. (2010) suggest the

distribution of these compounds relative to the cheilanthanes can be utilized to rank samples according to a relative marine-terrigenous composition, but the Myanmar samples fall outside the proposed trend (fig.8). However, the normalised distribution of the three compounds X, Y, Z serves excellently to discriminate the sampling areas (fig. 9).

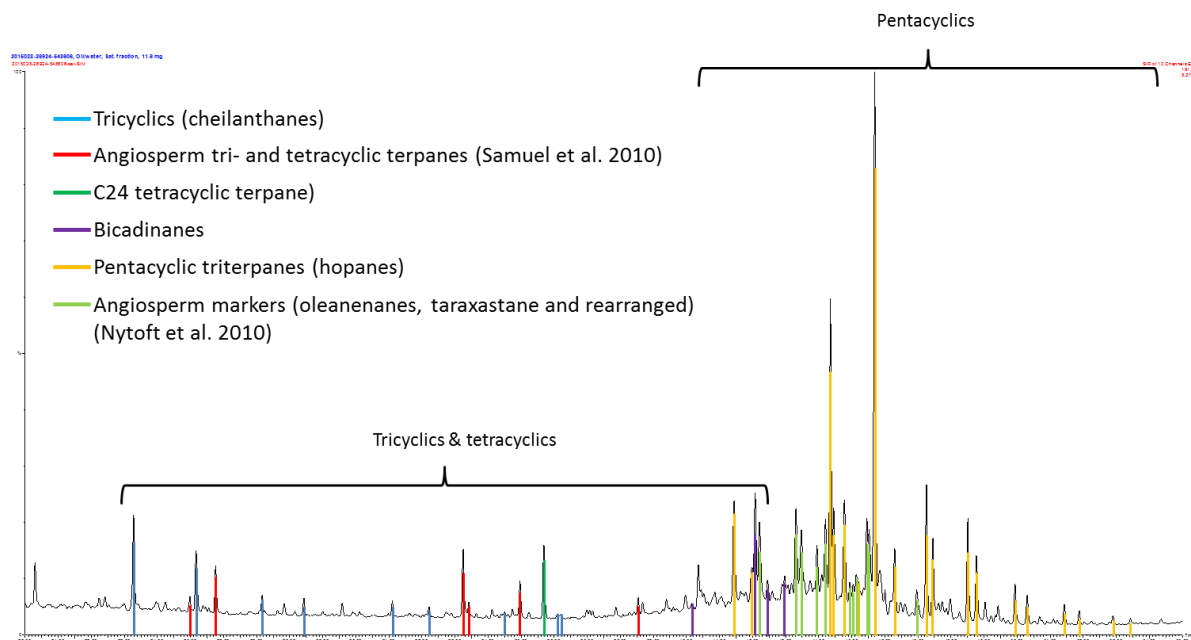


Fig. 7. GCMS_{SIM} -data, ion fragmentogram m/z 191.

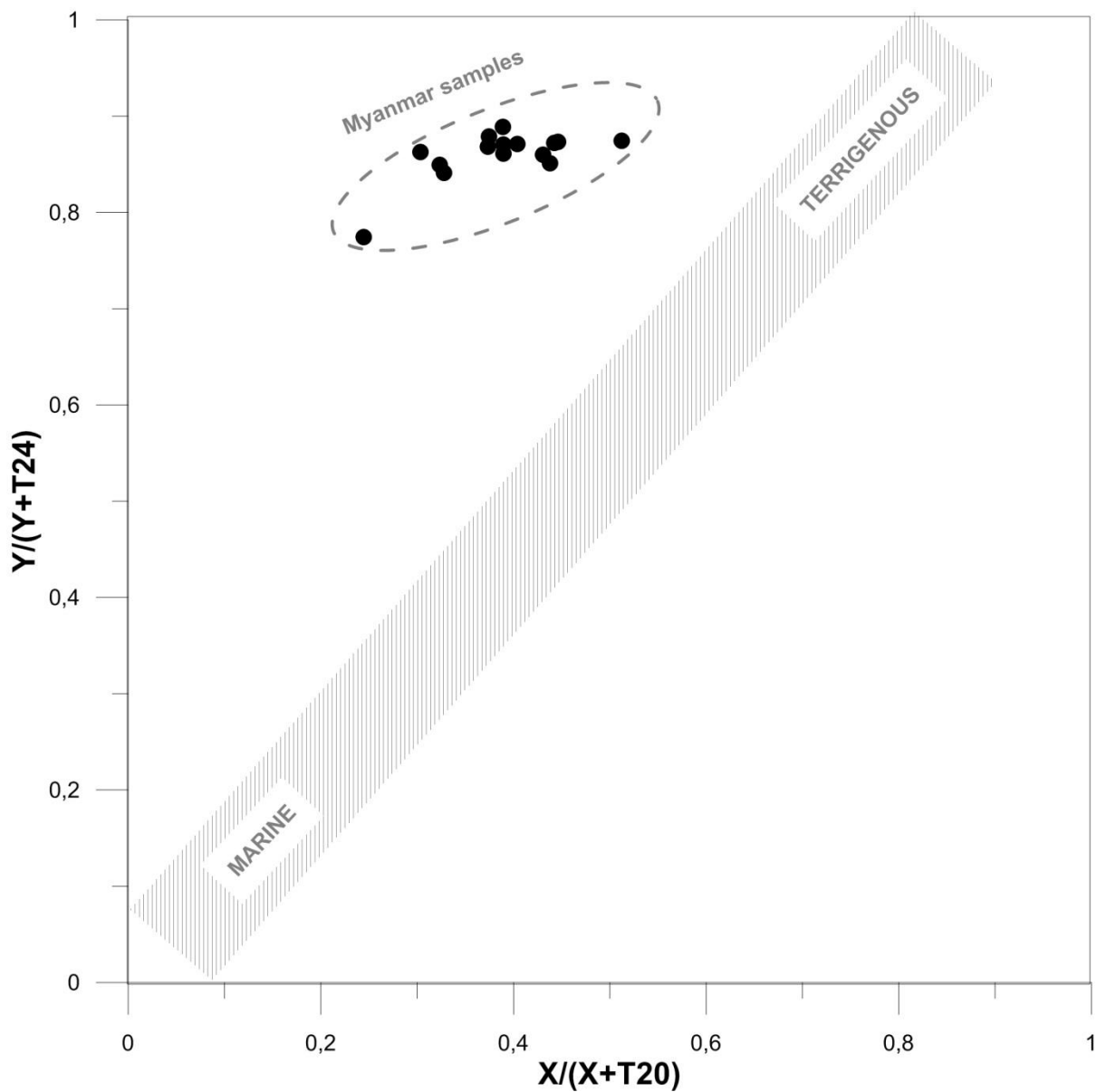


Fig. 8. Plot after Samuel et al. (2010). Hatched area show the approximate trend of marine to terrigenous composition defined by Samuel et al. (2010). The Myanmar samples fall outside the established trend.

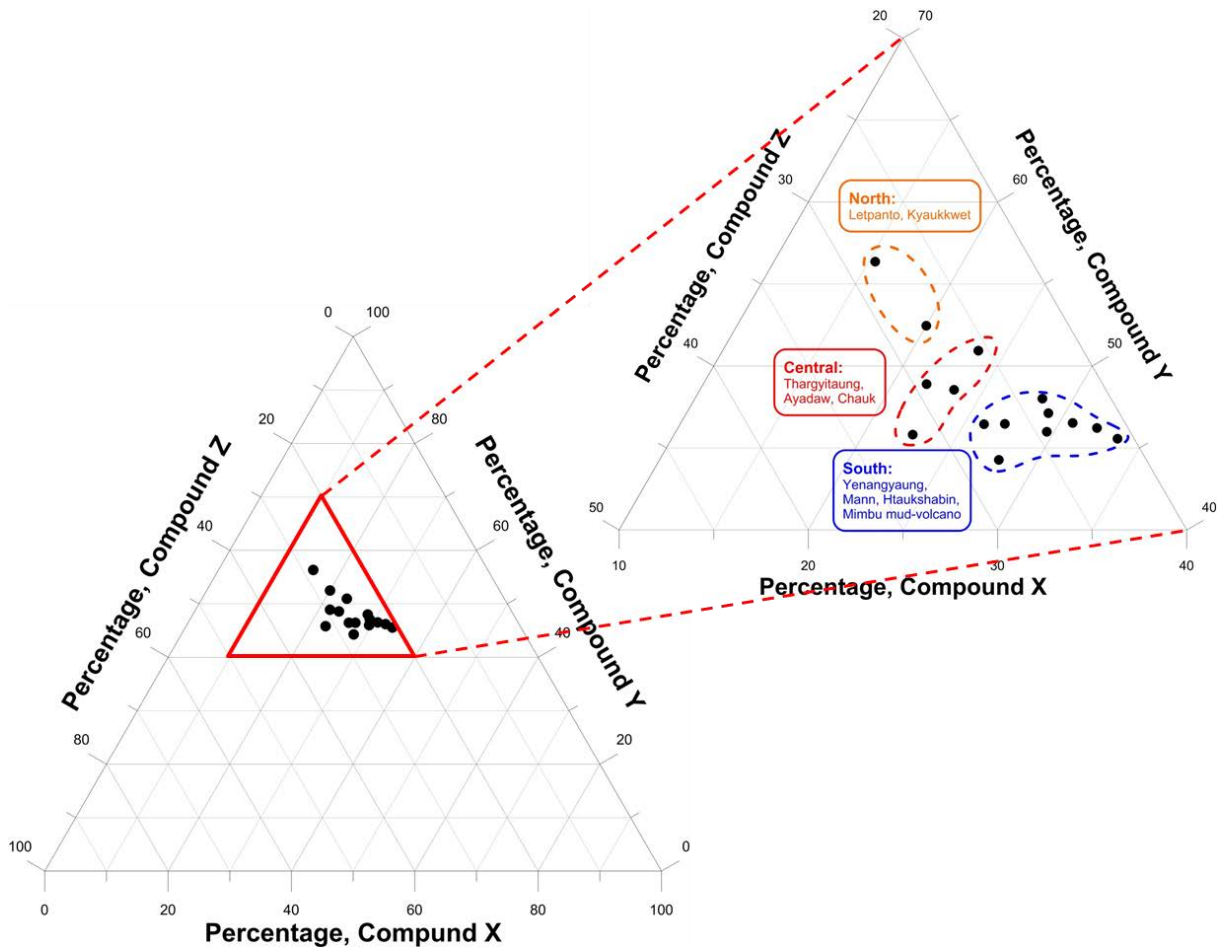


Fig. 9. Normalised distribution of compounds X, Y, Z, described by Samuel et al. (2010). The distribution of these compounds differs clearly among the three sampling areas.

The cheilanthane series may, combined with hopane and sterane parameters, be used for “fingerprinting oils from the three sampling areas. This can be achieved in several different ways that work more or less well, one example is shown in fig. 10.

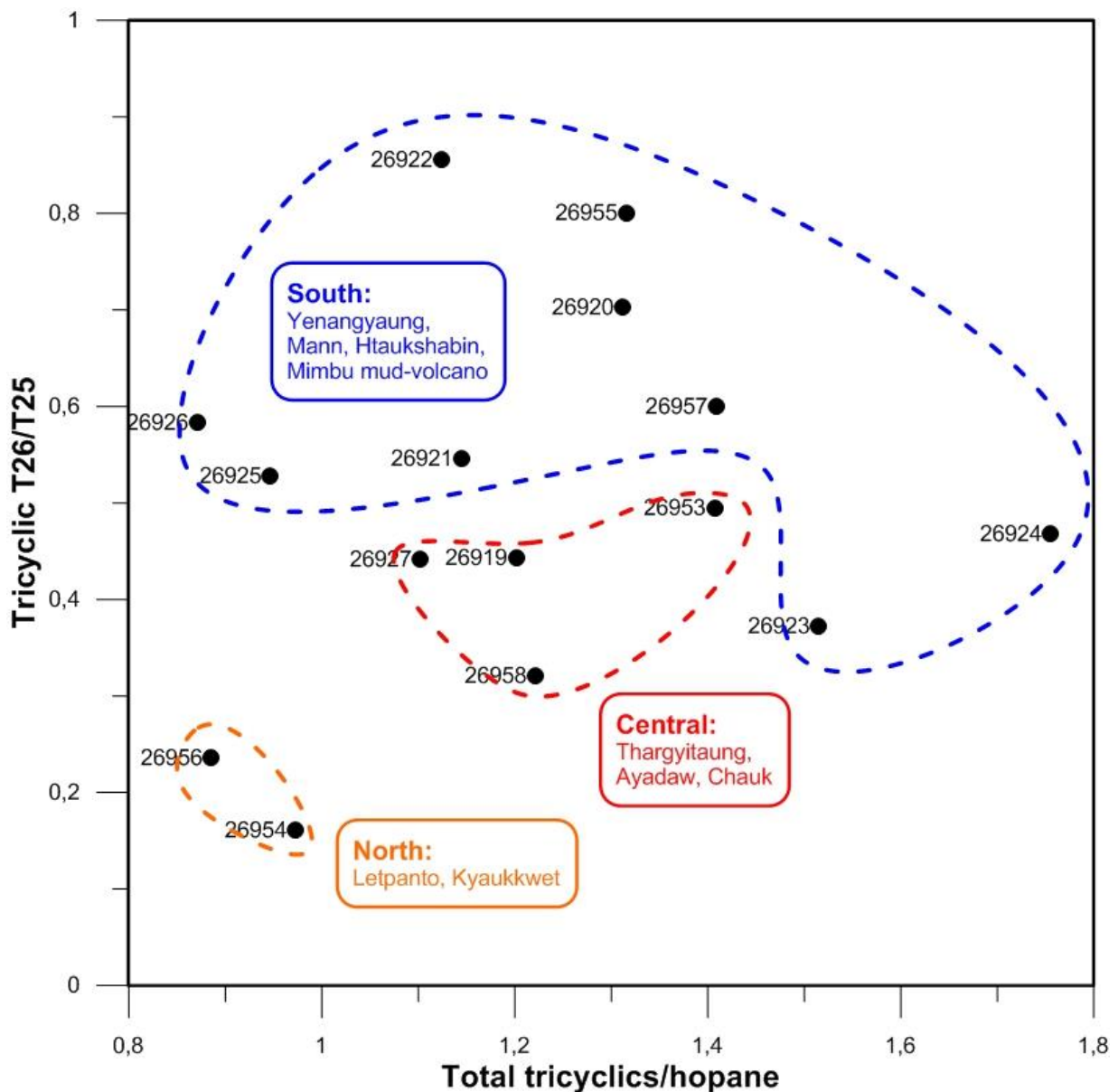


Fig. 10. Total C_{19-26} tricyclics (cheilanthanes) / C_{30} Hopane ratio versus C_{26} / C_{25} tricyclics (cheilanthane) ratio. The combination of these parameters seems discriminate the three sampling areas rather well, in particular the northern area is singled out.

The angiosperm higher land plant-derived tri- and tetracyclic components described by Samuel et al. (2010) may be used in a similar way to discriminate the sampling areas. This can also be achieved in several different ways, combined with both cheilanthane or hopane data and sterane data; two examples are shown in figs 11 and 12.

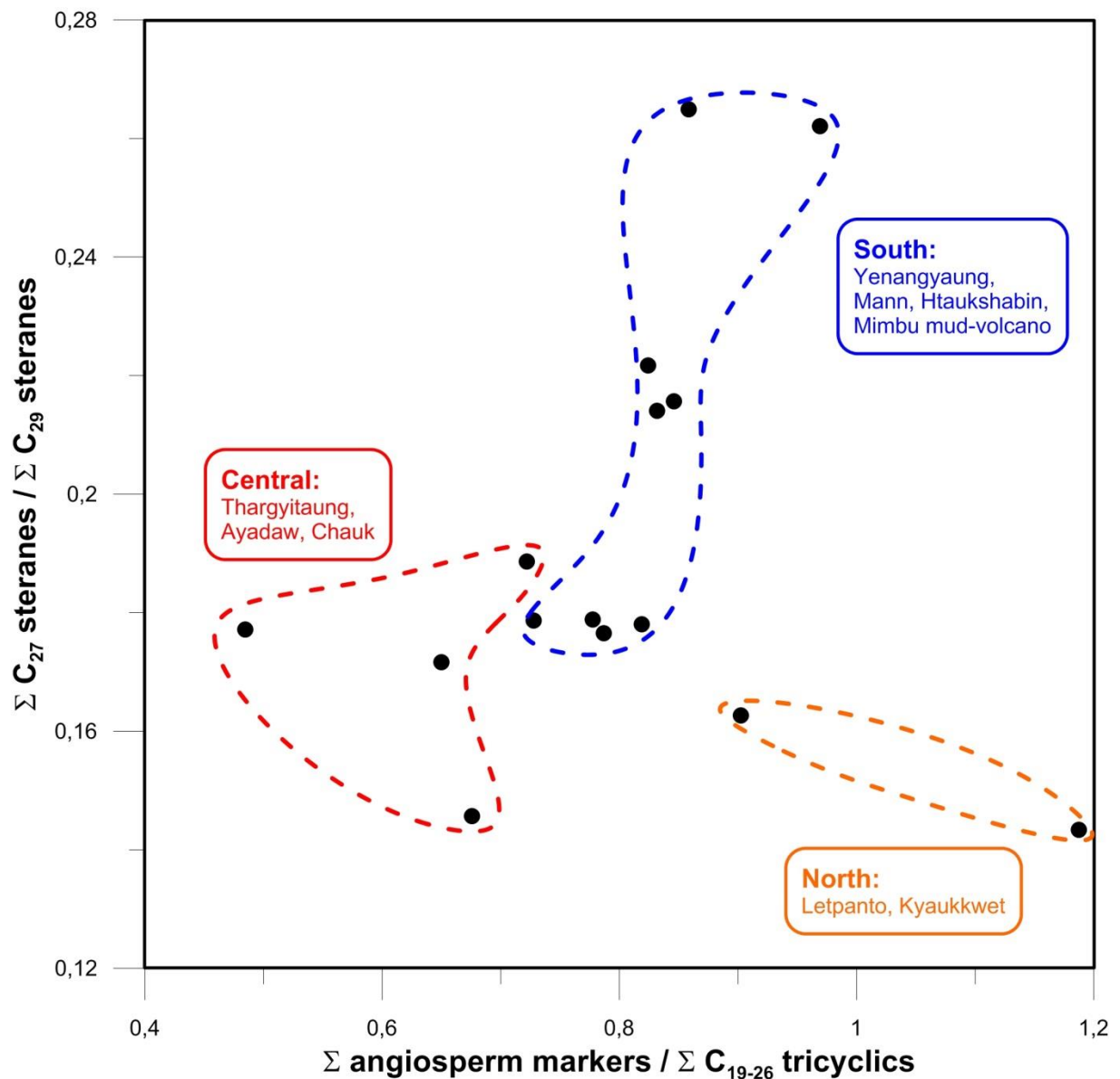


Fig. 11. Ratio of the sum of angiosperm higher land plant-derived tri- and tetracyclic components described by Samuel et al. (2010) to total C₁₉₋₂₃ tricyclics (cheilanthanes) versus ratio of total C₂₇ steranes (dia- plus regular) to total C₂₉ steranes (dia- plus regular). The three sampling areas are fairly well separated.

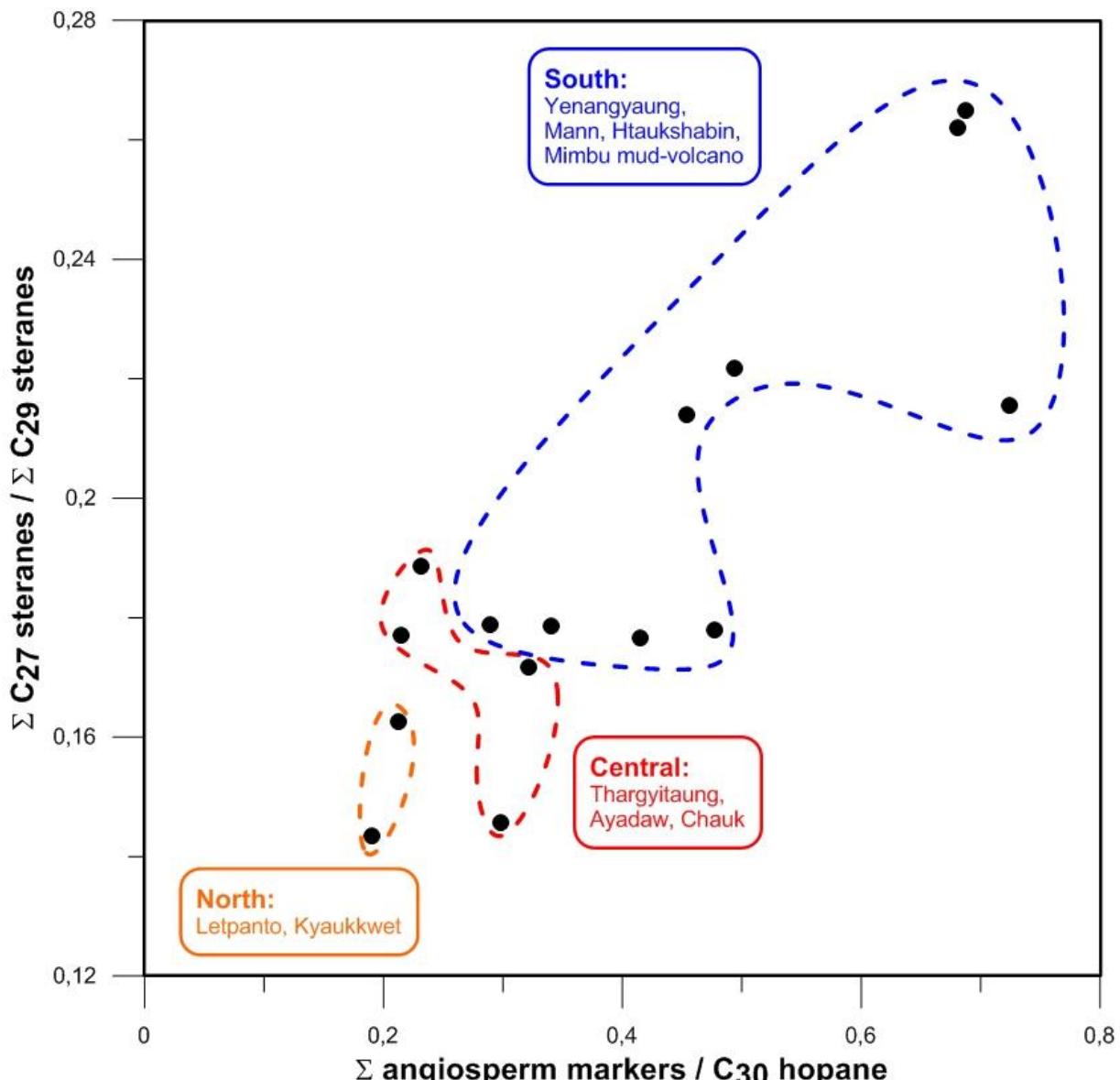


Fig. 12. Ratio of the sum of angiosperm higher landplant-derived tri- and tetracyclic components described by Samuel et al. (2010) to C₃₀ hopane versus ratio of total C₂₇ steranes (dia- plus regular steranes) to total C₂₉ steranes (dia- plus regular steranes). The three sampling areas are fairly well separated. Within the southern sampling areas the Mann and Htaukshabin fields plot together centrally in the cluster, four samples in the lower left part of the cluster all represent the Yenangyaung field, whereas the samples in the upper right part of the cluster represent the Yenangyaung field(2 samples) and the Mimbu mud volcano.

Traditional biological marker parameters derived from the sterane and hopane classes are not particularly useful in discriminating between the samples. The distribution of major hopanes is very similar in all samples and so is the distribution of steranes (fig. 13). A few ratios may be devised that allow the various samples to be grouped (eg. fig. 14) but in general the distribution of less commonly used compounds work better.

Isohopanes were documented by Nytoft (2011), and the isohopane ratio defined by this author is a strong tool for classifying terrestrially-derived oils. The IHR-values yielded by the Myanmar samples are rather extreme and surpasses even any sample cited by Nytoft (2011). When plotted against each other the 30-norhopane / hopane ratio and the IHR clearly distinguishes between the three sampling areas (fig. 15). Substituting the 30-norhopane / hopane ratio for the ratio of total C₂₇ steranes (dia- plus regular) to total C₂₉ steranes (dia- plus regular) yields a less clear-cut, but still acceptable separation of the sample clusters representing the sampling areas (fig 16).

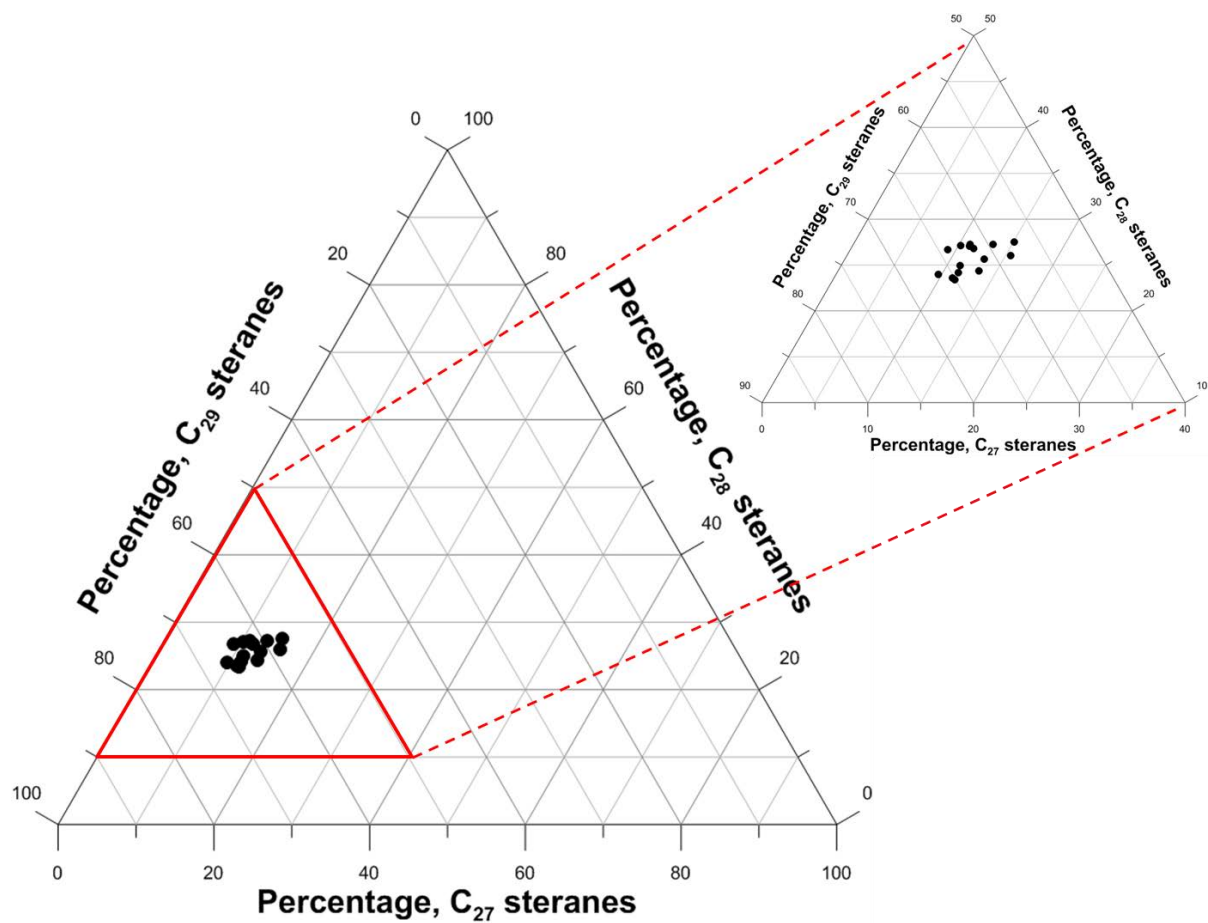


Fig. 13. Normalised distribution of C27-29 total steranes (dia- plus regular steranes). Note very homogeneous distribution.

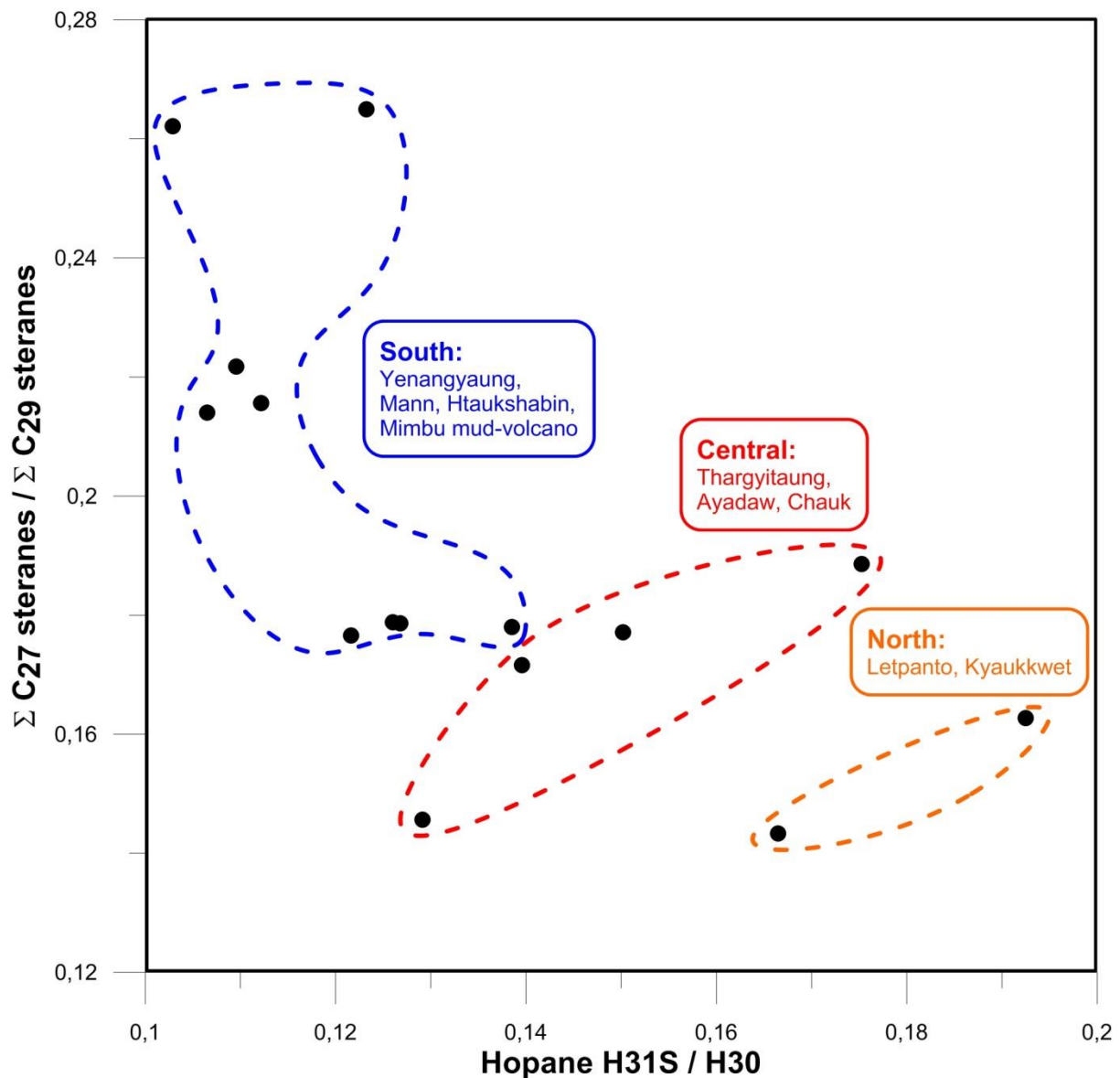


Fig. 14. Ratio of 22S-homohopane to hopane versus ratio of total C₂₇ steranes (dia- plus regular steranes) to total C₂₉ steranes (dia- plus regular steranes). The three sampling areas are fairly well separated.

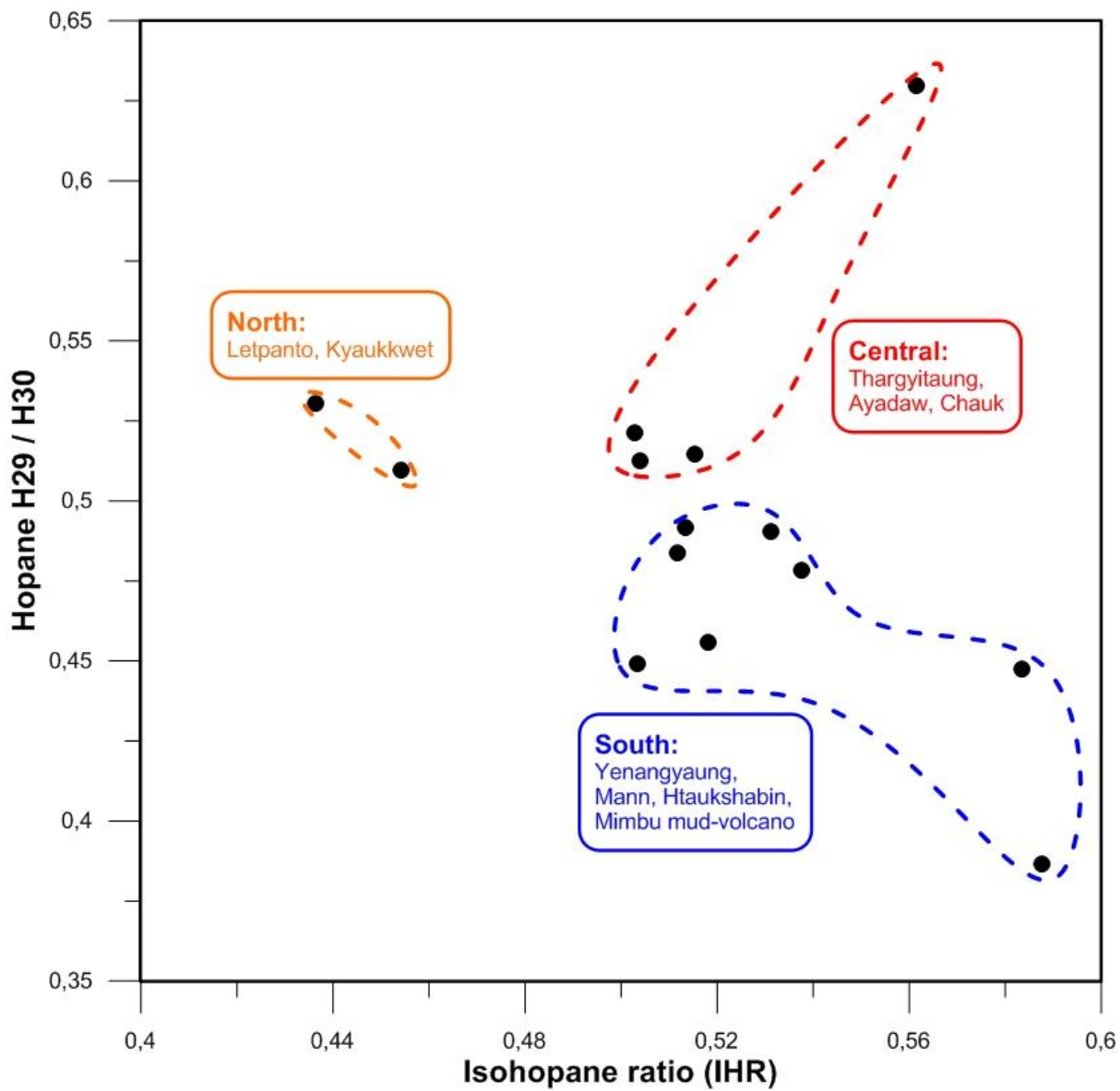


Fig. 15. Isohopane ratio, IHR (Nytoft 2011) versus ratio of 30-norhopane to hopane. The three sampling areas are clearly separated.

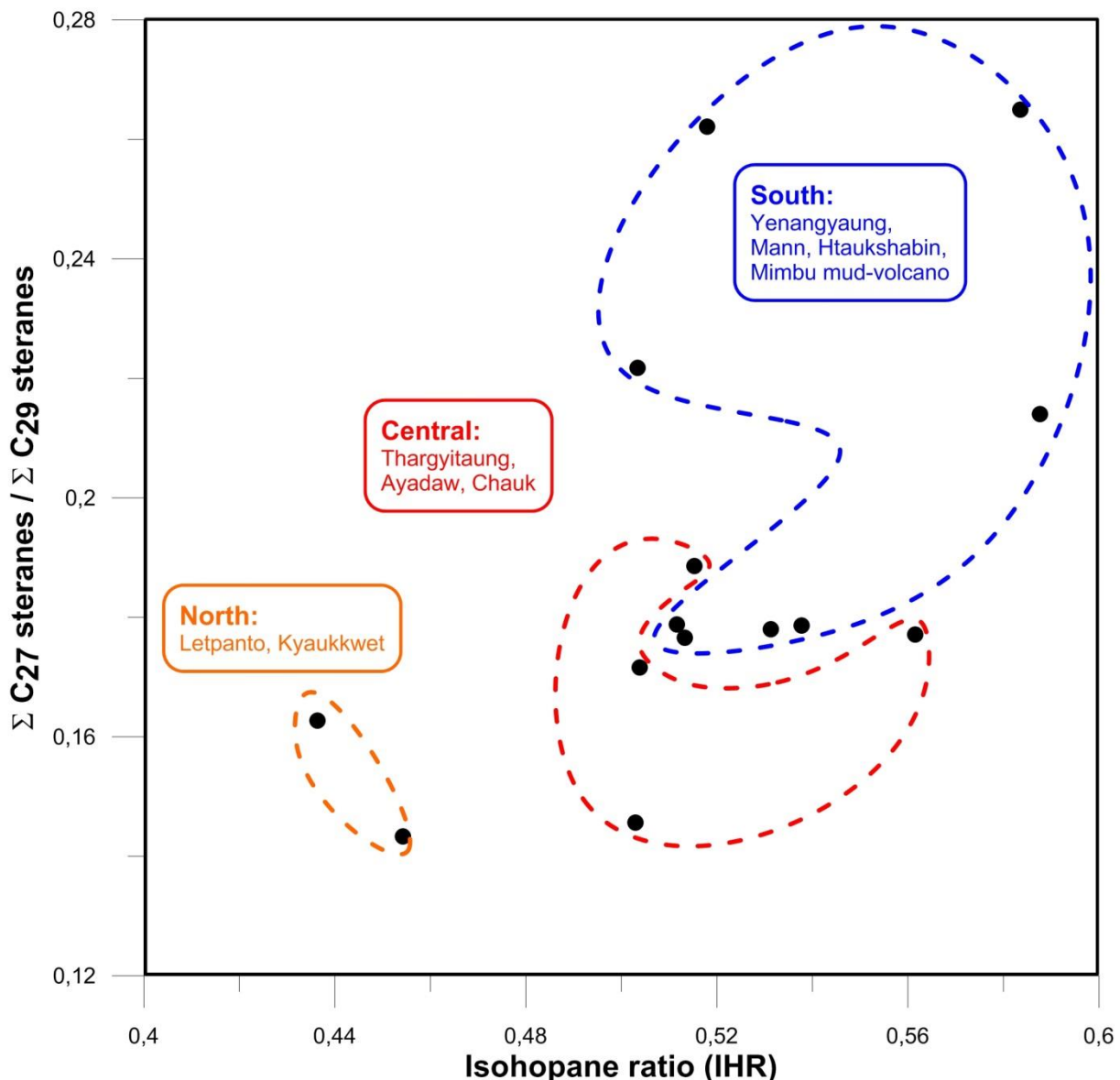


Fig. 16. Isohopane ratio, IHR (Nytoft 2011) versus ratio of total C_{27} steranes (dia- plus regular steranes) to total C_{29} steranes (dia- plus regular steranes). The three sampling areas are fairly well separated.

Bicadinanes may also serve to discriminate the three sampling areas (fig. 17) but it is noteworthy that one sample from the central area seems to show affinity towards the northern area. The sample in question represents the Thargyitaung (Sabe) field, which is the northernmost field sampled in the central area.

GCMSMS_{parent-daughter} m/z 412 \Rightarrow 369 fragmentograms showing the distribution of bicadinanes and several other compounds are shown in fig. 18. Samples from the northern area plus sample -26958, representing the Thargyitaung (Sabe) field of the central area all include a prominent peak (indicated by green asterisk), which absent or nearly absent from all other samples. This peak represents a compound that has been identified by Nytoft et al. (2010) as 5(4 \Rightarrow 3)abeo-3 α (H), 5 β (H), 18 α (H)-oleanane. This compound is one of series of rearranged compounds of the oleanane family,

described in detail by Nytoft et al. (2010). Several other members of this family are present in the Myanmar samples, but should be monitored using other ion transitions that have not been included in the present study.

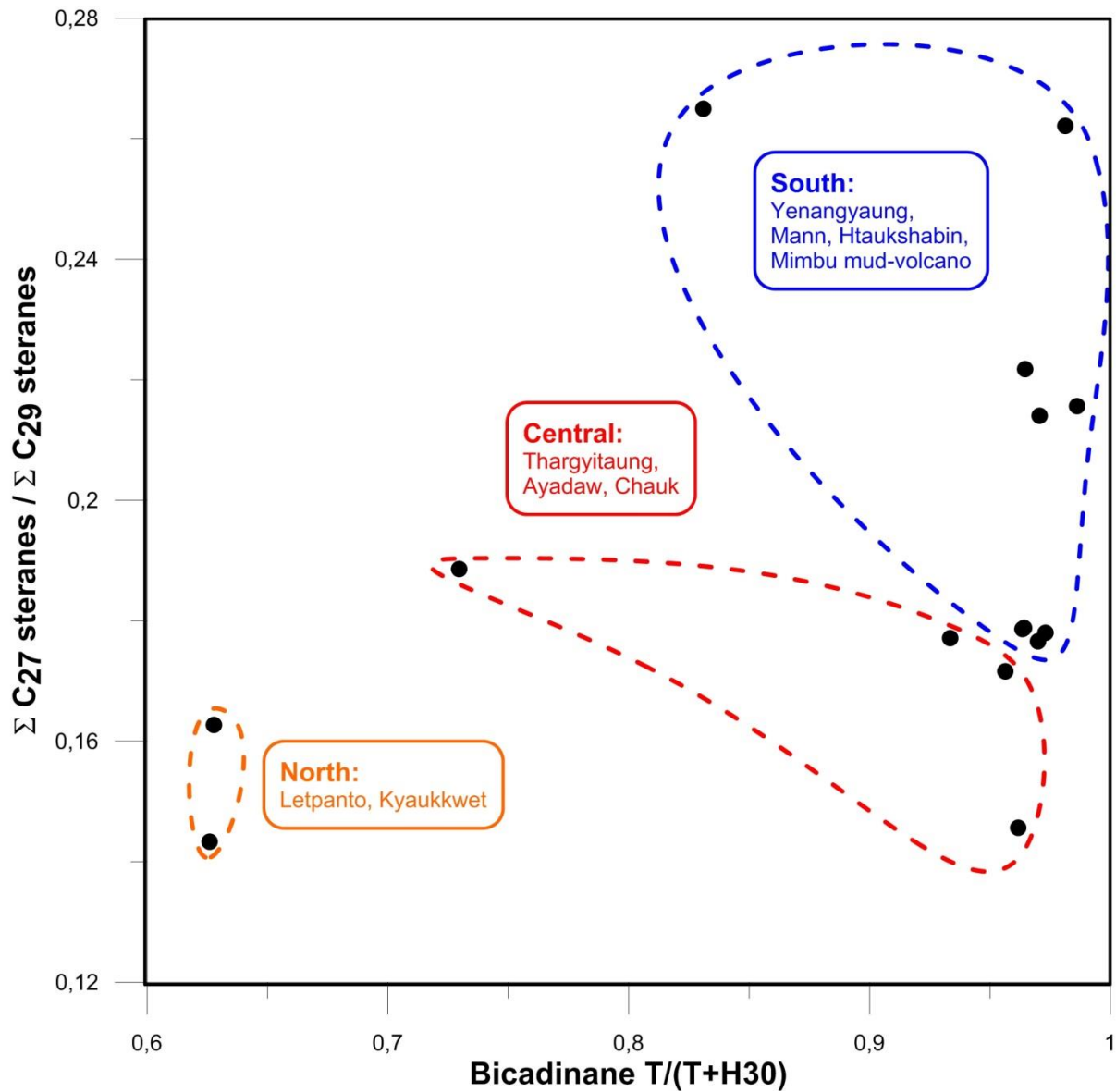


Fig. 17. Ratio of bicadinane T to T+hopane versus ratio of total C_{27} steranes (dia- plus regular steranes) to total C_{29} steranes (dia- plus regular steranes). The three sampling areas are fairly well separated. Note the “outlying” sample in the central area showing affinity to the northern area. The sample represents the Thargyitaung (Sabe) field, which is the northernmost field sampled in the central area.

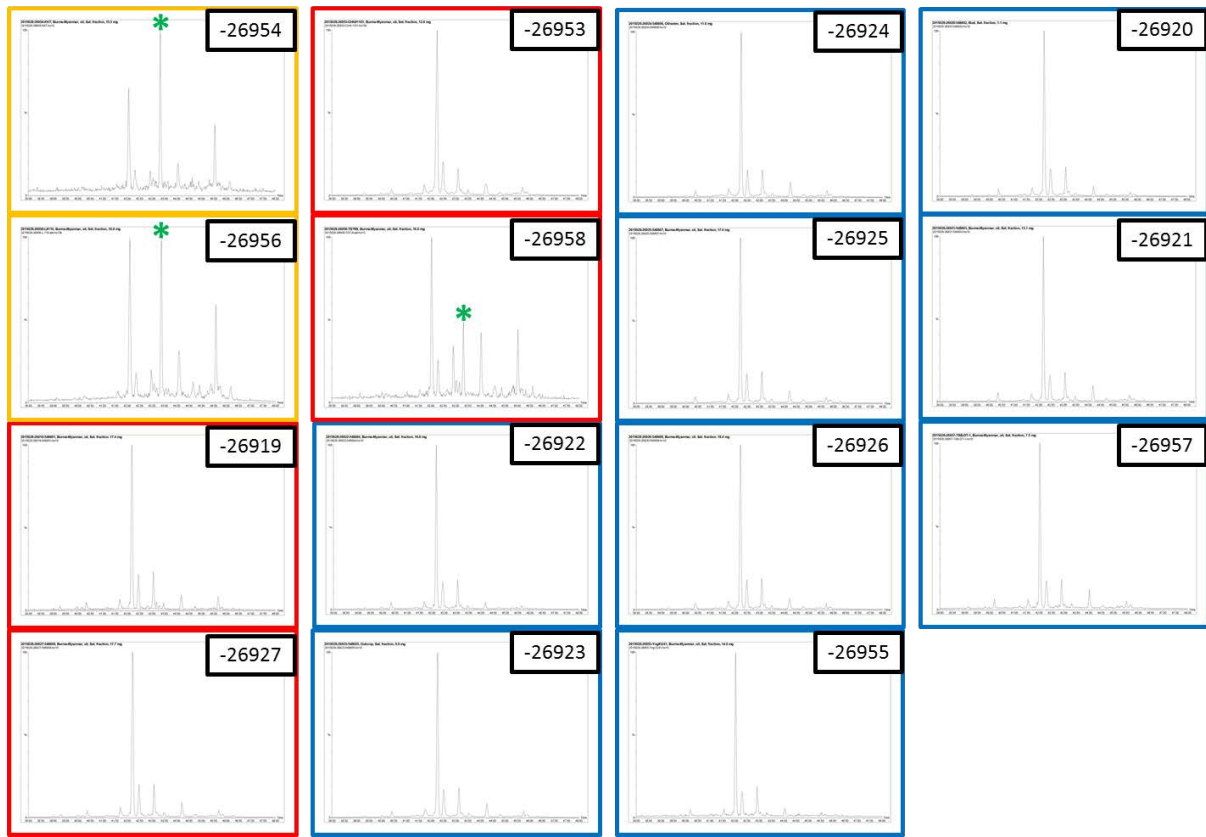


Fig. 18. GCMSMS_{parent-daughter} m/z 412 ⇌ 369 fragmentograms showing the distribution of bicadinanes and several other compounds. Green asterisk denotes 5(4 ⇌ 3)abeo-3α(H), 5β(H), 18α(H)-oleanane (Nytoft et al. 2010), which seems to be characteristic for samples from the northern sampling area plus the northernmost sample from the central area (-26958, Thargyitaung (Sabe) field).

4. Discussion

The overall paraffinic composition of non-degraded samples is conformable with an origin from sources dominated by terrestrial higher land-plant derived kerogen, and the rather high levels of heteroatomic compounds may indicate a low to moderate level of thermal maturity. Biodegradation initially affects primarily normal alkanes, thus leading to lower proportions of saturated hydrocarbons. The level of biodegradation can be initially assessed using gas chromatography data that show strong depletion in n-alkanes in surface and mud-volcano samples. The Mann and Htaukshabin field samples have suffered some biodegradation and appear somewhat depleted in n-alkanes. Very high levels of asphaltenes in the Htaukshabin field may be caused by concurrent biodegradation and replenishment by fresh petroleum charges during part of the fields history, but based on available data this cannot be further investigated. The remainder of samples from the southern area, i.e. Yenangyaung field samples seem essentially undegraded. Based on bimodal n-alkane distributions and CPI clearly >1 , samples from the Letpanto and Kyaukkwet fields in the northern area appear less thermally mature than samples from the southern area, whereas the central area seems to occupy an intermediate position in this respect too. Hence, gaschromatographic data hint at the existence of an overall N – S increase in thermal maturity.

Sterane and hopane thermal maturity indicators confirm the variation in thermal maturity that is suggested by GC data. Both the N–S trend in maturity across the basin and the separation of the sampling areas are well defined. The fact that a maturity assessment based on bicadinane distribution does not provide meaningful results may be attributed to mixing of contributions from several sources with different bicadinane distributions and concentrations. Bicadinanes can be regarded as “trace-components” that may be present or absent, whereas steranes and hopanes are ubiquitous and thus not similarly susceptible to mixing of sources.

The tricyclic terpanes of the cheilanthane series are routinely used for geochemical correlation, and high concentrations relative to pentacyclic compounds are often seen in oils derived from marine algal material, whereas low concentrations are usually a characteristic of terrigenous oils. Hence, the low concentrations observed in the Myanmar samples are in accordance with their general terrigenous character. However, the distribution of angiosperm higher land-plant derived tricyclic and tetracyclic components falls outside the marine-terrigenous trend defined by Samuel et al. (2010) (fig. 9). This is probably due to mixing of sources; the oils sampled resulting from contributions from several source intervals with different characteristics and varying concentrations of different biological marker compounds in the thick sedimentary succession filling the Central Burma Depression.

A number of different biological marker parameters based on commonly used hopanes and steranes have proven useful in grouping and discriminating the samples analysed, and a number of lesser used components have added further to this. The various parameters may in different combinations classify the samples according to origin in the sense that the three sampling area are clearly distinguished by a number of parameters. In particular, the northern sampling area is commonly very well distinguished from the central and southern areas. However, with respect to source rock characterisation in terms of relative contributions to the kerogen of terrigenous versus marine organic matter the results are ambiguous. For instance, low values of the 22S-homohopane to

hopane ratio are often characteristic of lacustrine source rocks, whereas high sterane C₂₇/C₂₉ ratios can be taken as a crude indicator marine source rocks (eg. Peters et al. 2005). However, when these parameters are cross-plotted (fig. 14), the ostensibly more marine samples are also the more lacustrine samples. Similar contradictory or ambiguous indications are seen when using the parameters H₂₉/H₃₀ that is often used as carbonate indicator (fig. 15) and the sterane C₂₇/C₂₉ ratio, which when cross plotted against IHR (fig. 16), suggests that the ostensibly more marine influenced samples are also the more terrigenous samples. In this respect it should be borne in mind that the differences between the samples are consistent, but subtle, and the variation observed in the parameters used is generally too small to allow detailed interpretations of source depositional environments. I.e the significance of the various parameters in terms of source depositional environment commonly accepted is not valid in the present case. The distribution of bicadinanes also has the potential to discriminate between the sample-groups, but hint at a compositional relationship between the oils in the northern area, and the northernmost field sampled in the central area. This is further substantiated by the preponderance of 5(4 \Rightarrow 3)abeo-3 α (H), 5 β (H), 18 α (H)-oleanane (Nytoft et al., 2010) in samples from the northern area and the northernmost field sampled in the central area. This compound is present in low proportions only in other samples from the central area and is essentially absent from samples collected in the southern area.

5. Conclusions

Based on analysis of a sample set from the Salin basin it has proven possible to add further insight to the results previously published by Curiale et al. (1994):

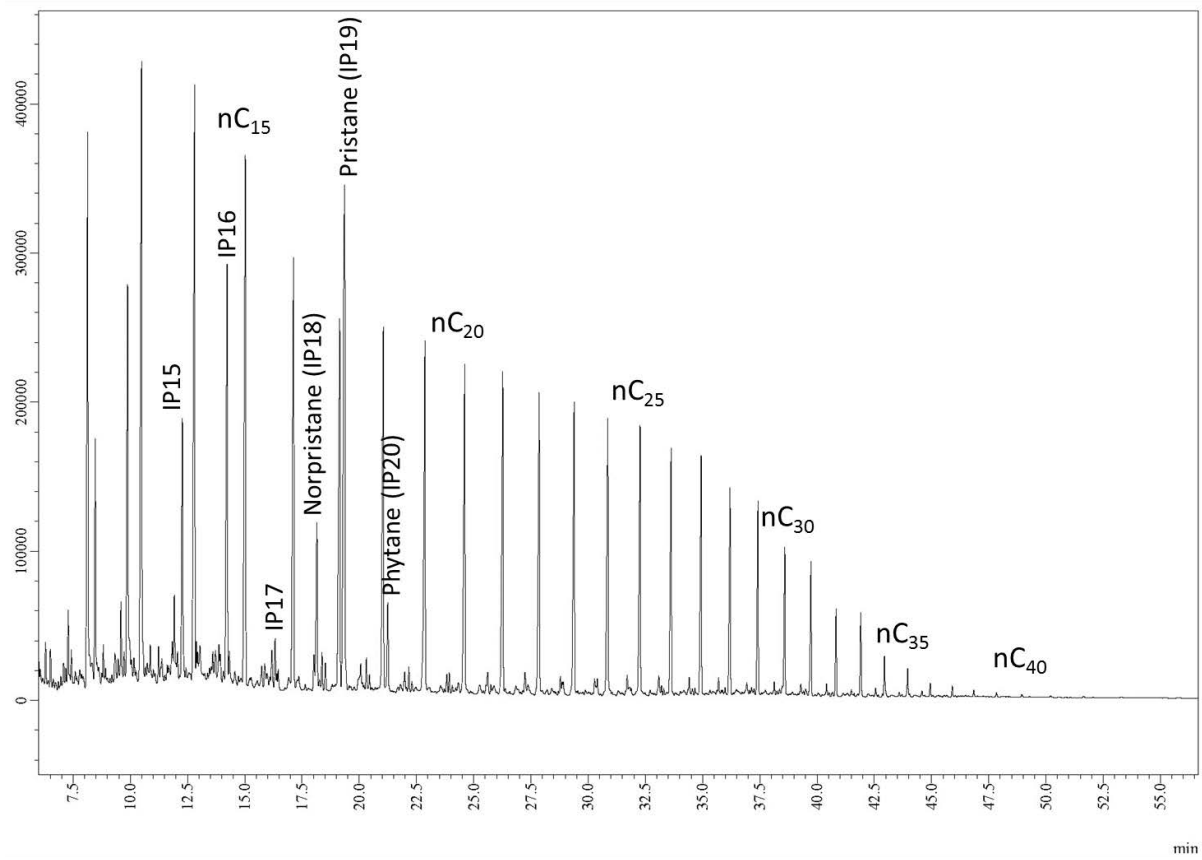
- The general conclusions of Curiale et al. (1994) can be confirmed:
 - the oils in the Salin Basin belong to one single family
 - the oils are essentially terrigenous in origin
 - the oils primarily differ with respect to their level of biodegradation
- The proposed exploration model of Curiale et al. (1994) can neither be confirmed nor contested by the new data reported herein.
- The data reported herein add the following new insights:
 - A gradient in thermal maturity exists, increasing from North to South across the Salin Basin. This is shown by both sterane and triterpane biomarker thermal maturity indicators
 - Hence, the three geographical areas covered by samples can be clearly distinguished in terms of thermal maturity
 - Uncorrelated to the level of thermal maturity and biodegradation, subtle variations in petroleum composition allow the three said geographical areas to be distinguished.
 - This distinction can be achieved through a combination of a variety of biomarker-derived parameters that include both cheilanthanes, unknown angiosperm derived tri- and tetracyclic compounds, bicadinanes, rearranged pentacyclic angiosperm higher land plant markers of the oleanane family and isohomohopanes in addition to commonly used sterane and hopane markers.
 - The distinction is, however, a “fingerprint” only, since the various parameters are not consistent in terms of marine versus terrigenous predominance in the source-rock kerogen.
 - One important reason for this is that the differences in various parameters that serve to discriminate between sample-groups are, albeit consistent, subtle and small, which precludes their normal use as facies indicators.
 - A secondary reason is probably the effect of multiple sources contributing to both pooled and seeping oils. Each contributing unit will show different concentrations and distributions of biological marker compounds, leading to contradictory indications of predominant source rock type in the resulting oil accumulations.
- The results obtained show good promise for a continuation of the study to include oil and source rock samples from other areas of Myanmar, pending procurement of necessary funding.
- Provided a larger set of samples can be procured in the future a classification based on multivariate statistics will be considered.

6. References

- Curiale, J.A., Pe Kyi, I., Collins, I.D., Din, A., Nyein, K., Nyunt, M. & Stuart, C.J. 1994: The central Myanmar (Burma) oil family--composition and implications for source. *Organic Geochemistry* 22, 237–255,
- Goswami, B.G., Bisht, R.S., Bhatnagar, A.K., Kumar, D., Pangtey, K.L., Mittal, A.K., Goel, J.P., Datta, G.C., Thomas, N.J., 2005. Geochemical characterization and source investigation of oils discovered in Khoraghat–Nambar structures of the Assam-Arakan Basin, India. *Organic Geochemistry* 36, 161–181.
- Holba, A. G., Dzou, L. I. P., Masterson, W. D., Hughes, W. B., Huizinga, B. J., Singletary, M. S., Moldowan, J. M., Mello, M. R. and Tegelaar, E., 1998: Application of 24-norcholestanes for constraining source age of petroleum. *Organic Geochemistry* 29, 1269–1283.
- Murray, A.P., Summons, R., Boreham, C.J. & Dowling, L.M. 1994: Biomarker and n-alkane isotope profiles for Tertiary oils: relationship to source rock depositional setting. *Organic Geochemistry* 22, 521–542
- Nytoft, H.P. 2011: Novel side chain methylated and hexacyclic hopanes: Identification by synthesis, distribution in a worldwide set of coals and crude oils and use as markers for oxic depositional environments. *Organic Geochemistry* 42, 520–539
- Nytoft, H.P., Kildahl-Andersen, G. & Rise, F. 2016: Unusual hexacyclic oleananes in Late Cretaceous/Tertiary terrigenous oils: NMR characterisation of the major hexacyclic oleanane in Niger Delta oil. *Organic Geochemistry* 101, 196–206
- Nytoft, H.P., Kildahl-Andersen, G., & Samuel, O.J. 2010: Rearranged oleananes: Structural identification and distribution in a worldwide set of Late Cretaceous/Tertiary oils. *Organic Geochemistry* 41, 1104–1118
- Peters, K. E., Walters, C. C. & Moldowan, J. M., 2005. The Biomarker Guide, volumes 1+2, 1155pp., Cambridge University Press.
- Radke, M., Wilisch, N. & Welte, D.H. 1980: Preparative Hydrocarbon Group Type Determination by Automated Medium Pressure Liquid Chromatography. *Analytical Chemistry*, 52, 406-411
- Ridd, M.F. & Racey, A. 2015: Onshore petroleum geology of Myanmar: Central Burma Depression. In: Racey, A. & Ridd, M.F. (eds): Petroleum Geology of Myanmar. Geological Society, London, Memoirs, vol. 45, p.
- Samuel, O.J., Kildahl-Andersen, G., Nytoft, H.P., Johansen, J.E., Jones, M., 2010: Novel tricyclic and tetracyclic terpanes in Tertiary deltaic oils: Structural identification, origin and application to petroleum correlation. *Organic Geochemistry* 41, 1326–1337

Appendix 1: Separation, n-alkane and acyclic isoprenoid data

Separation and Gas Chromatographic data



Compound identification key

Lab. #	Alt. name	Asphaltenes %	Saturates %	Aromatics %	Polars %
20150028-26919	548601	0,3	39,6	9,8	50,7
20150028-26920	548602	17,5	21,6	27,5	51,0
20150028-26921	548603	0,3	32,7	28,9	38,4
20150028-26922	548604	0,6	38,7	16,7	44,7
20150028-26923	548605	2,0	25,06	23,54	51,39
20150028-26924	548606	4,8	24,37	24,37	51,26
20150028-26925	548607	7,0	43,6	15,8	40,6
20150028-26926	548608	9,6	41,9	15,5	42,6
20150028-26927	548609	10,3	43,9	13,4	42,7
20150028-26953	CHK # 1101	6,7	48,5	16,5	35,0
20150028-26954	KKT	8,9	43,8	19,2	37,0
20150028-26955	Yng # 3241	6,1	45,5	17,5	37,0
20150028-26956	L # 110	5,8	44,9	17,3	37,9
20150028-26957	TSB-DT-1	39,2	24,0	27,9	48,1
20150028-26958	TGT # 9	12,6	44,4	19,2	36,4

Asphaltenes % = 100* Asphaltenes (mg) / total sample (mg)

Saturates % = 100* saturates / (saturates+aromatics+polars) by weight in asphaltene-free sample

Aromatics % = 100* aromatics / (saturates+aromatics+polars) by weight in asphaltene-free sample

Polars % = 100* polars / (saturates+aromatics+polars) by weight in asphaltene-free sample

Lab. #	Alt. name	Iso/nC	Pr/Ph	Pr/nC ₁₇	Ph/nC ₁₈	Bias	Wax	CPI	Norpristane %	Pristane %	Phytane %
20150028-26919	548601	0,66	7,89	1,68	0,23	1,84	0,28	1,04	18,1	72,7	9,2
20150028-26920	548602	1,24	2,88	5,28	1,18	1,99	0,25	1,19	12,3	65,1	22,6
20150028-26921	548603	2,39	5,44	5,24	1,23	1,76	0,3	1,05	20,1	67,5	12,4
20150028-26922	548604	0,38	6,79	0,92	0,15	2,11	0,21	1,02	20,9	69,0	10,2
20150028-26923	548605	n.d.	n.d.	n.d.	n.d.	n.d.	n.d.	n.d.	n.d.	n.d.	n.d.
20150028-26924	548606	n.d.	n.d.	n.d.	n.d.	n.d.	n.d.	n.d.	n.d.	n.d.	n.d.
20150028-26925	548607	0,53	7,16	1,39	0,19	1,55	0,28	1,02	19,1	71,0	9,9
20150028-26926	548608	0,46	7,12	1,13	0,16	1,74	0,25	1,03	19,9	70,3	9,9
20150028-26927	548609	0,47	7,48	1,25	0,18	1,81	0,26	1,02	18,9	71,5	9,6
20150028-26953	CHK # 1101	0,46	6,73	1,24	0,19	1,69	0,31	1,03	18,8	70,7	10,5
20150028-26954	KKT	1,06	7,5	3,65	0,51	0,88	1,03	1,1	14,4	75,5	10,1
20150028-26955	Yng # 3241	0,4	6,22	0,95	0,17	1,94	0,23	1,01	20,3	68,7	11,1
20150028-26956	L # 110	0,9	7,37	2,76	0,42	1,25	0,68	1,09	16,0	74,0	10,0
20150028-26957	TSB-DT-1	2,24	5,34	5,27	1,2	1,83	0,28	1,06	19,6	67,8	12,7
20150028-26958	TGT # 9	0,7	6,3	2,27	0,34	1,03	0,44	1,08	15,9	72,6	11,5

Iso/nC = C₁₅₋₂₀ linear isoprenoids / C₁₅₋₂₀ n-alkanes

Pr/Ph = pristane / phytane ratio

Pr/nC₁₇ = pristane / nC₁₇

Ph/nC₁₈ = phytane / nC₁₈

Bias = Sum(nC₁₅₋₂₂) / Sum (nC₂₃₋₃₀)

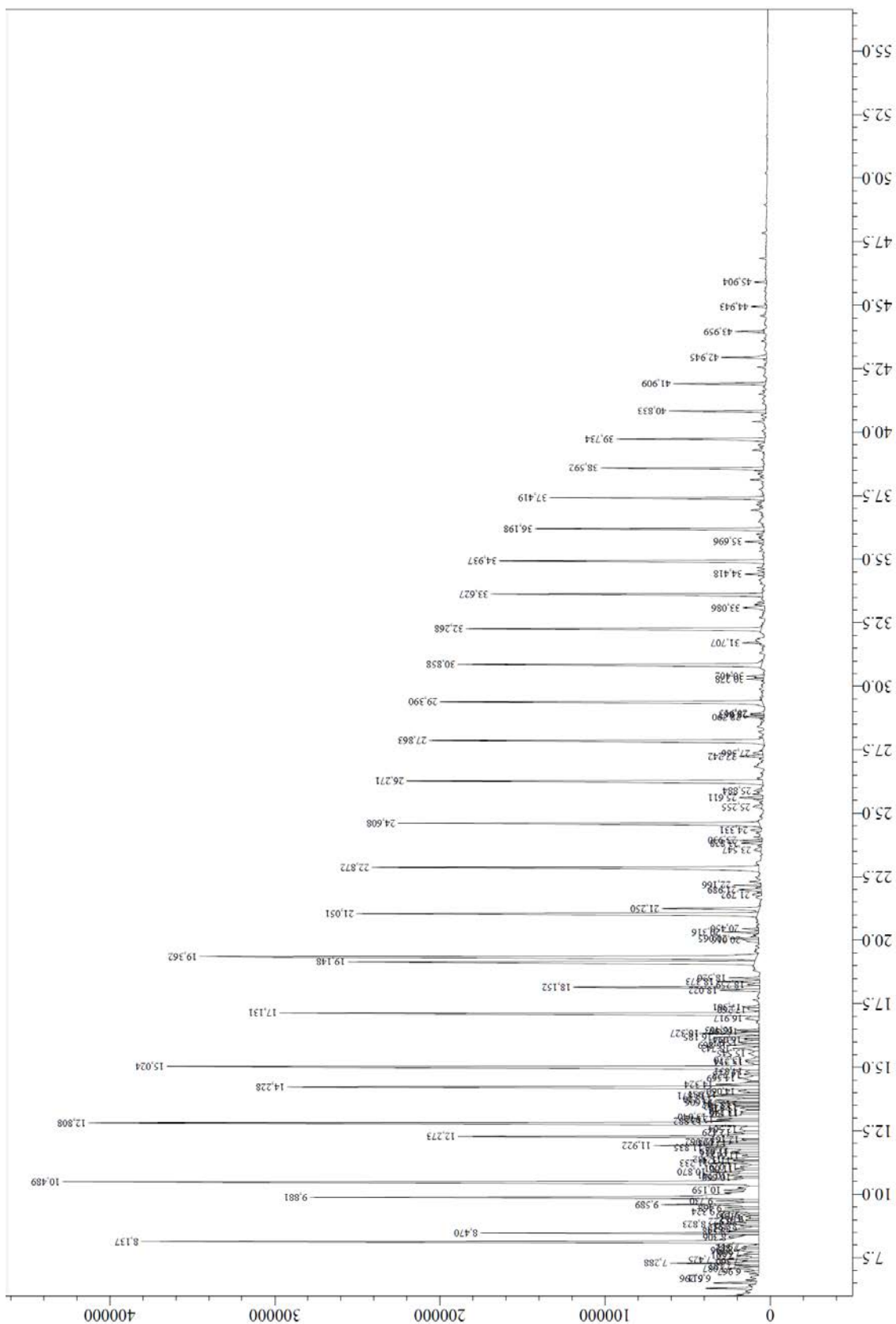
Wax = nC₃₁ / nC₁₉

CPI = Carbon Preference Index, $(2^*(nC_{21}+nC_{23}+nC_{25}+nC_{27}+nC_{29})+nC_{31}+nC_{19}) / (2^*(nC_{20}+nC_{22}+nC_{24}+nC_{26}+nC_{28}+nC_{30}))$

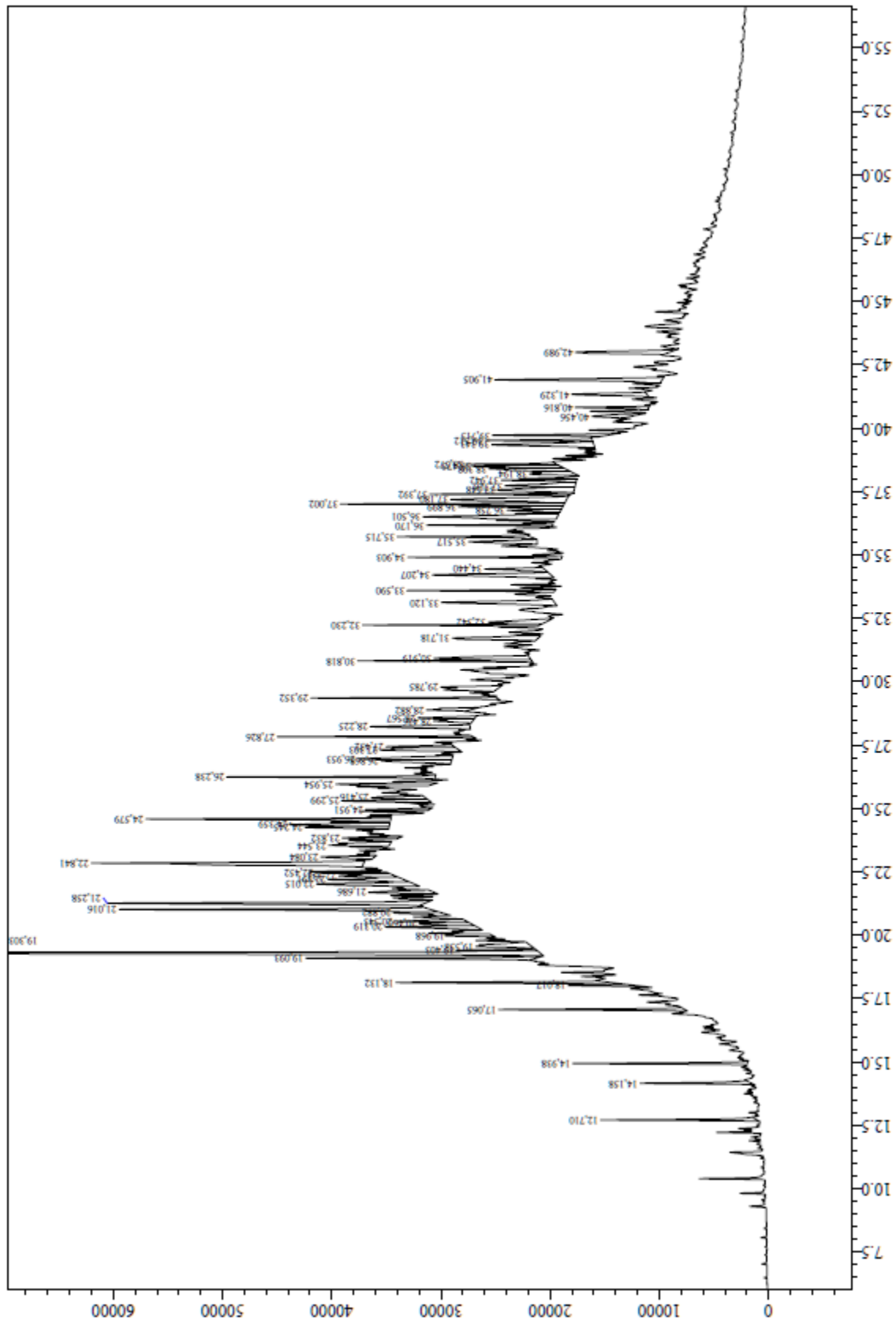
Norpristane % = 100* norpristane / (norpristane+pristane+phytane)

Pristane % = 100* pristane / (norpristane+pristane+phytane)

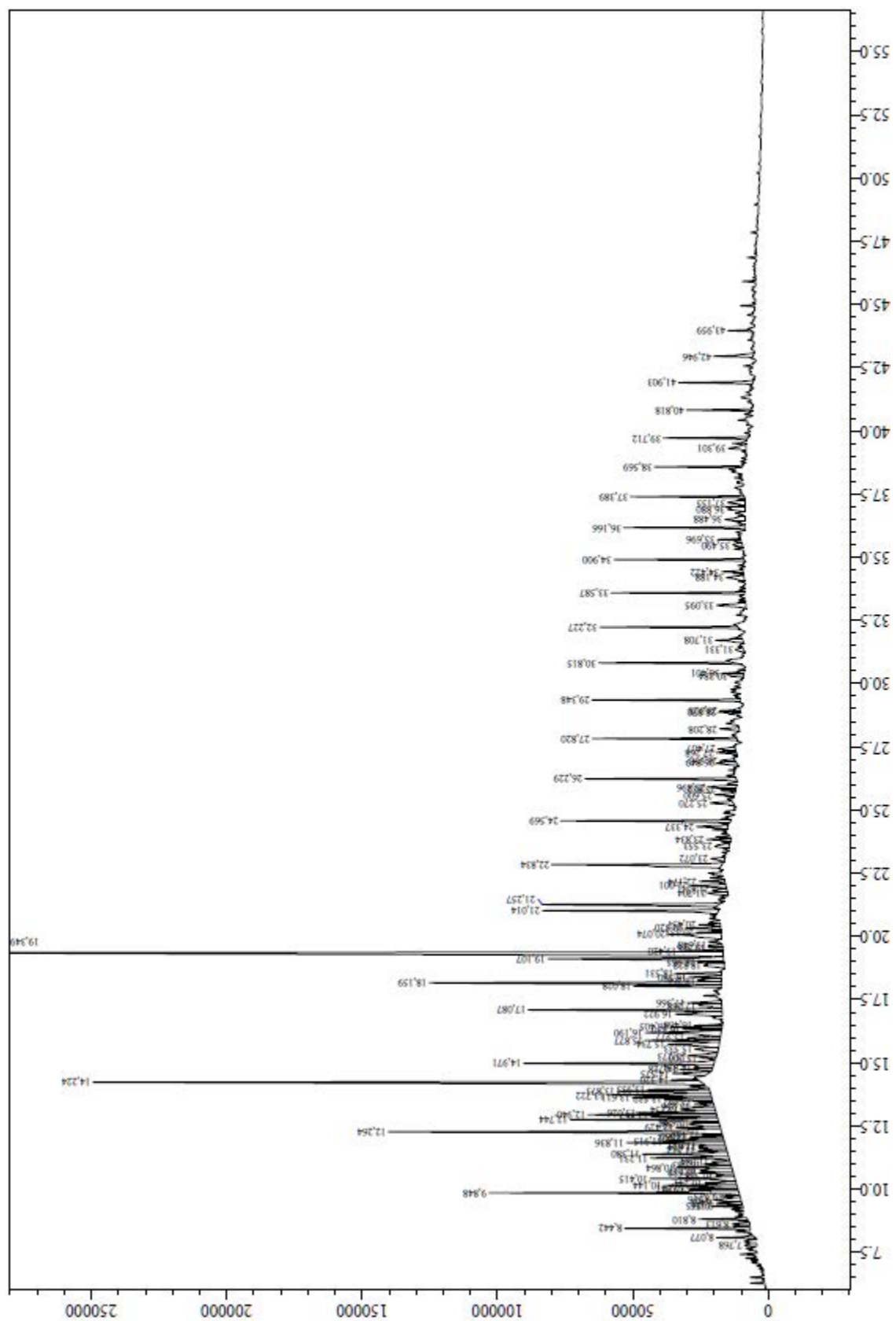
Phytane % = 100* phytane / (norpristane+pristane+phytane)



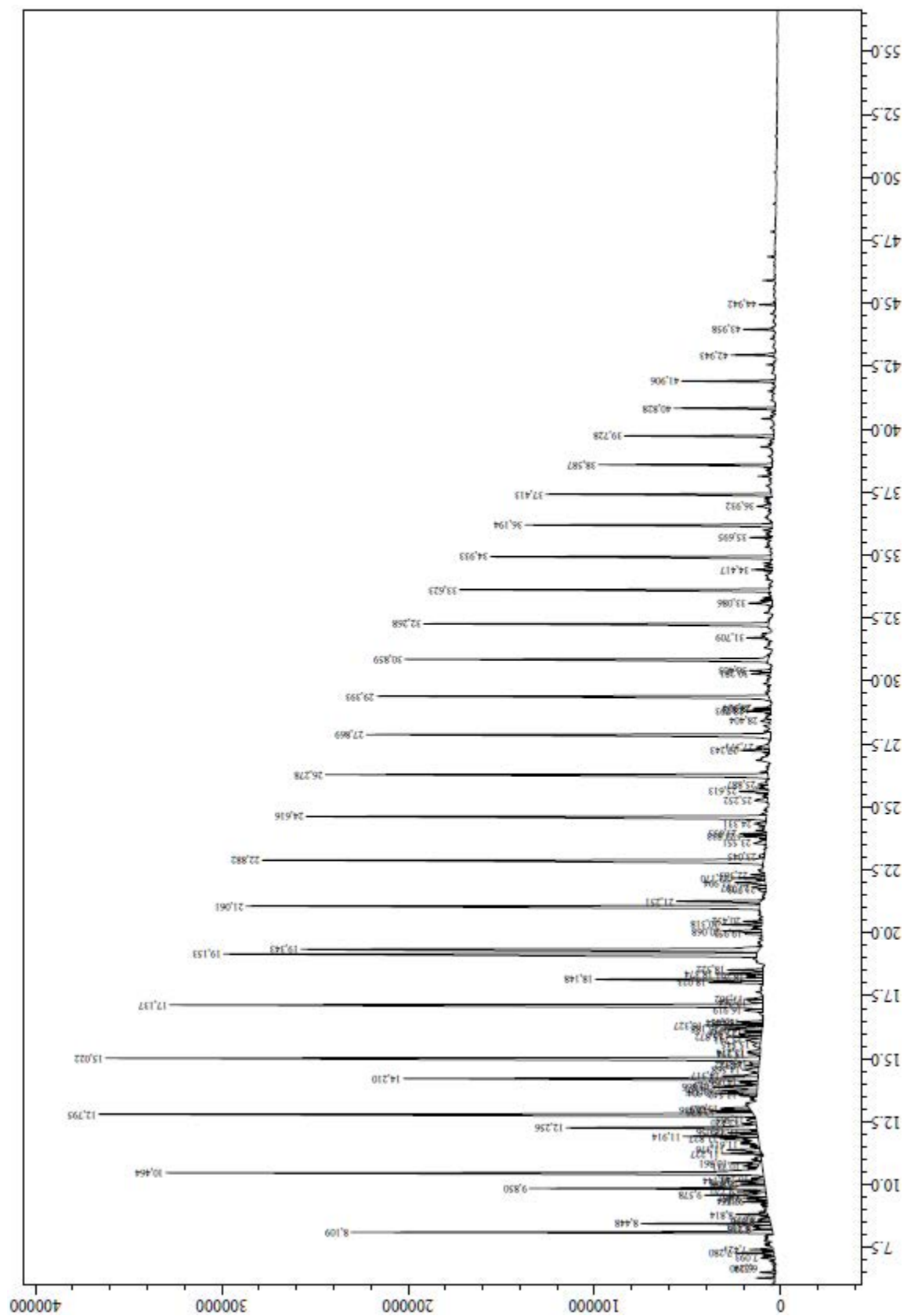
Sample 2015028-26919



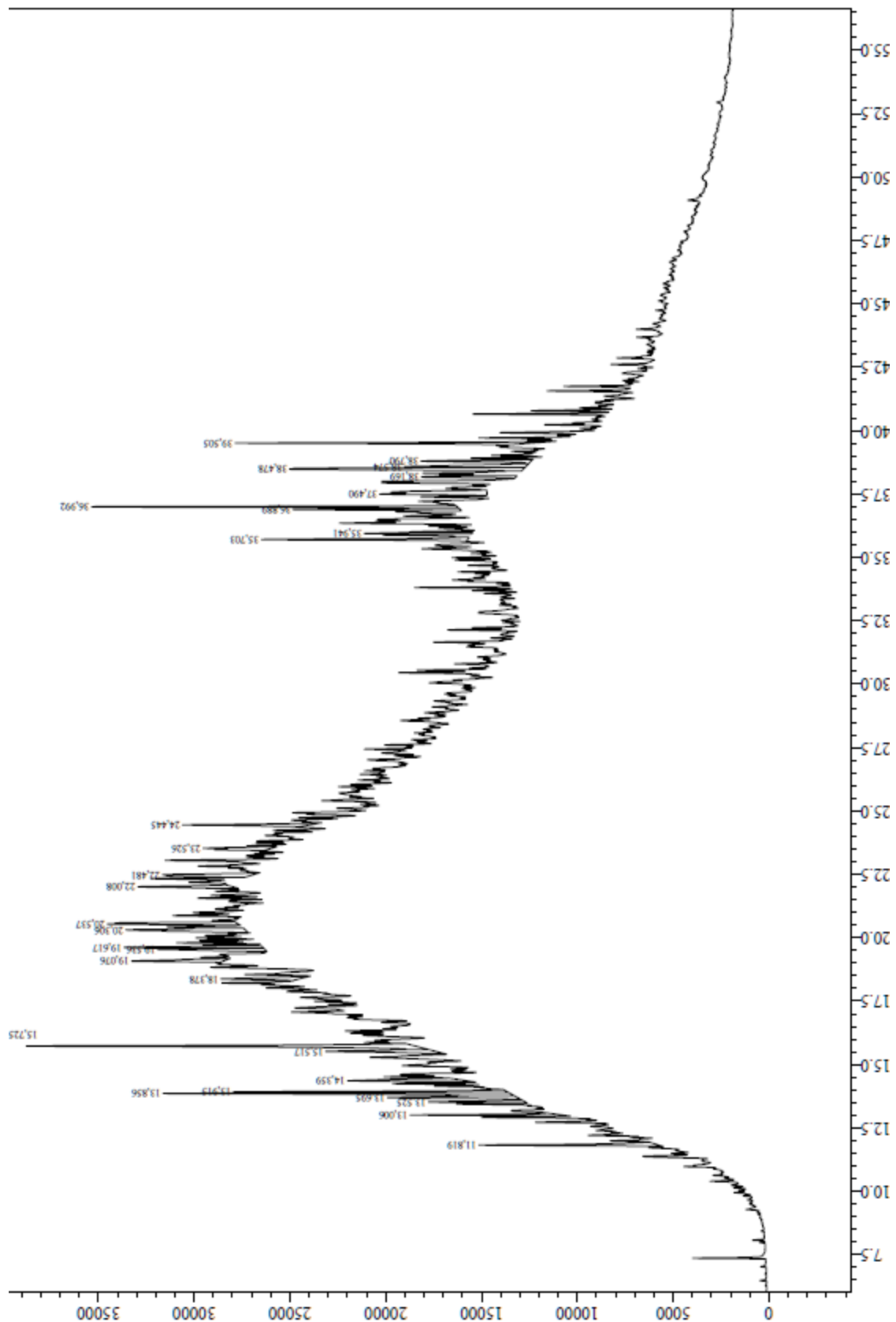
Sample 2015028-26920



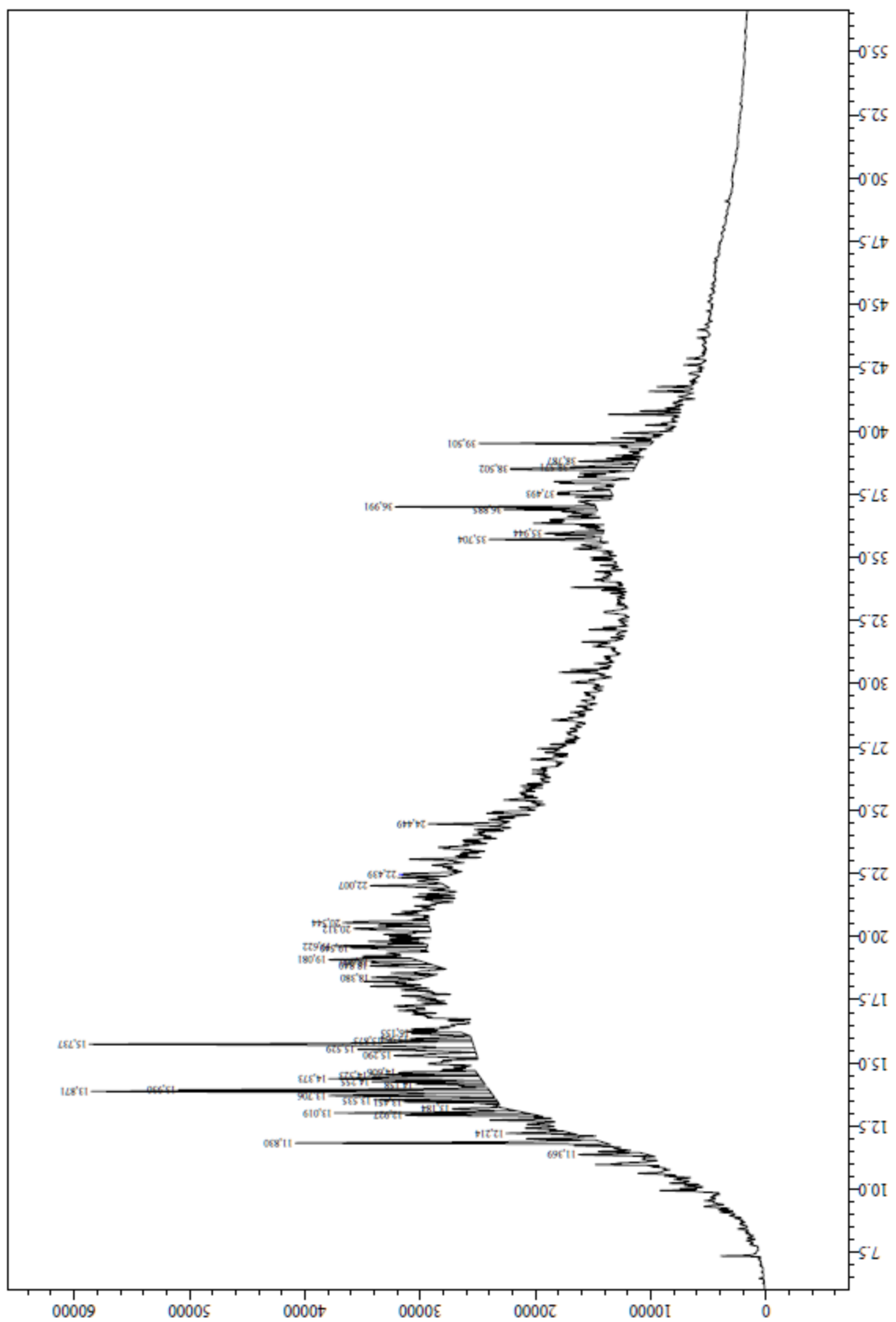
Sample 2015028-26921



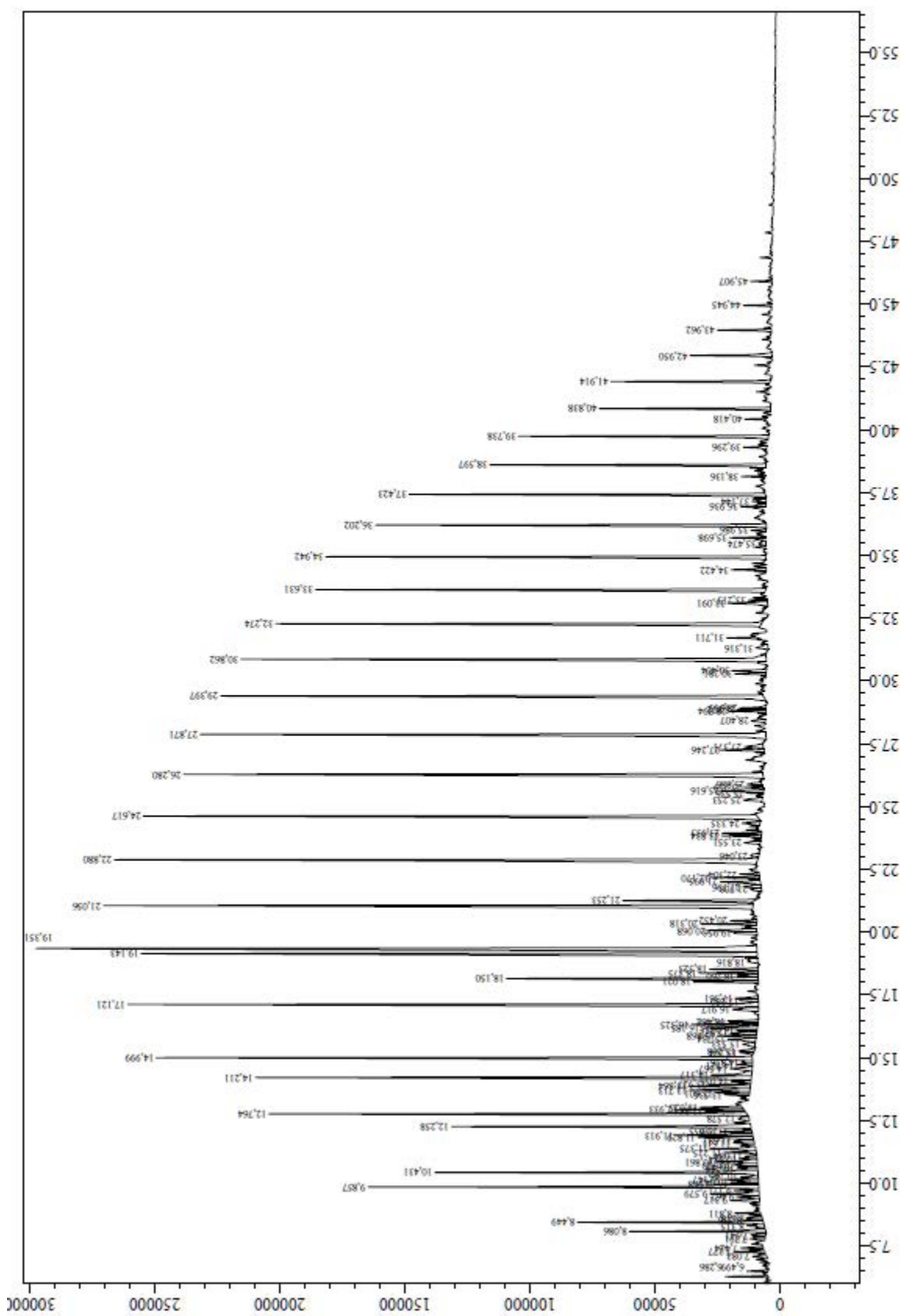
Sample 2015028-26922



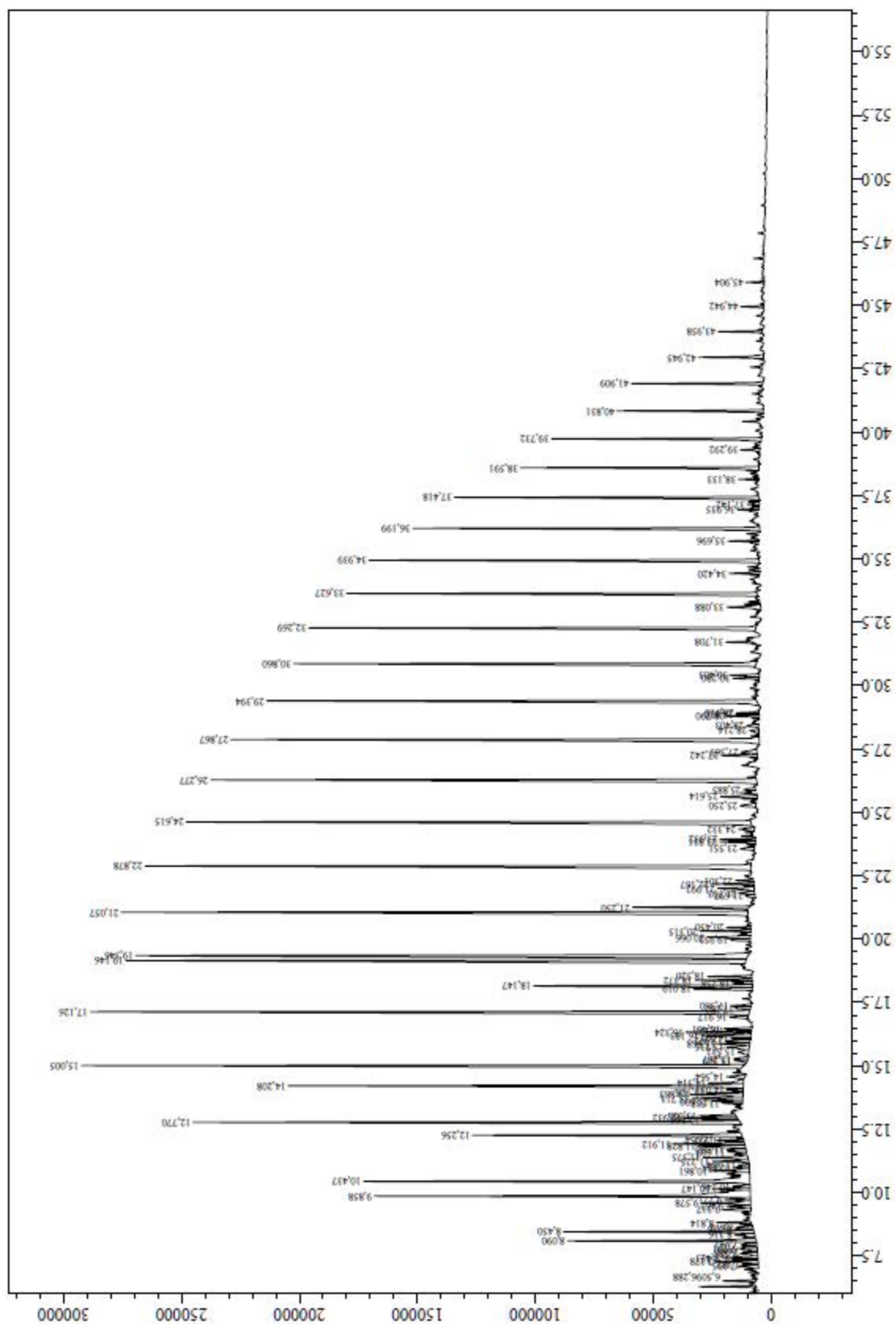
Sample 2015028-26923



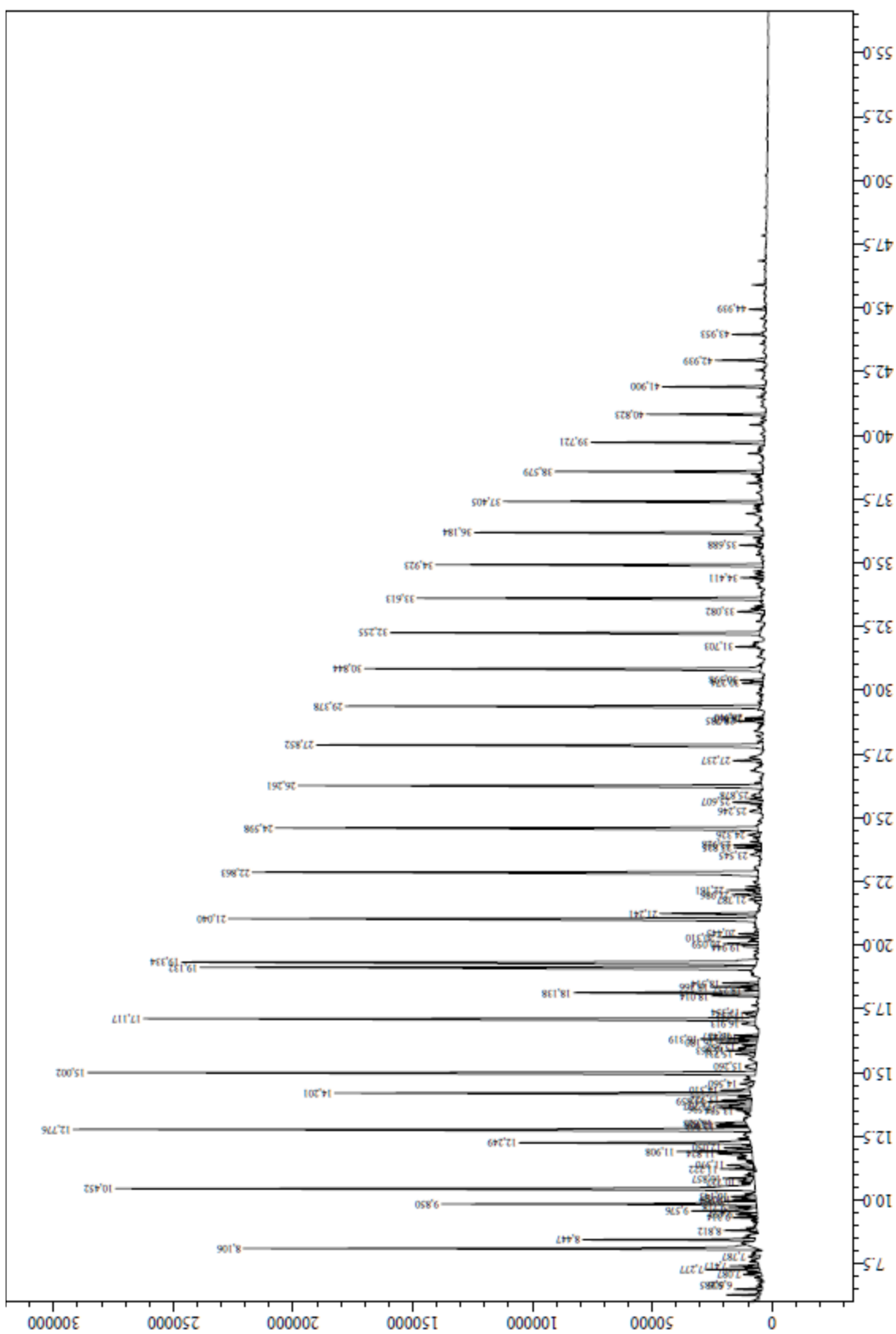
Sample 2015028-26924



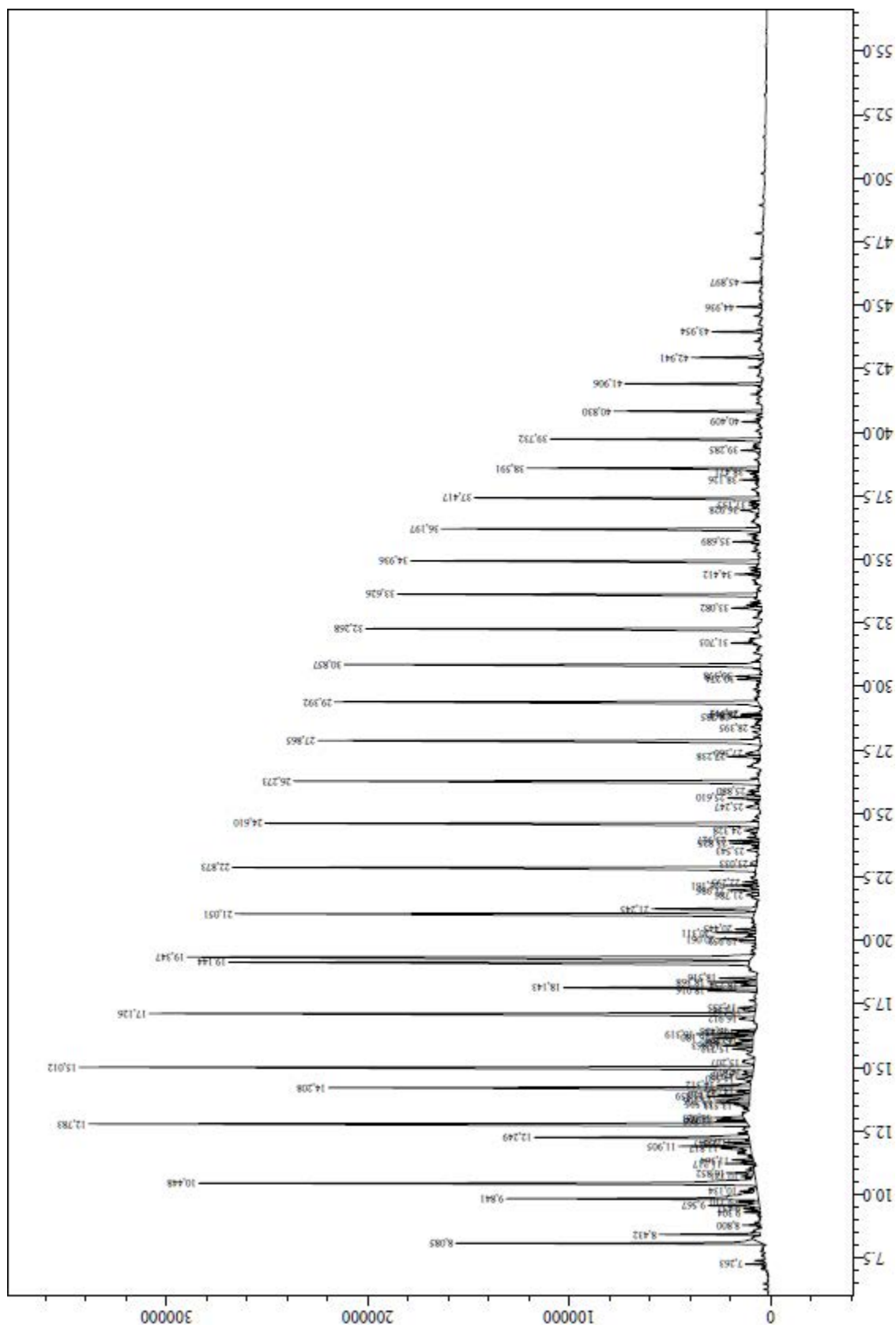
Sample 2015028-26925



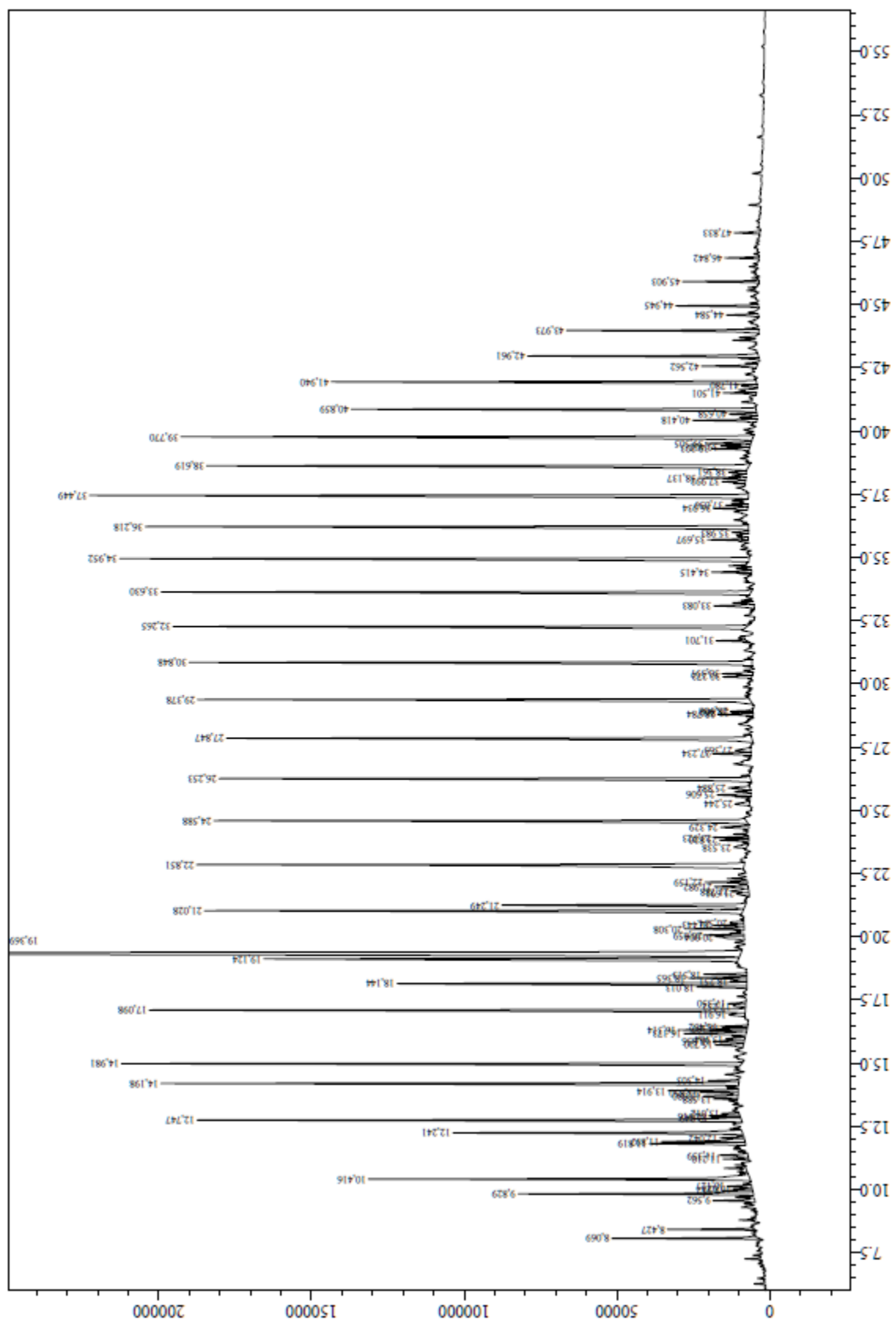
Sample 2015028-26926



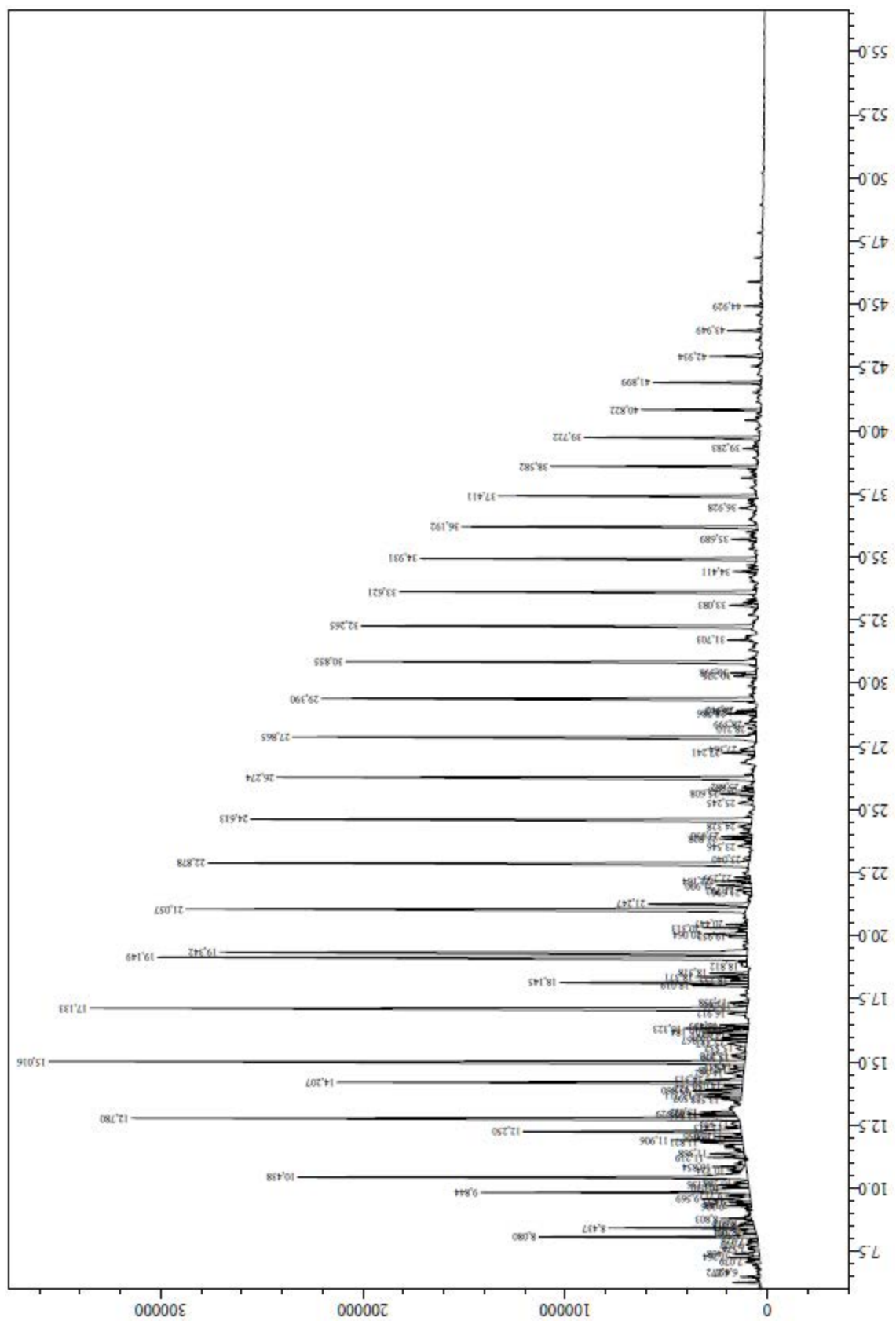
Sample 2015028-26927



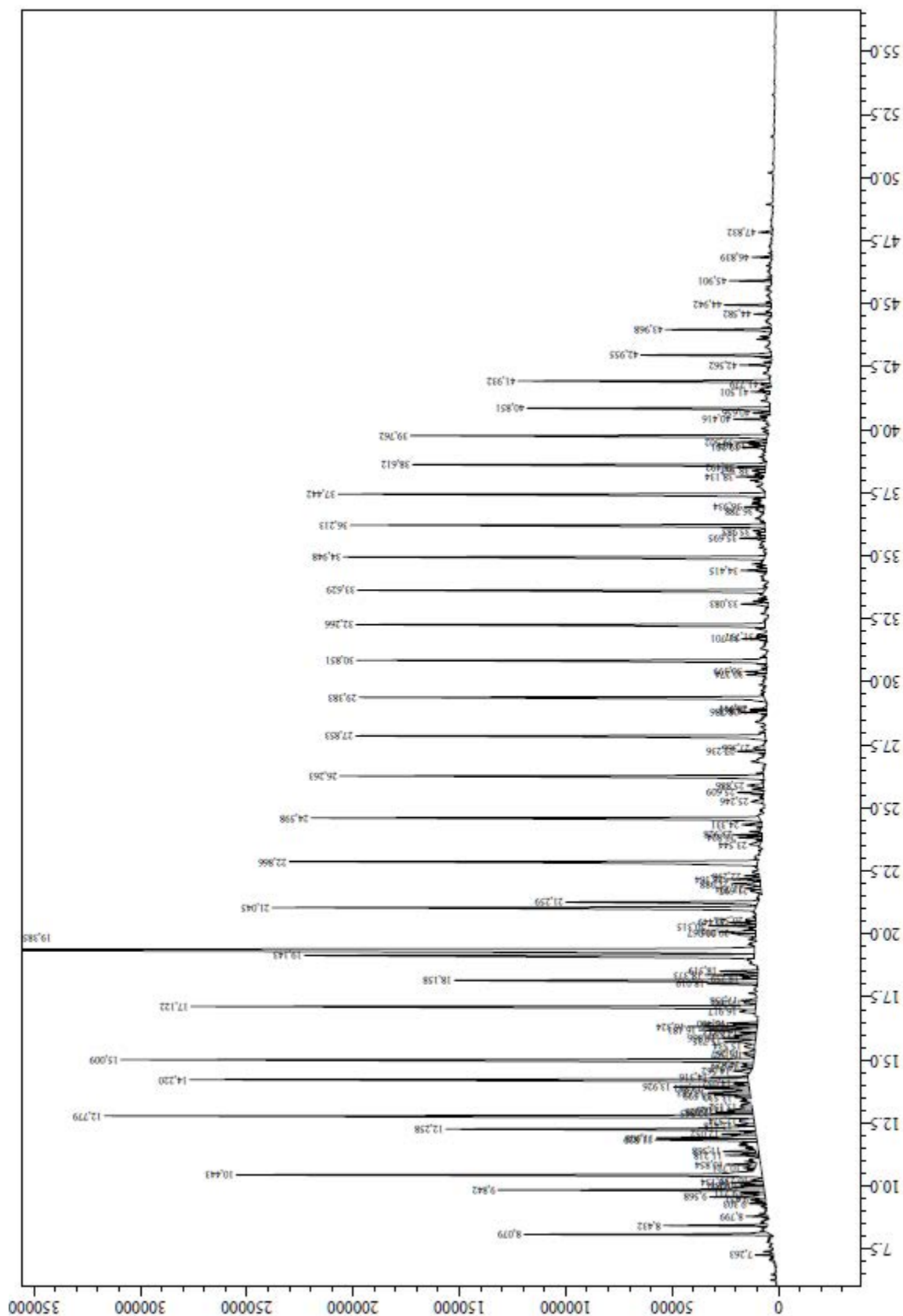
Sample 2015028-26953



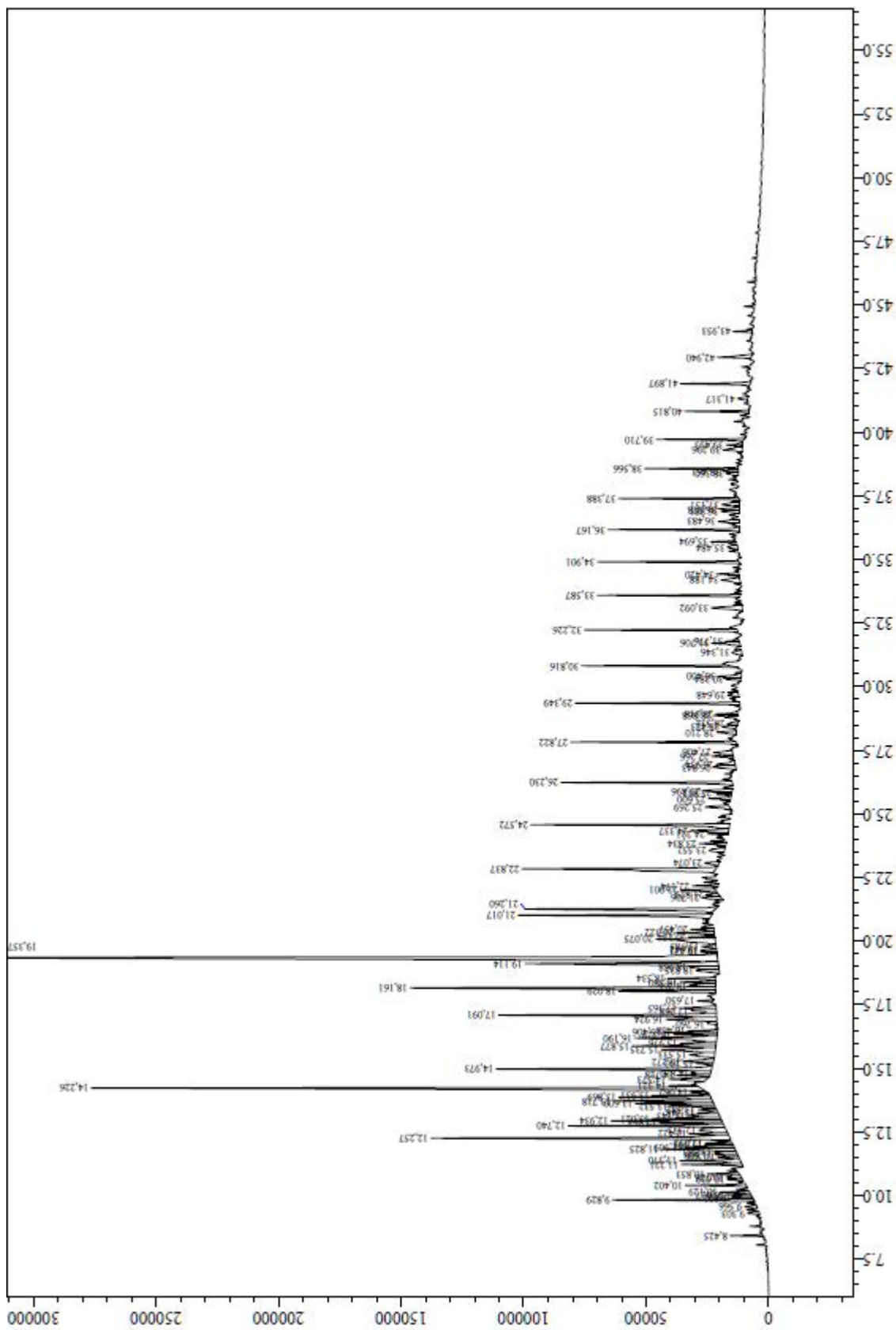
Sample 2015028-26954



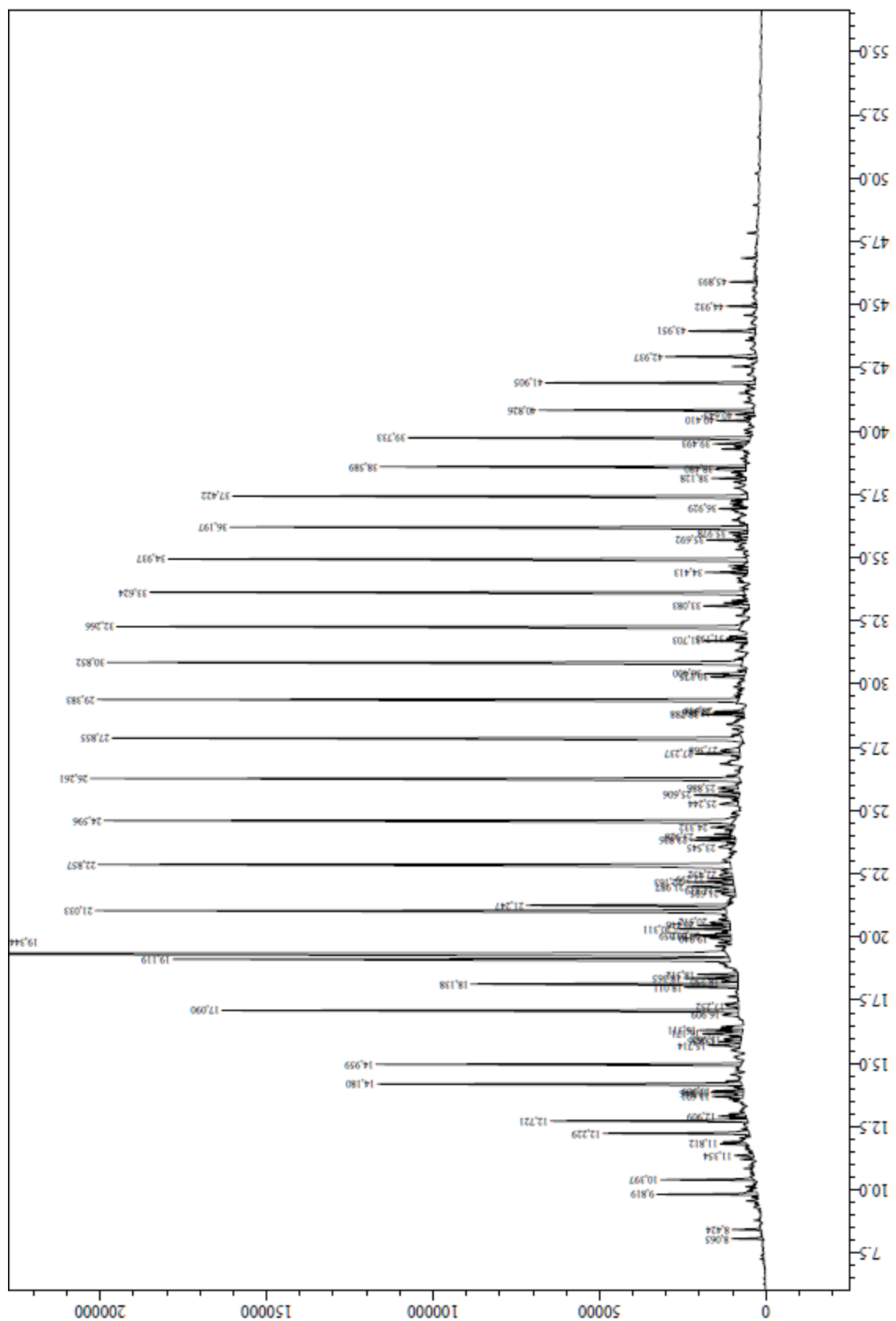
Sample 2015028-26955



Sample 2015028-26956



Sample 2015028-26957



Sample 2015028-26958

Appendix 2: Tri- and tetracyclic terpanes

GC-MS_{SIM} data

Lab. #	Alt. Lab. #	T/H30	T23/H30	T26/25	TE24 / H30	H31S / H30	%X	%Y	%Z	Angio / Hopane	Angio/T	X / (X+T20)	Y / (Y+T24)
20150028-26919	548601	0,44	0,03	1,20	0,17	0,30	22,60	45,82	31,58	0,21	0,48	0,24	0,77
20150028-26920	548602	0,70	0,06	1,31	0,17	0,24	33,56	45,56	20,87	0,68	0,97	0,51	0,87
20150028-26921	548603	0,55	0,03	1,14	0,15	0,20	30,71	46,54	22,76	0,45	0,83	0,45	0,87
20150028-26922	548604	0,86	0,07	1,12	0,23	0,23	29,61	46,00	24,39	0,72	0,85	0,43	0,86
20150028-26923	548605	0,37	0,02	1,51	0,11	0,22	28,36	48,00	23,64	0,29	0,78	0,39	0,89
20150028-26924	548606	0,47	0,03	1,76	0,13	0,22	29,13	47,12	23,75	0,34	0,73	0,40	0,87
20150028-26925	548607	0,53	0,04	0,95	0,20	0,23	26,06	46,45	27,49	0,42	0,79	0,37	0,87
20150028-26926	548608	0,58	0,05	0,87	0,20	0,23	27,15	46,47	26,39	0,48	0,82	0,39	0,87
20150028-26927	548609	0,44	0,03	1,10	0,19	0,24	21,80	48,90	29,30	0,30	0,68	0,30	0,86
20150028-26953	CHK # 1101	0,49	0,04	1,41	0,19	0,28	23,43	48,56	28,01	0,32	0,65	0,32	0,85
20150028-26954	KKT	0,16	0,02	0,97	0,07	0,39	15,36	56,36	28,29	0,19	1,19	0,37	0,88
20150028-26955	Yng # 3241	0,80	0,06	1,32	0,19	0,25	27,94	44,27	27,79	0,69	0,86	0,44	0,85
20150028-26956	L # 110	0,24	0,02	0,89	0,08	0,35	20,00	52,46	27,54	0,21	0,90	0,39	0,86
20150028-26957	TSB-DT-1	0,60	0,05	1,41	0,16	0,22	32,14	46,22	21,64	0,49	0,82	0,44	0,87
20150028-26958	TGT # 9	0,32	0,03	1,22	0,10	0,33	23,52	50,93	25,56	0,23	0,72	0,33	0,84

T/H30 = Ratio of total C₁₉₋₂₆ tricyclics (cheilanthanes) to C₃₀ hopane

T23/H30 = Ratio of C₂₃ tricyclic (cheilanthane) to C₃₀ hopane

T26/T25 = Ratio of C₂₆ tricyclic (cheilanthane) to C₂₅ tricyclic (cheilanthane)

Te24/H30 = Ratio of C₂₄ tetracyclic terpane to C₃₀ hopane

H31S/H30 = Ratio of C₃₁ homohopane-22S to C₃₀ hopane

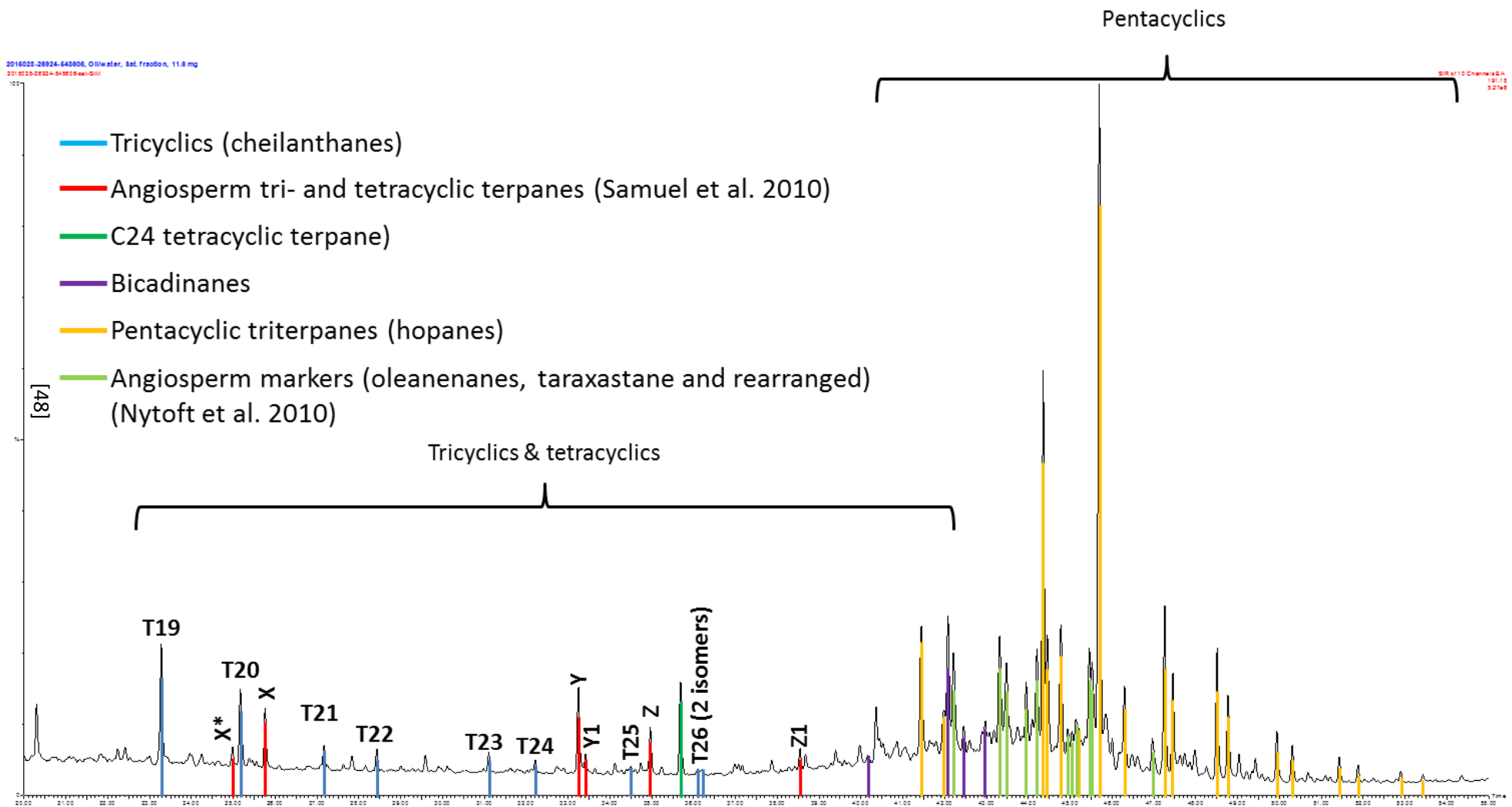
%X, %Y, %Z = Normalised distribution of tri and tetracyclic angiosperm-derived compounds described by Samuel et al (2010), all isomers.

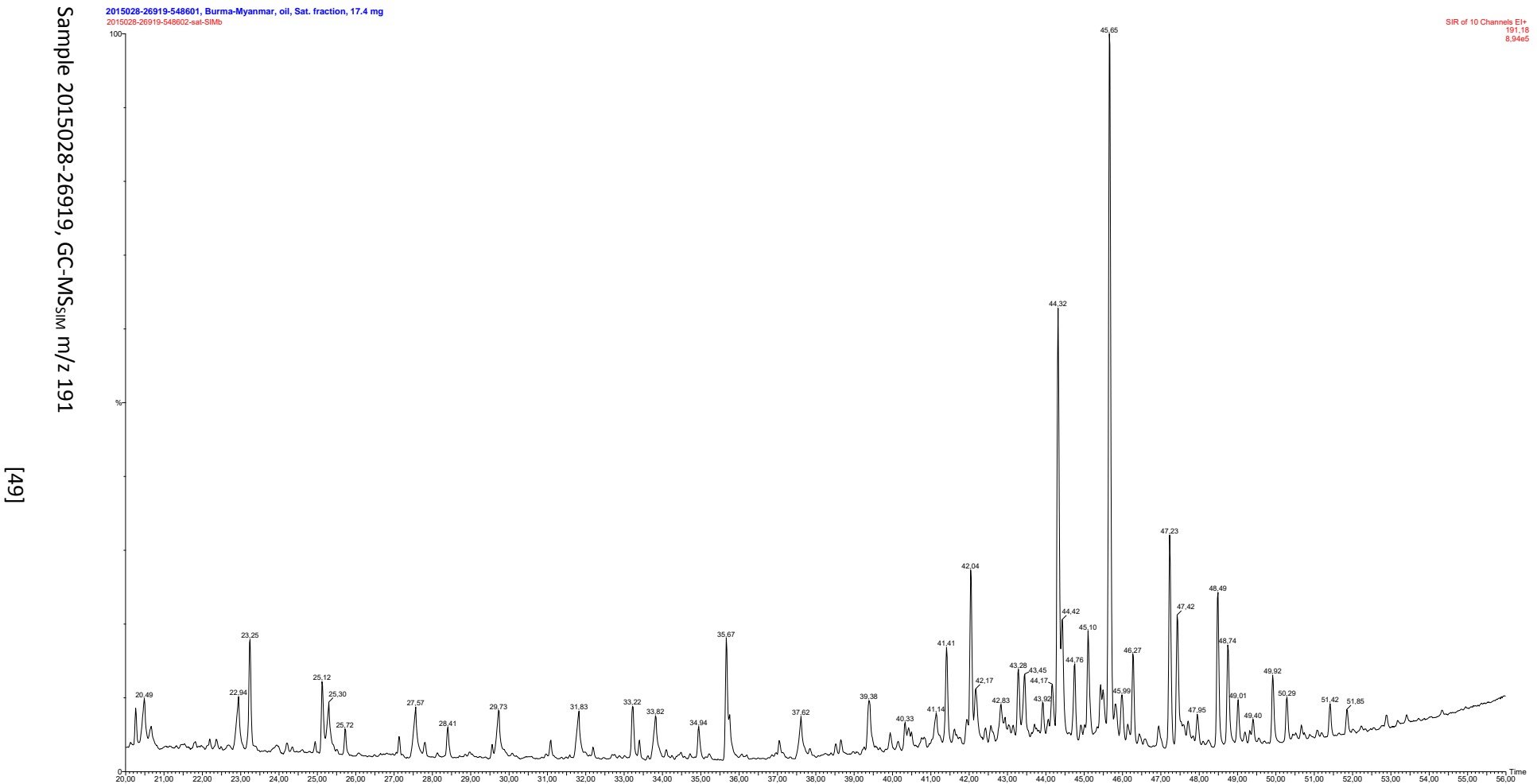
Angio/Hopane = Ratio of the sum of compounds X, Y, Z to hopane

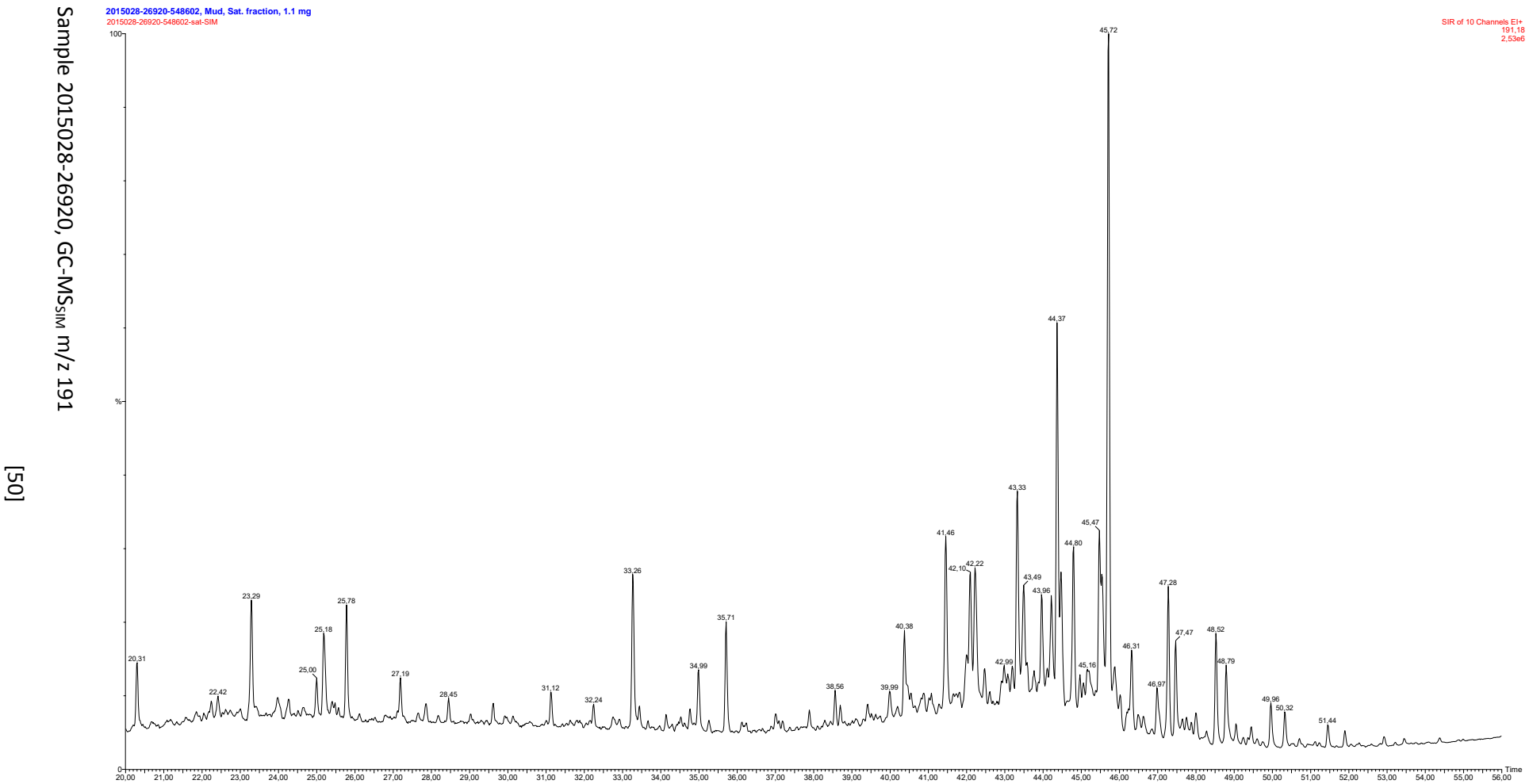
Angio/T = Ratio of the sum of compounds X, Y, Z to total C₁₉₋₂₆ tricyclics (cheilanthanes)

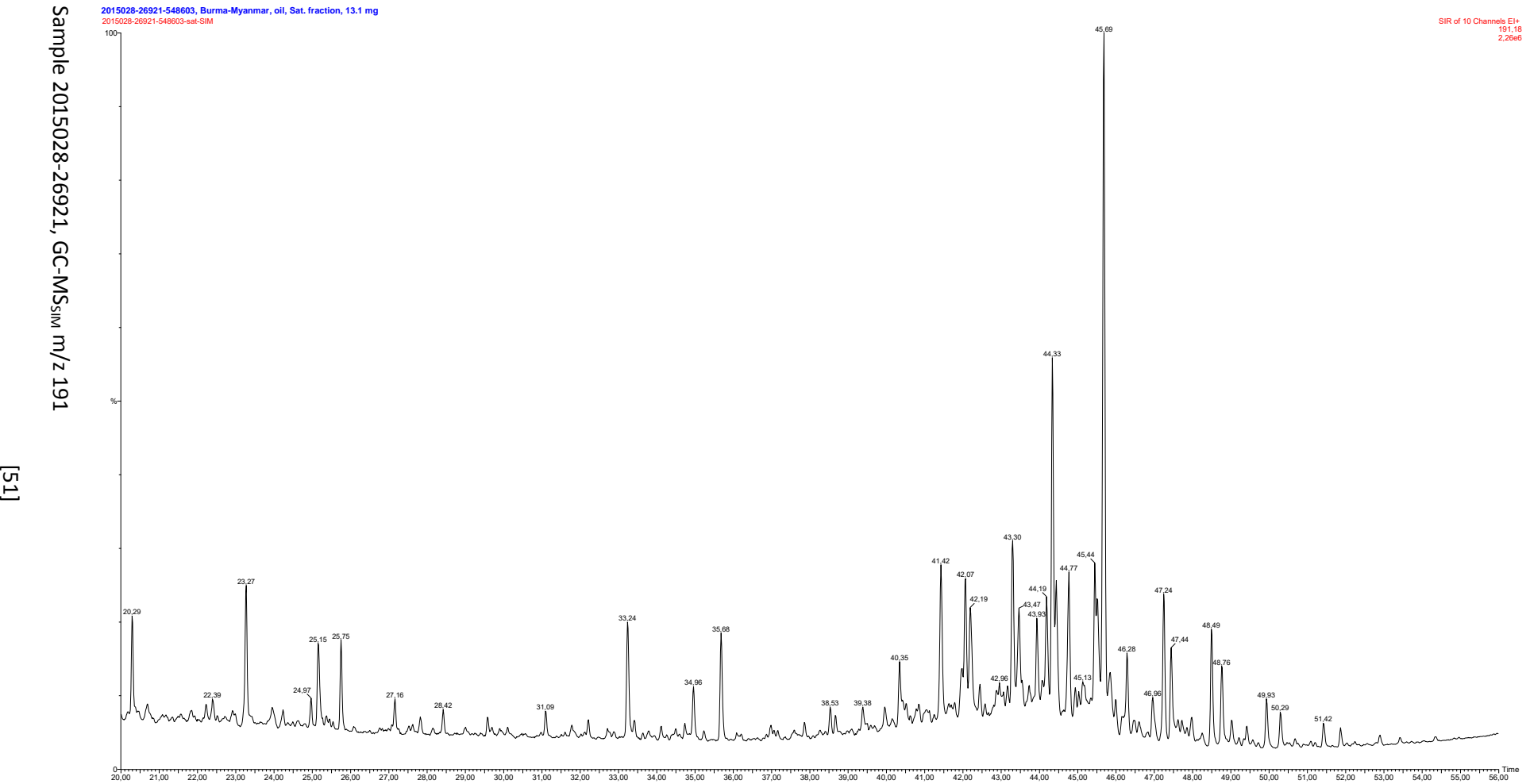
X/(X+T20) = Ratio of Compound X to the sum of Compound X plus C₂₀ tricyclic (cheilanthane). Ratio devised by Samuel et al. (2010)

Y/(Y+T24) = Ratio of Compound Y to the sum of Compound Y plus C₂₄ tricyclic (cheilanthane). Ratio devised by Samuel et al. (2010)



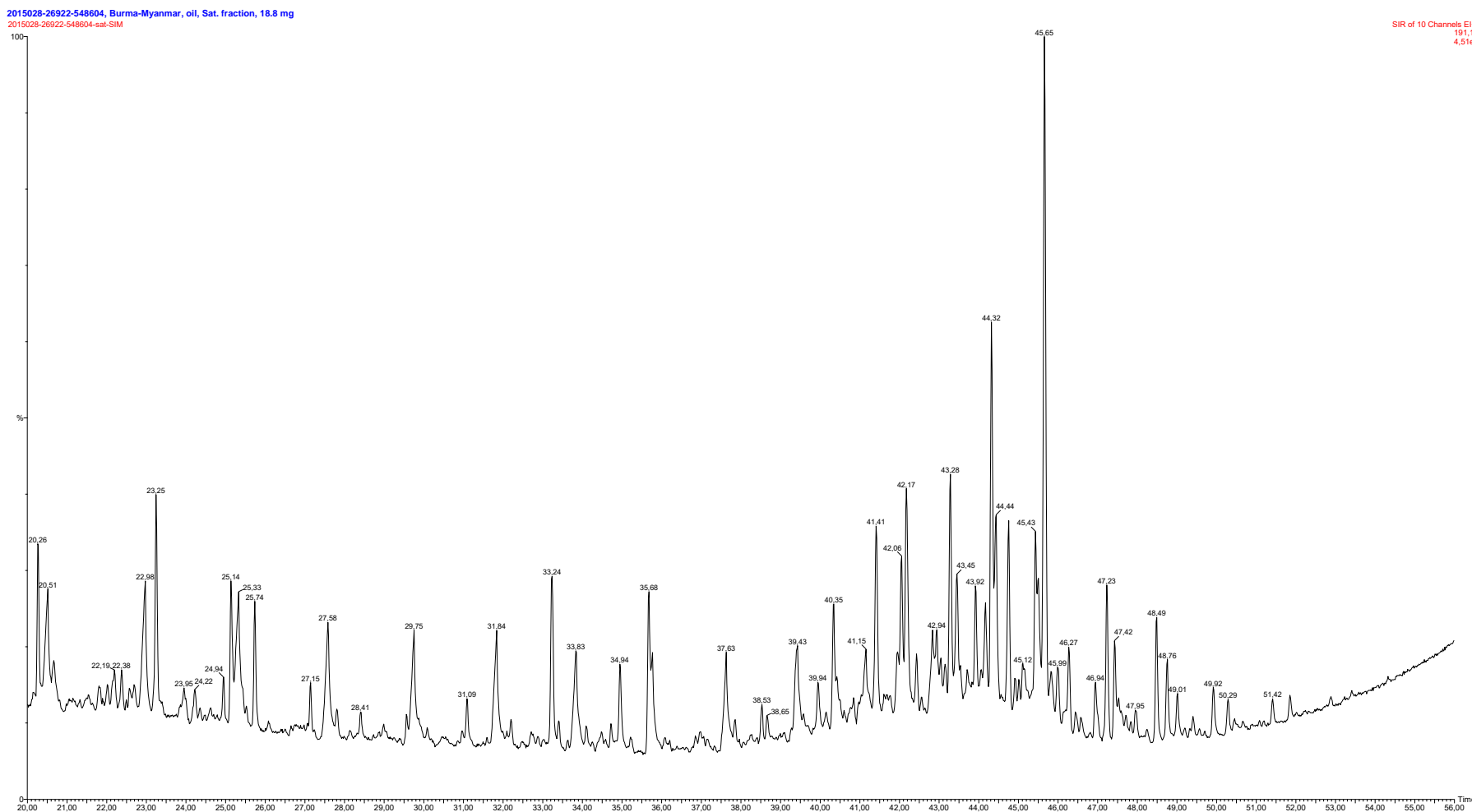






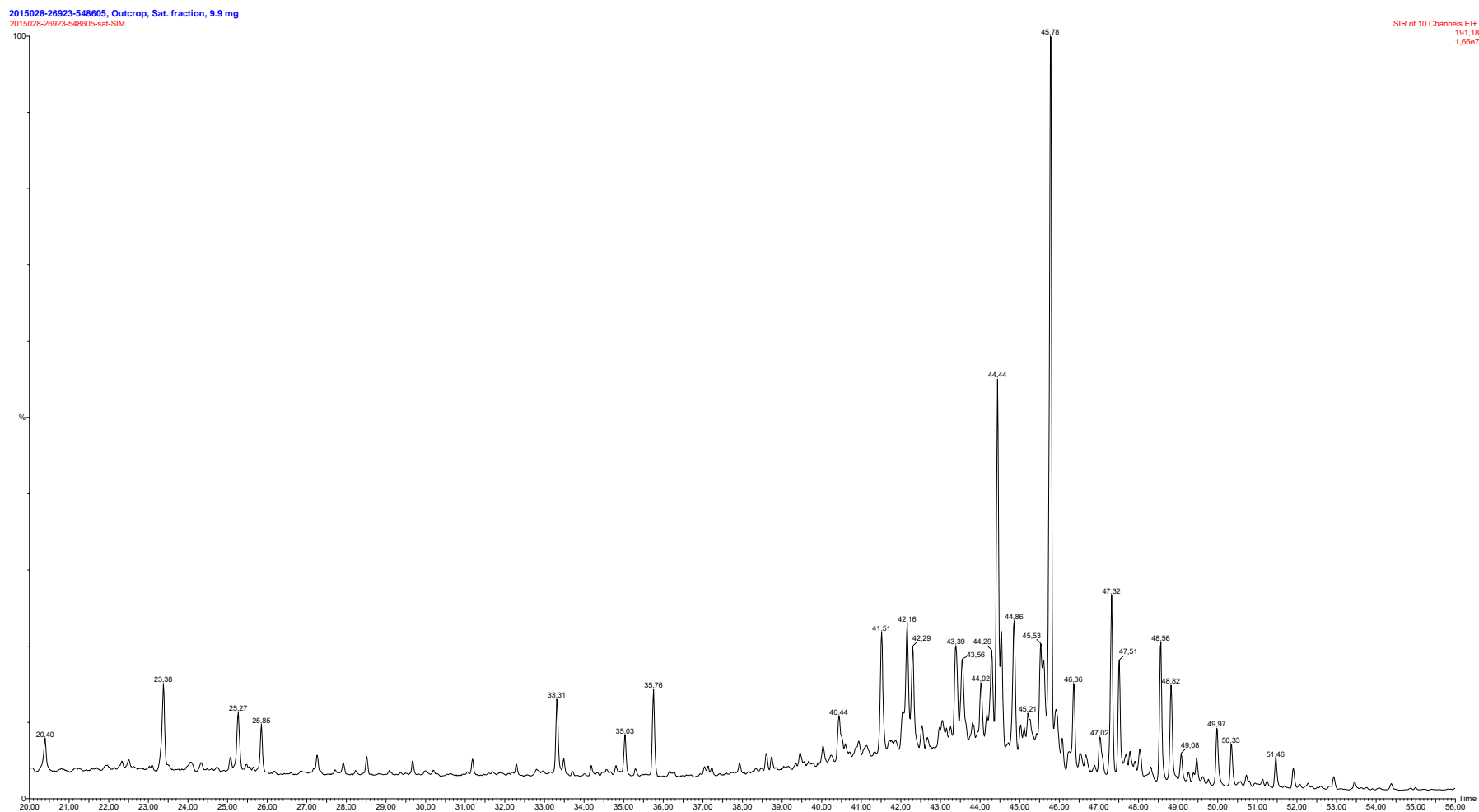
[52]

Sample 2015028-26922, GC-MS_{SIM} m/z 191



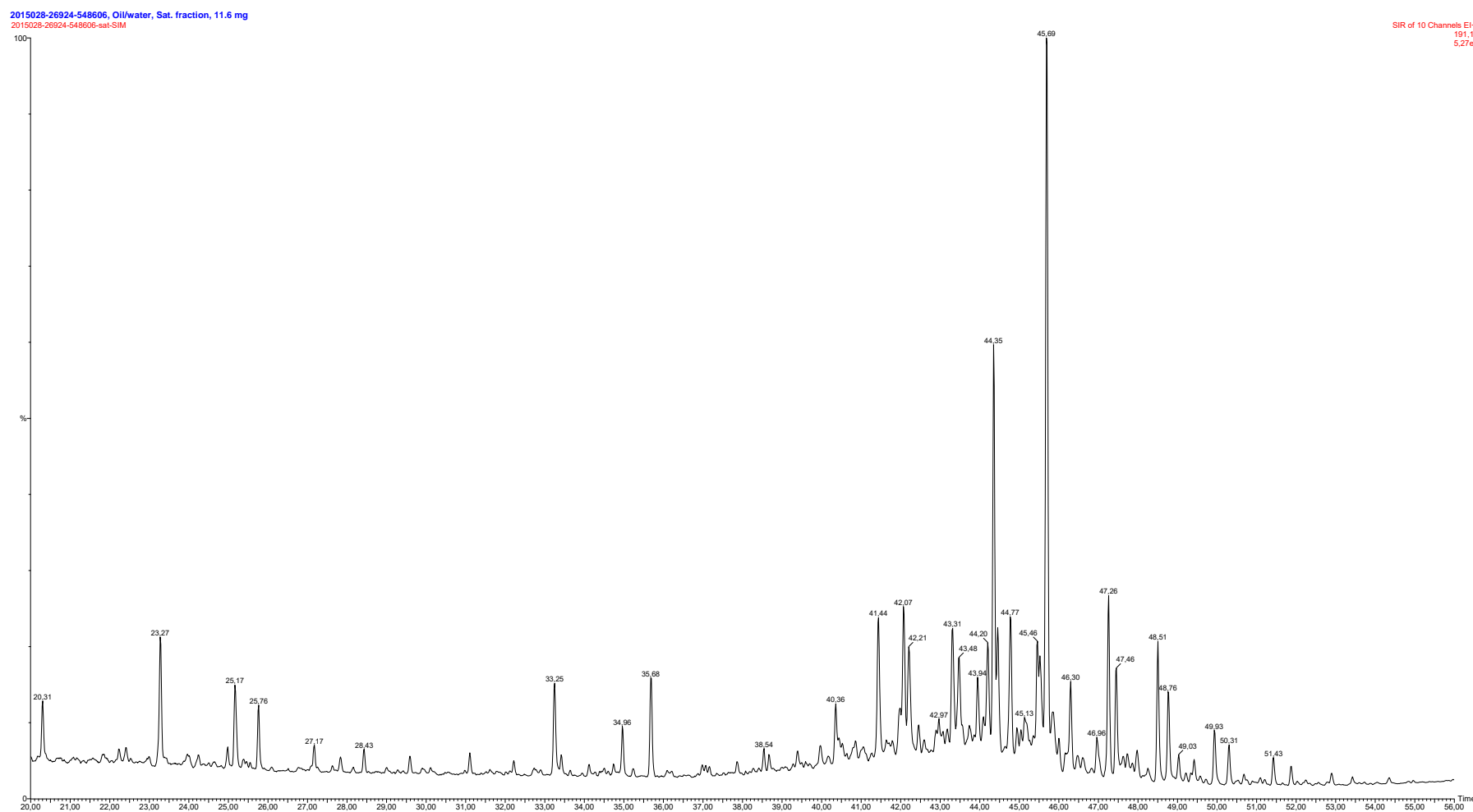
[53]

Sample 2015028-26923, GC-MS_{Sim} m/z 191



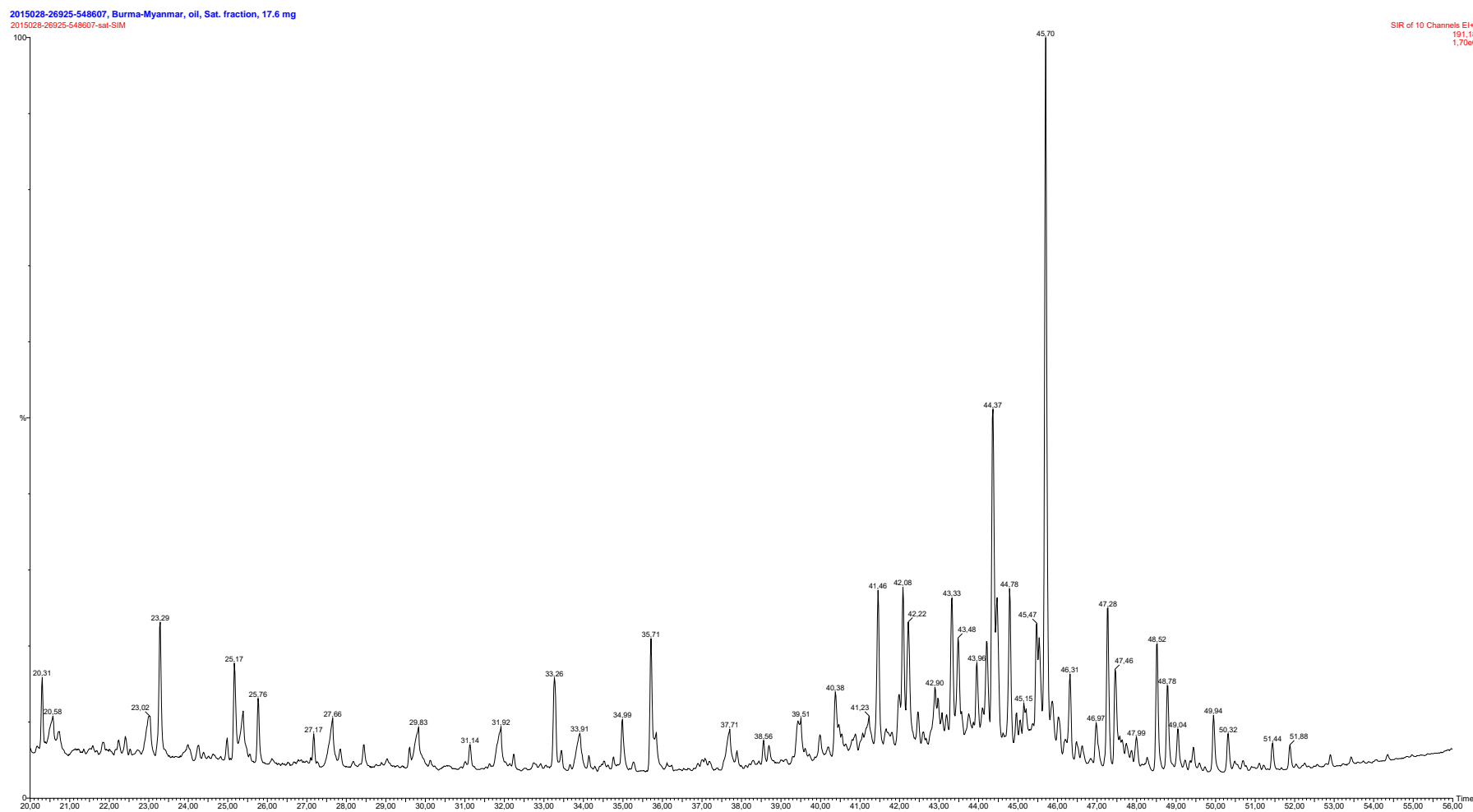
[54]

Sample 2015028-26924, GC-MS_{Sim} m/z 191



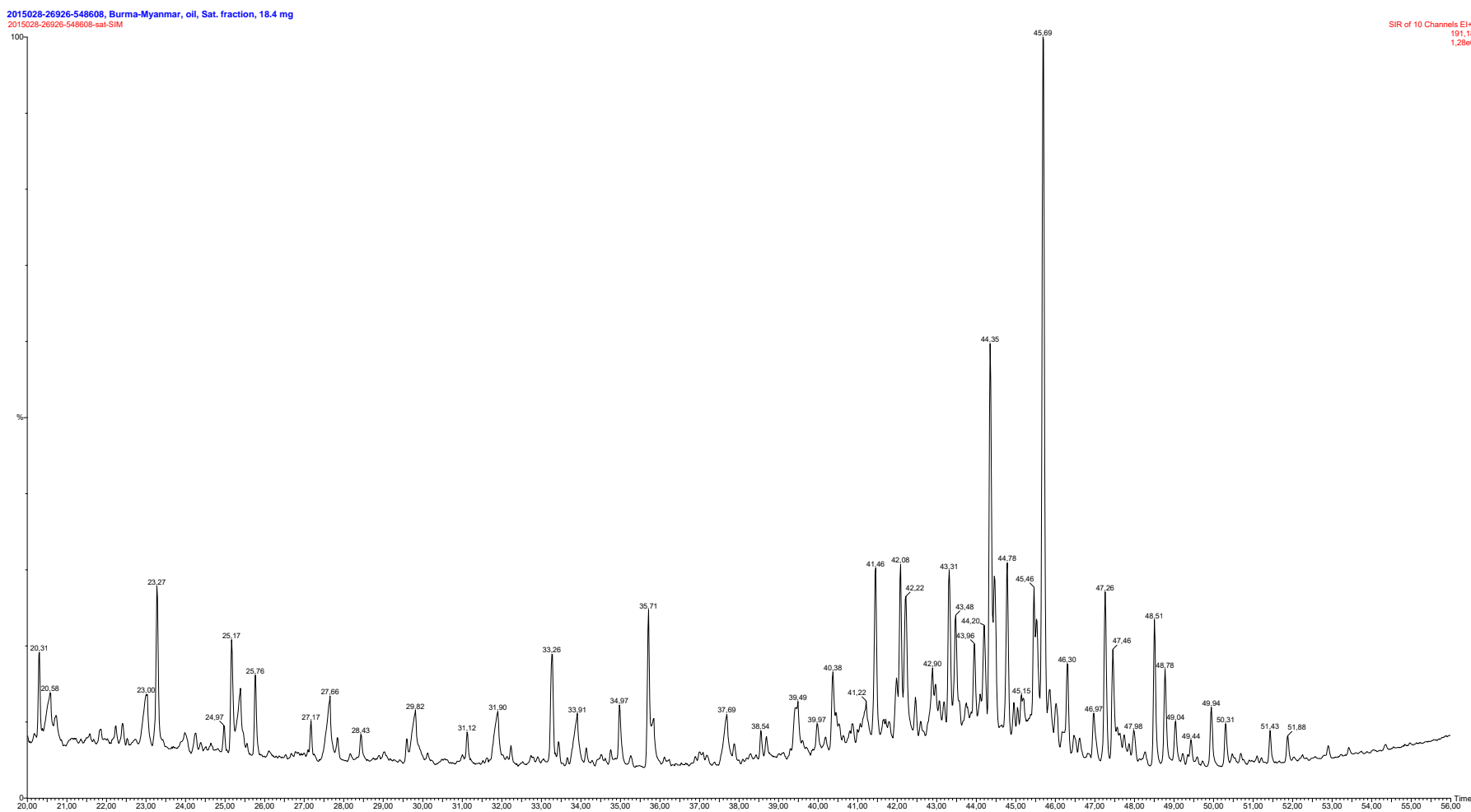
[55]

Sample 2015028-26925, GC-MS_{Sim} m/z 191



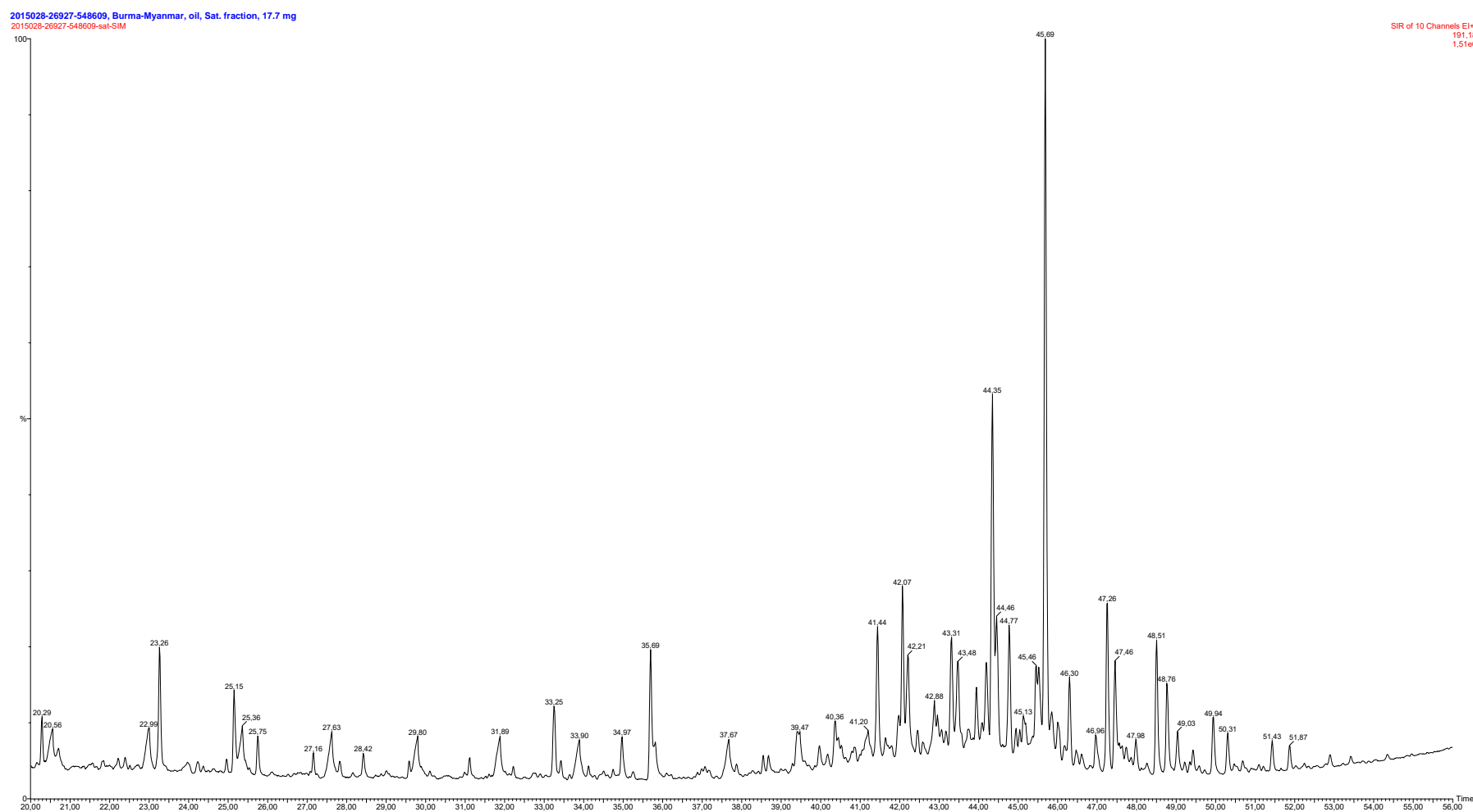
[56]

Sample 2015028-26926, GC-MS_{SIM} m/z 191



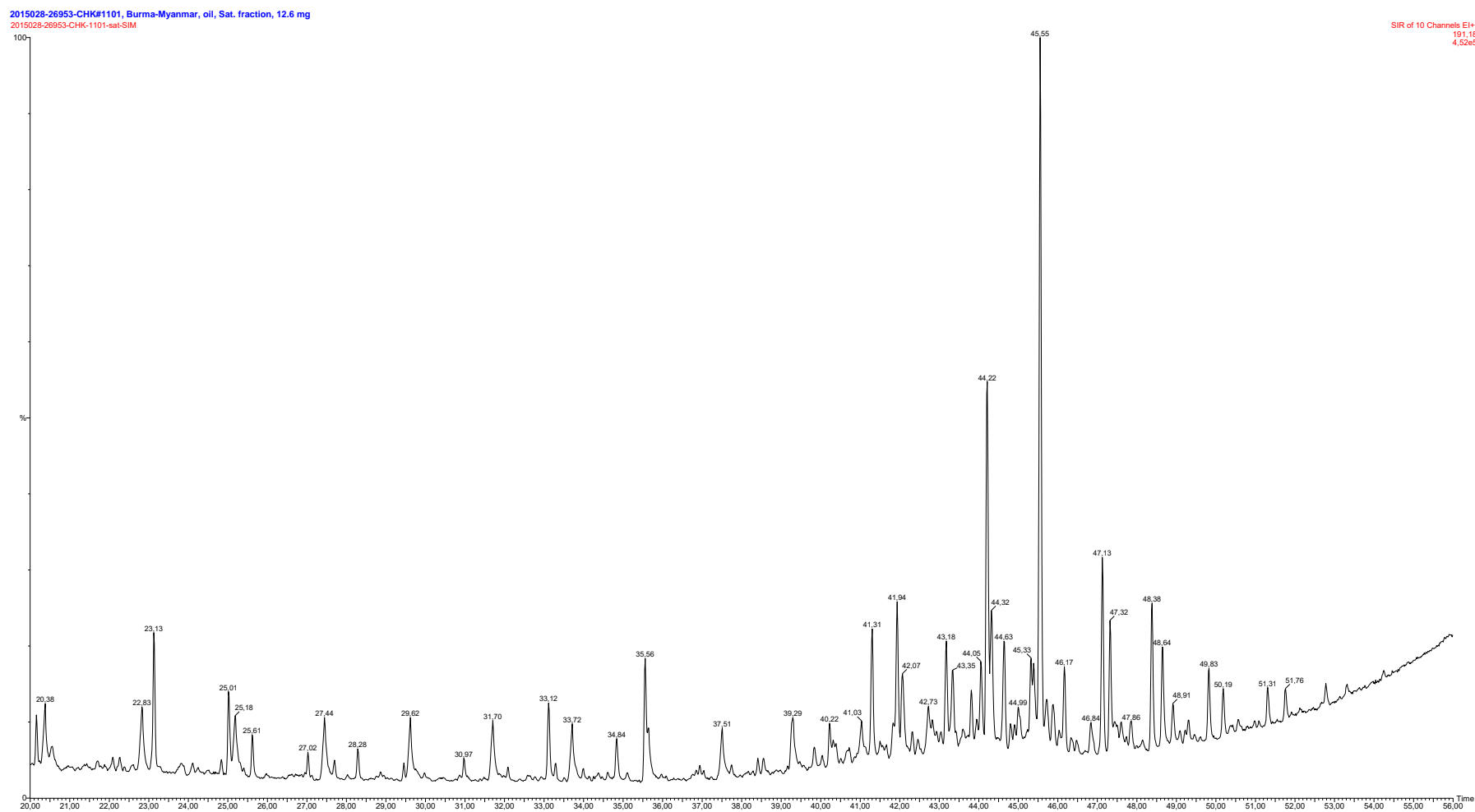
[57]

Sample 2015028-26927, GC-MS_{Sim} m/z 191



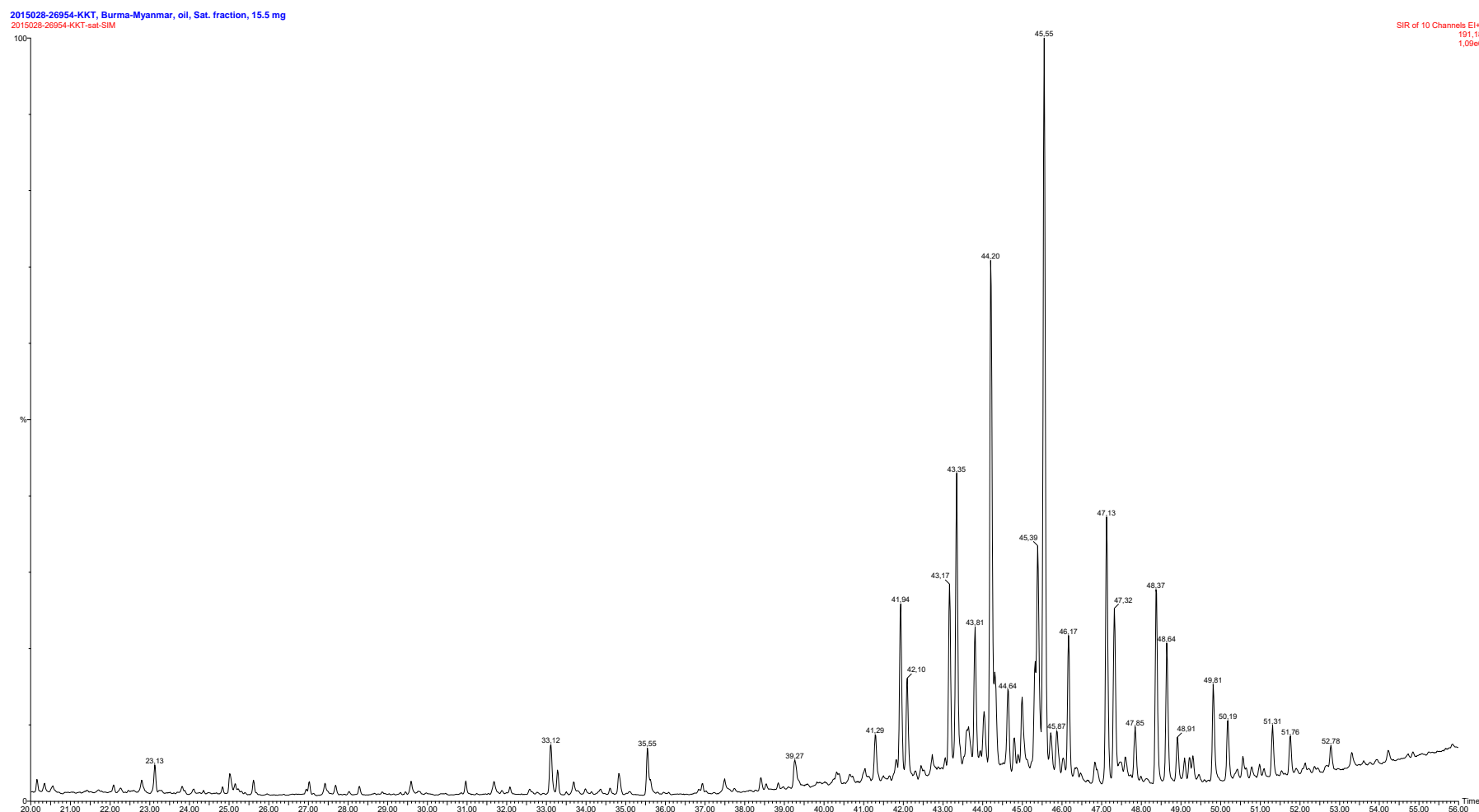
[58]

Sample 2015028-26953, GC-MS_{Sim} m/z 191

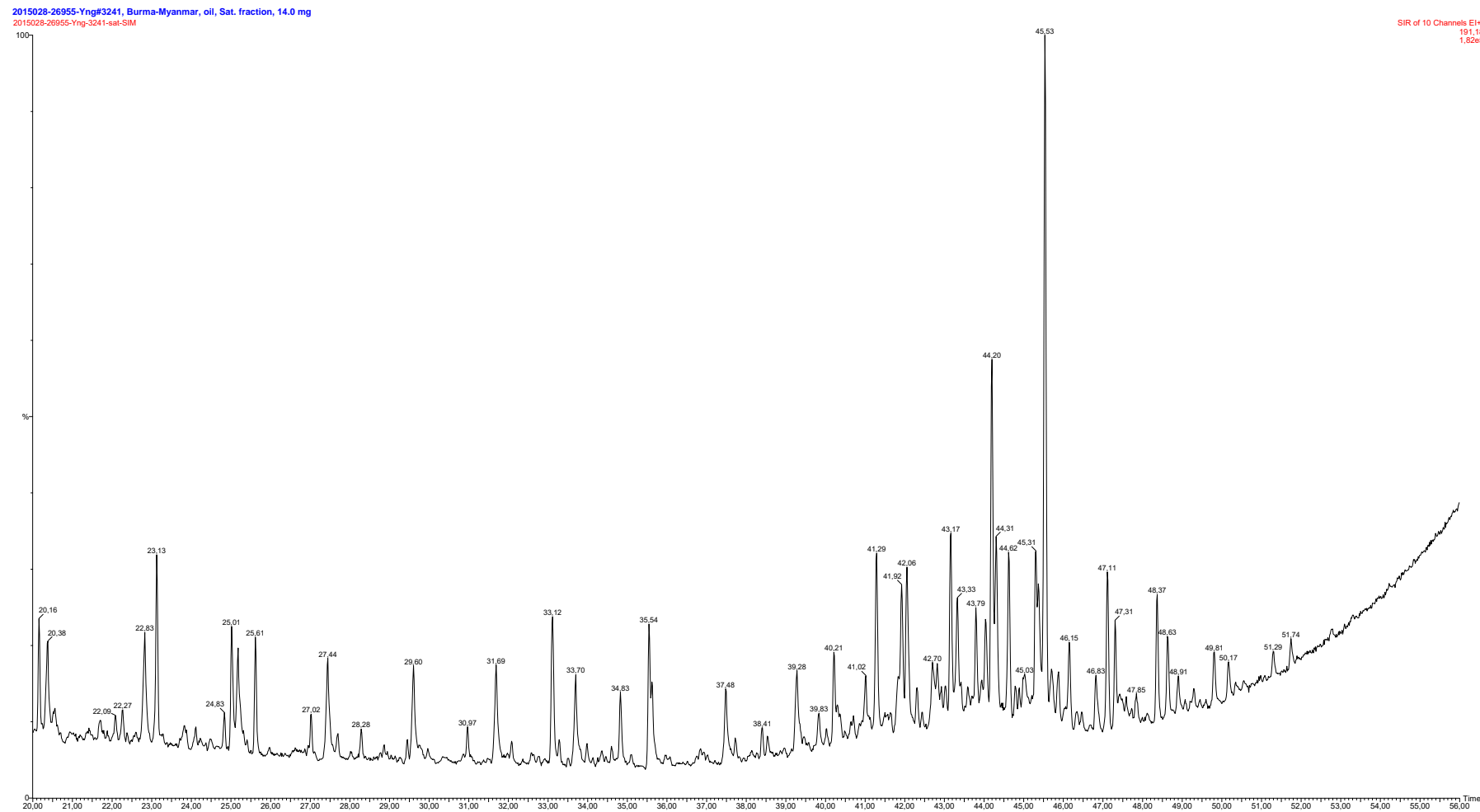


[59]

Sample 2015028-26954, GC-MS_{Sim} m/z 191

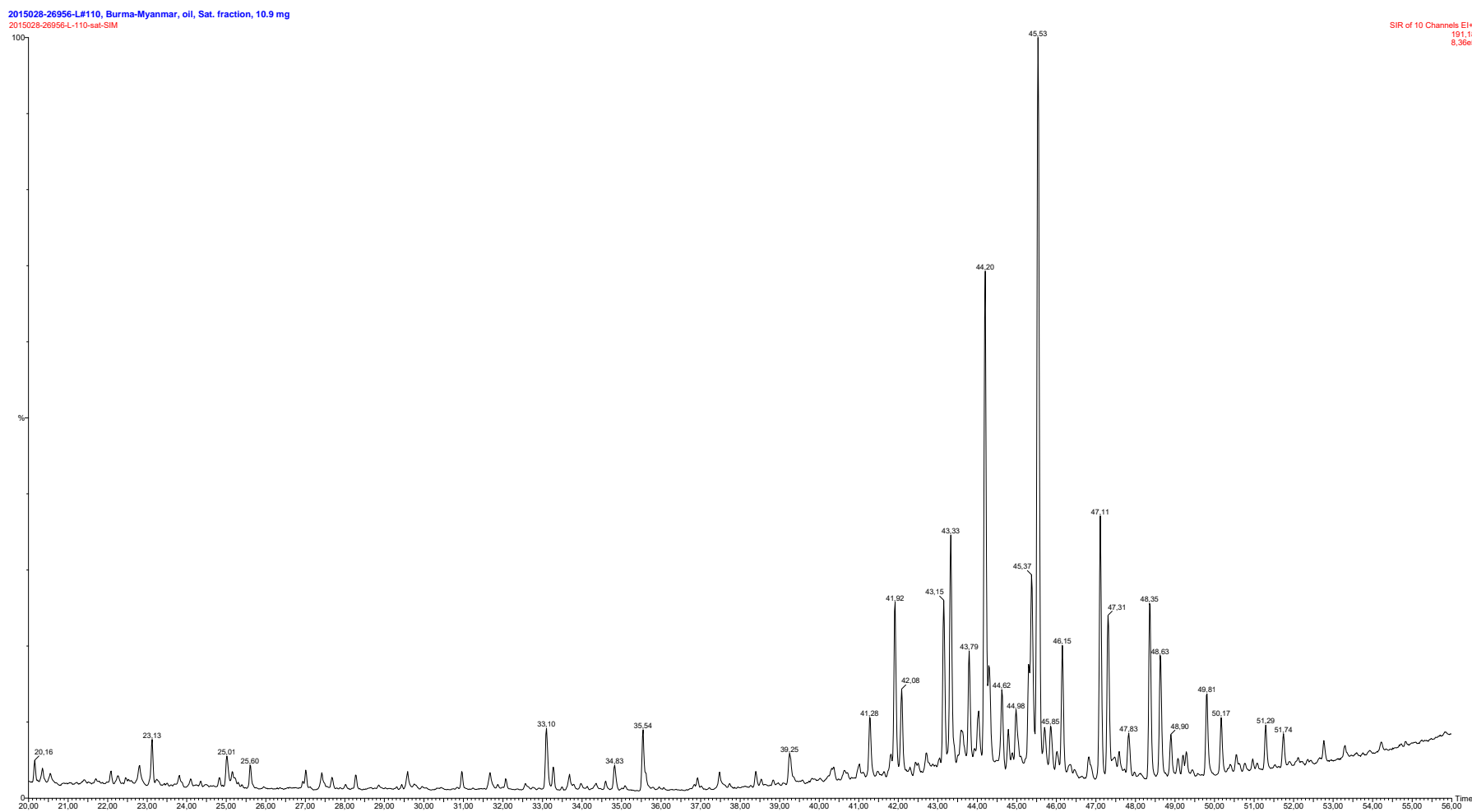


Sample 2015028-26955, GC-MS_{Sim} m/z 191



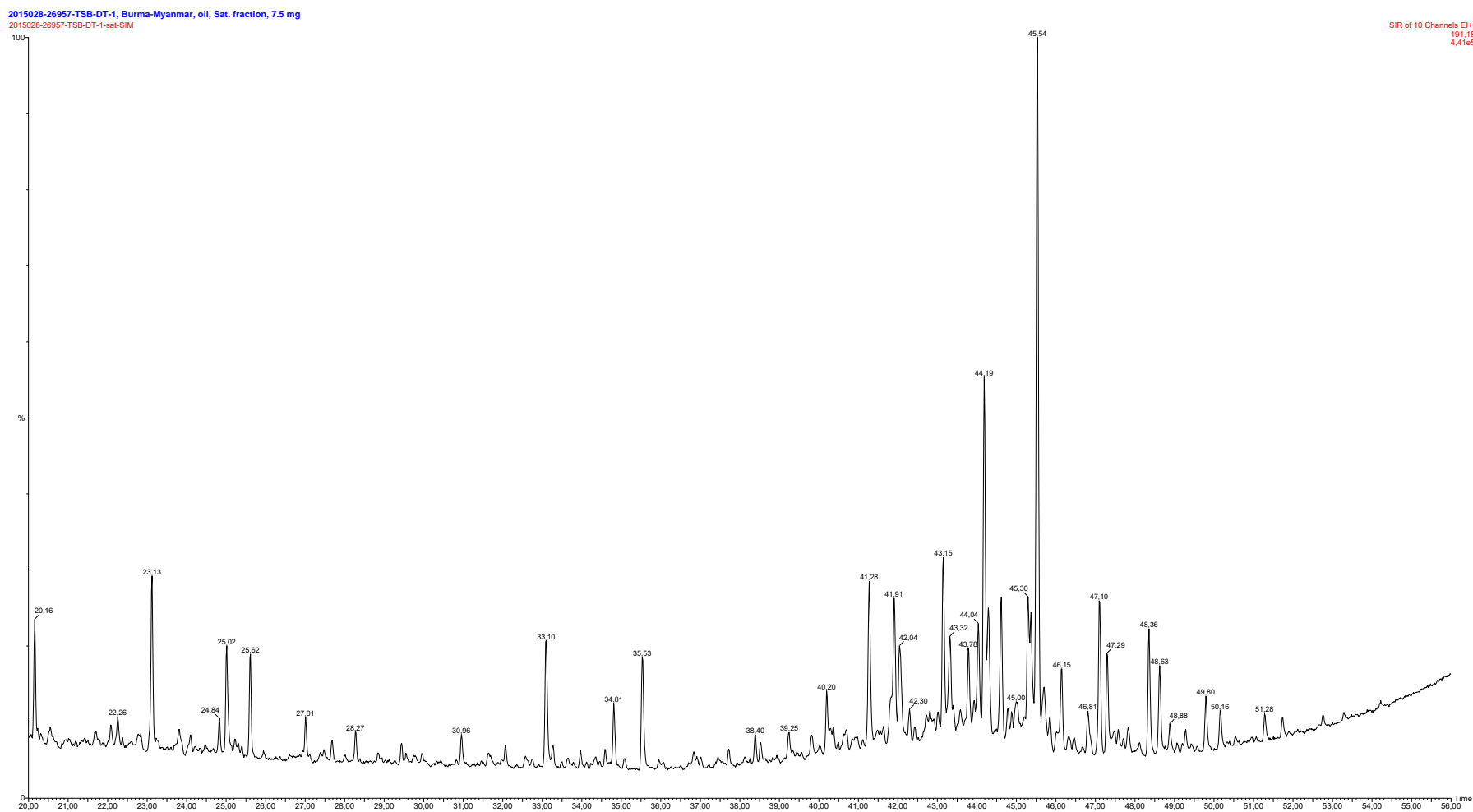
[61]

Sample 2015028-26956, GC-MS_{Sim} m/z 191



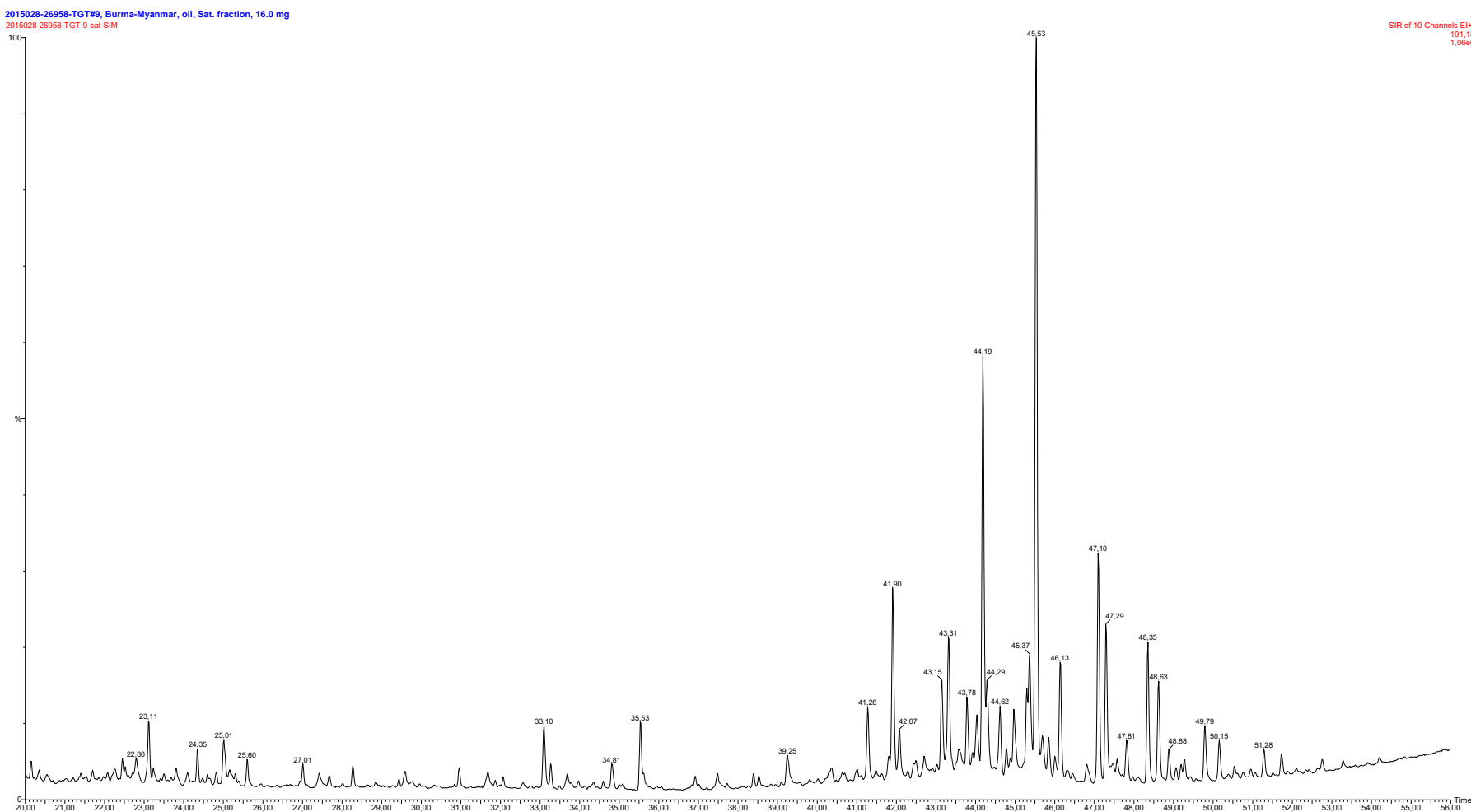
[62]

Sample 2015028-26957, GC-MS_{Sim} m/z 191



[63]

Sample 2015028-26958, GC-MS_{Sim} m/z 191



Appendix 3: Hopanes

GC-MS-MS Parent \Rightarrow Daughter data

C₂₇-C₃₅ pentacyclic triterpanes

m/z 370 \Rightarrow 191

m/z 384 \Rightarrow 191

m/z 398 \Rightarrow 191

m/z 412 \Rightarrow 191

m/z 426 \Rightarrow 191

m/z 440 \Rightarrow 191

m/z 454 \Rightarrow 191

m/z 468 \Rightarrow 191

m/z 482 \Rightarrow 191

[5]

Lab. #	Alt. Lab. #	Ts / (Ts+Tm)	M30-index	H31-iso	H32-iso	H31S / H30	DH30-index	H29 / H30	Oleanane-index	Taxastane-index
20150028-26919	548601	0,44	7,42	0,61	0,62	0,15	13,77	0,63	19,06	2,24
20150028-26920	548602	0,63	7,77	0,59	0,57	0,10	24,69	0,46	34,72	5,06
20150028-26921	548603	0,60	6,40	0,59	0,78	0,11	24,20	0,39	31,77	6,06
20150028-26922	548604	0,75	7,64	0,59	0,61	0,11	29,46	0,50	36,45	4,43
20150028-26923	548605	0,57	7,06	0,59	0,58	0,13	20,86	0,48	28,37	3,84
20150028-26924	548606	0,56	7,26	0,59	0,61	0,13	20,45	0,48	19,99	3,40
20150028-26925	548607	0,60	7,99	0,58	0,62	0,12	5,02	0,49	21,51	3,54
20150028-26926	548608	0,61	6,20	0,76	0,57	0,14	5,47	0,49	28,97	6,93
20150028-26927	548609	0,55	7,43	0,60	0,62	0,13	4,72	0,52	27,31	3,52
20150028-26953	CHK # 1101	0,46	5,94	0,60	0,59	0,14	14,73	0,51	27,12	3,12
20150028-26954	KKT	0,24	6,79	0,59	0,60	0,17	17,52	0,51	38,42	2,08
20150028-26955	Yng # 3241	0,71	7,50	0,59	0,54	0,12	25,89	0,45	35,28	9,23
20150028-26956	L # 110	0,30	8,42	0,59	0,60	0,19	9,39	0,53	30,22	2,05
20150028-26957	TSB-DT-1	0,60	7,69	0,59	0,60	0,11	5,20	0,45	21,85	6,67
20150028-26958	TGT # 9	0,35	7,86	0,59	0,57	0,18	13,86	0,51	29,61	1,35

M30 index = 100* moretane / (moretane+hopane)

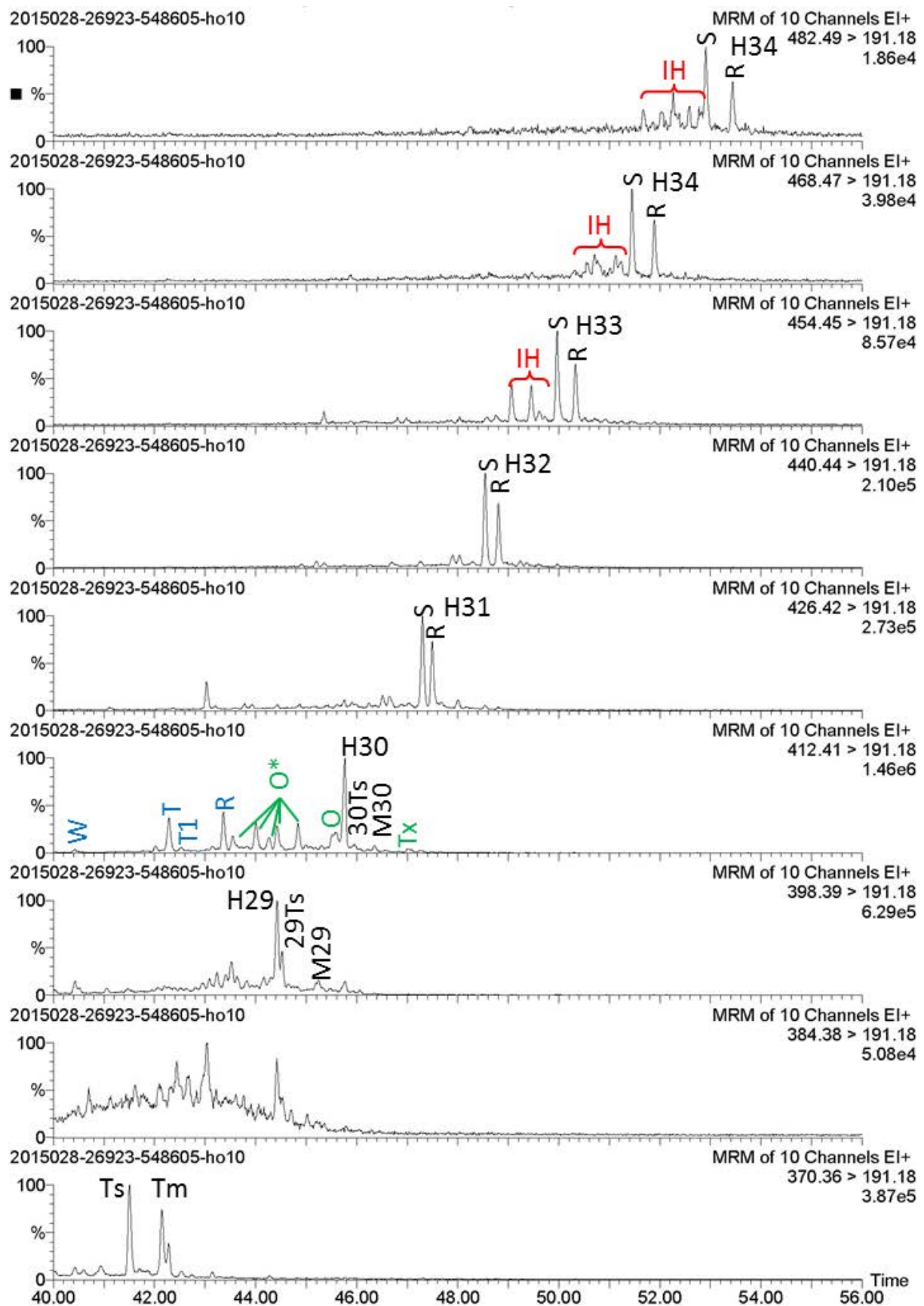
H31-iso = homohopane 22S/(22S+22R) isomerisation ratio

H32-iso = bishomohopane 22S/(22S+22R) isomerisation ratio

DH30-index = 100* diahopane / (diahopane + hopane)

Oleanane index = 100* oleanane / (oleanane+hopane)

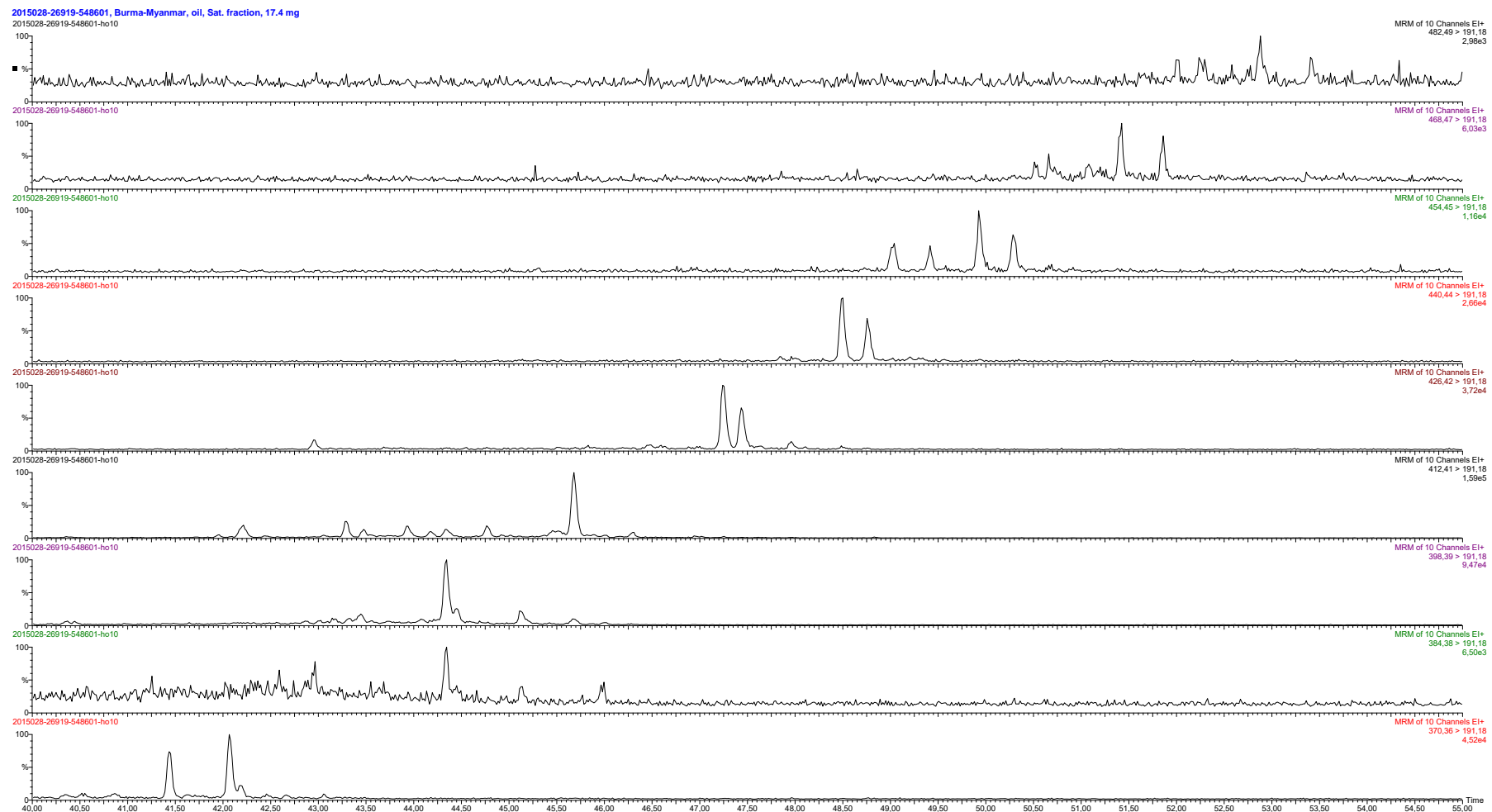
Taraxastane index = 100* taraxastane / (taraxastane + hopane)



Compound identification key

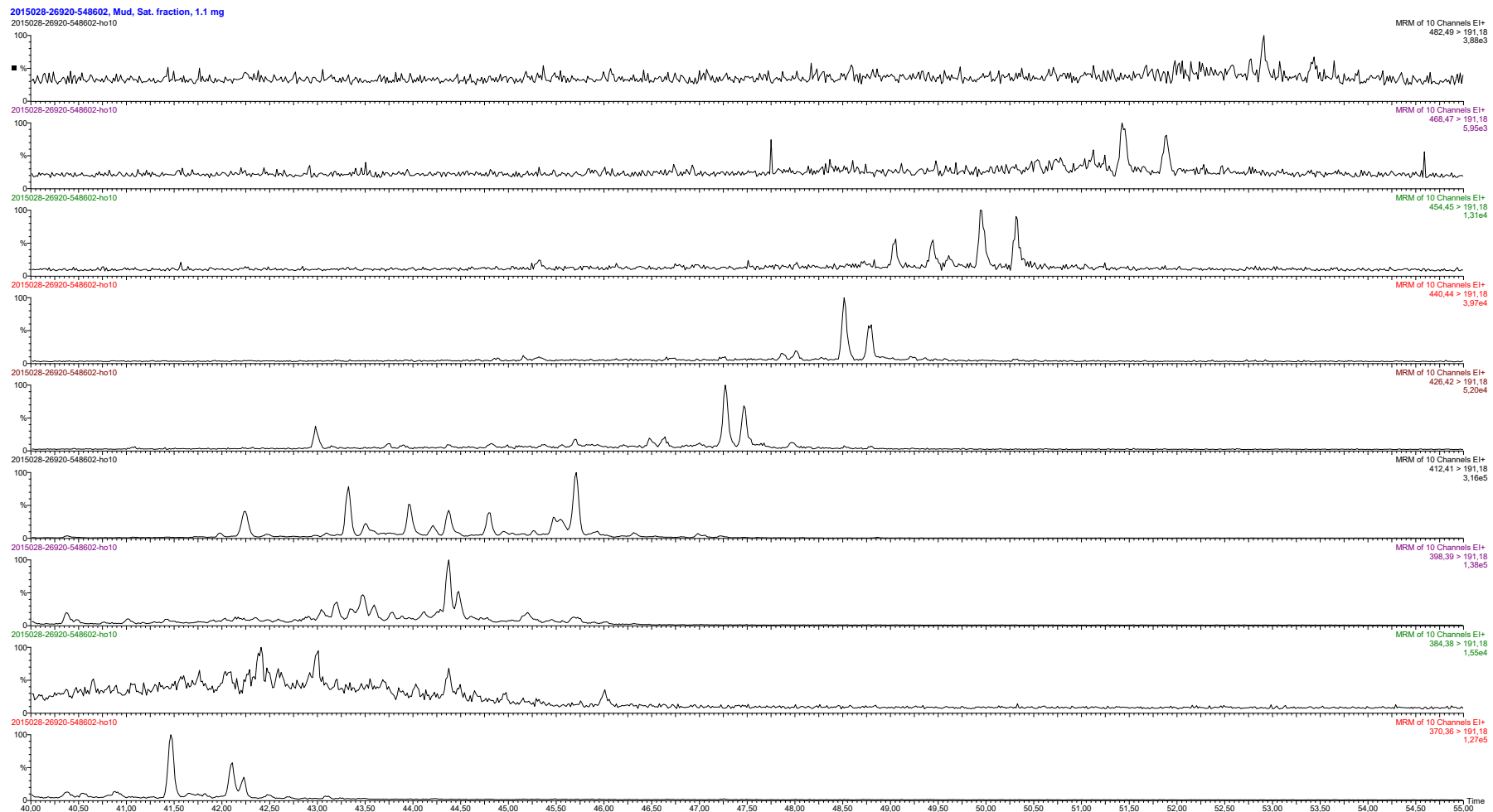
Sample 2015028-26919, GC-MSMS data

[67]



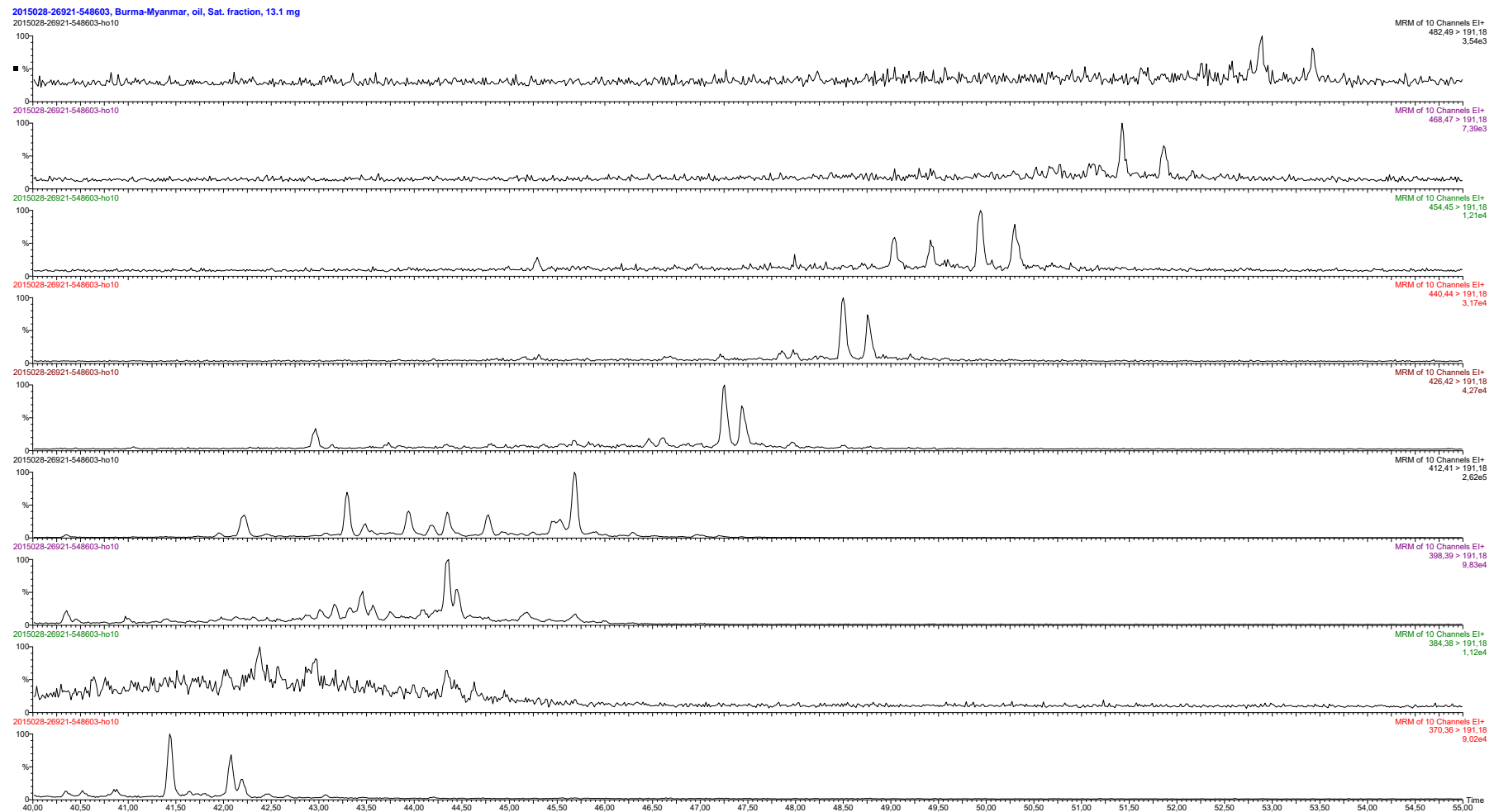
Sample 2015028-26920, GC-MSMS data

[68]

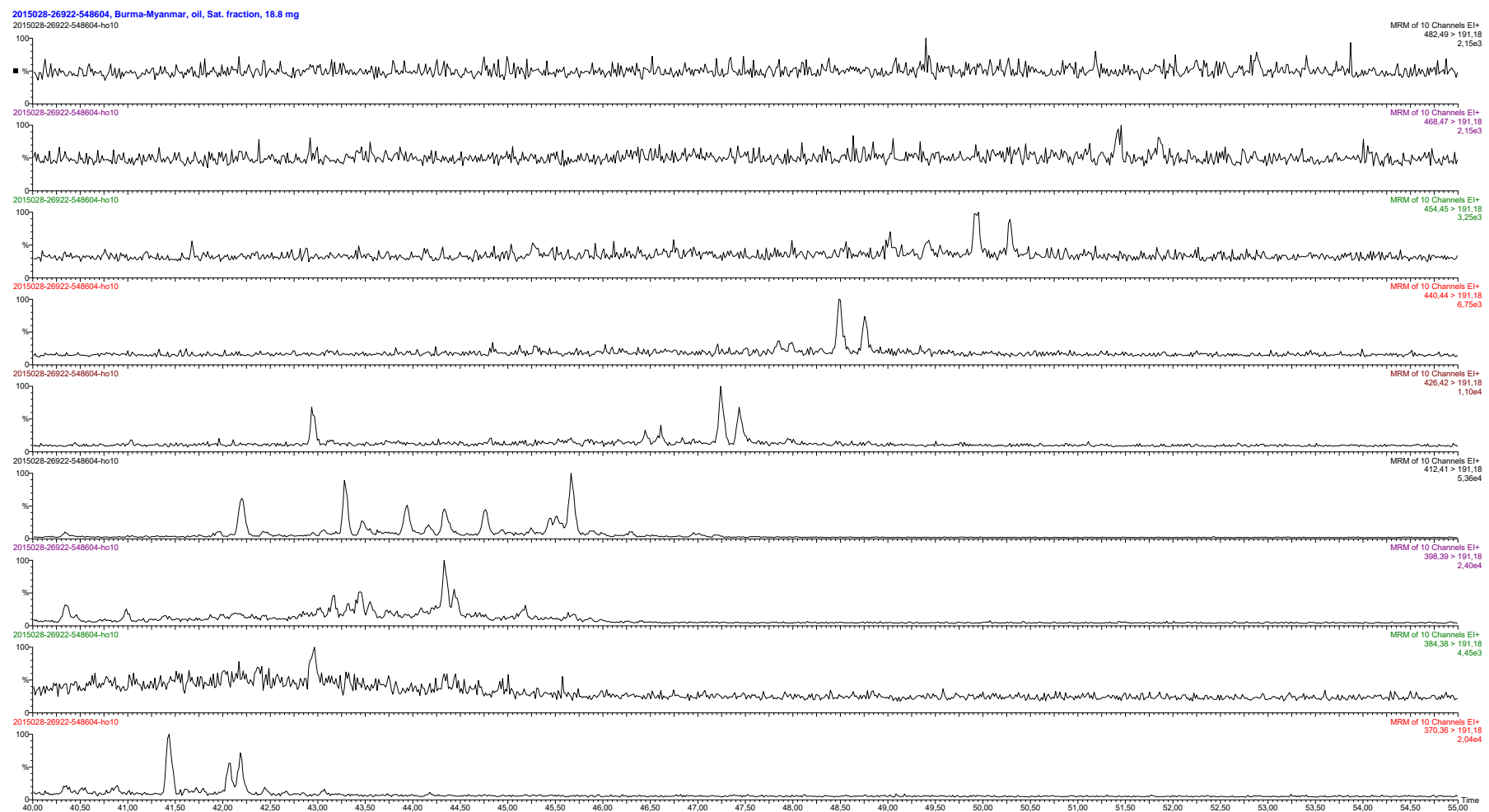


Sample 2015028-26921, GC-MSMS data

[69]

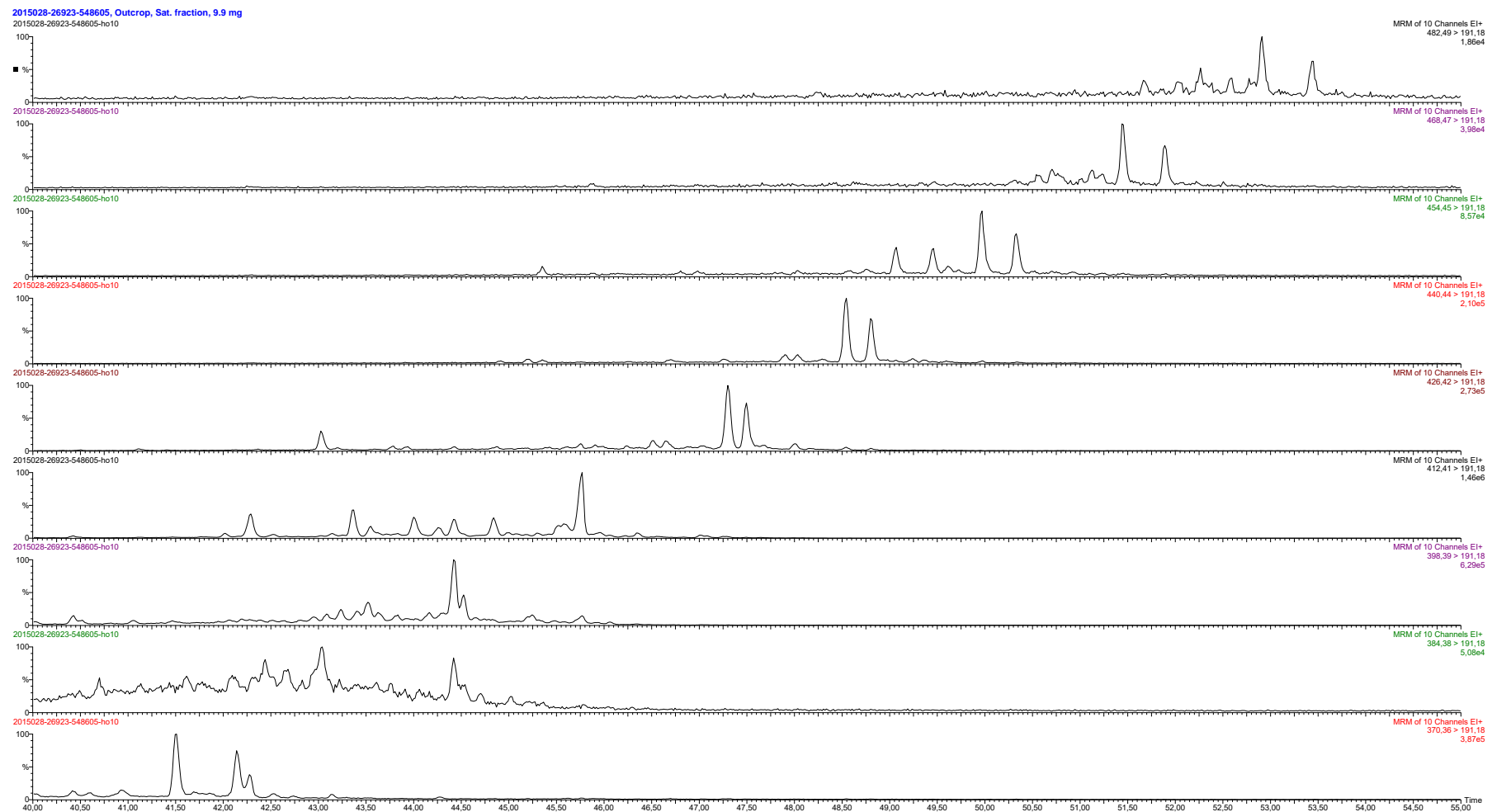


Sample 2015028-26922, GC-MSMS data



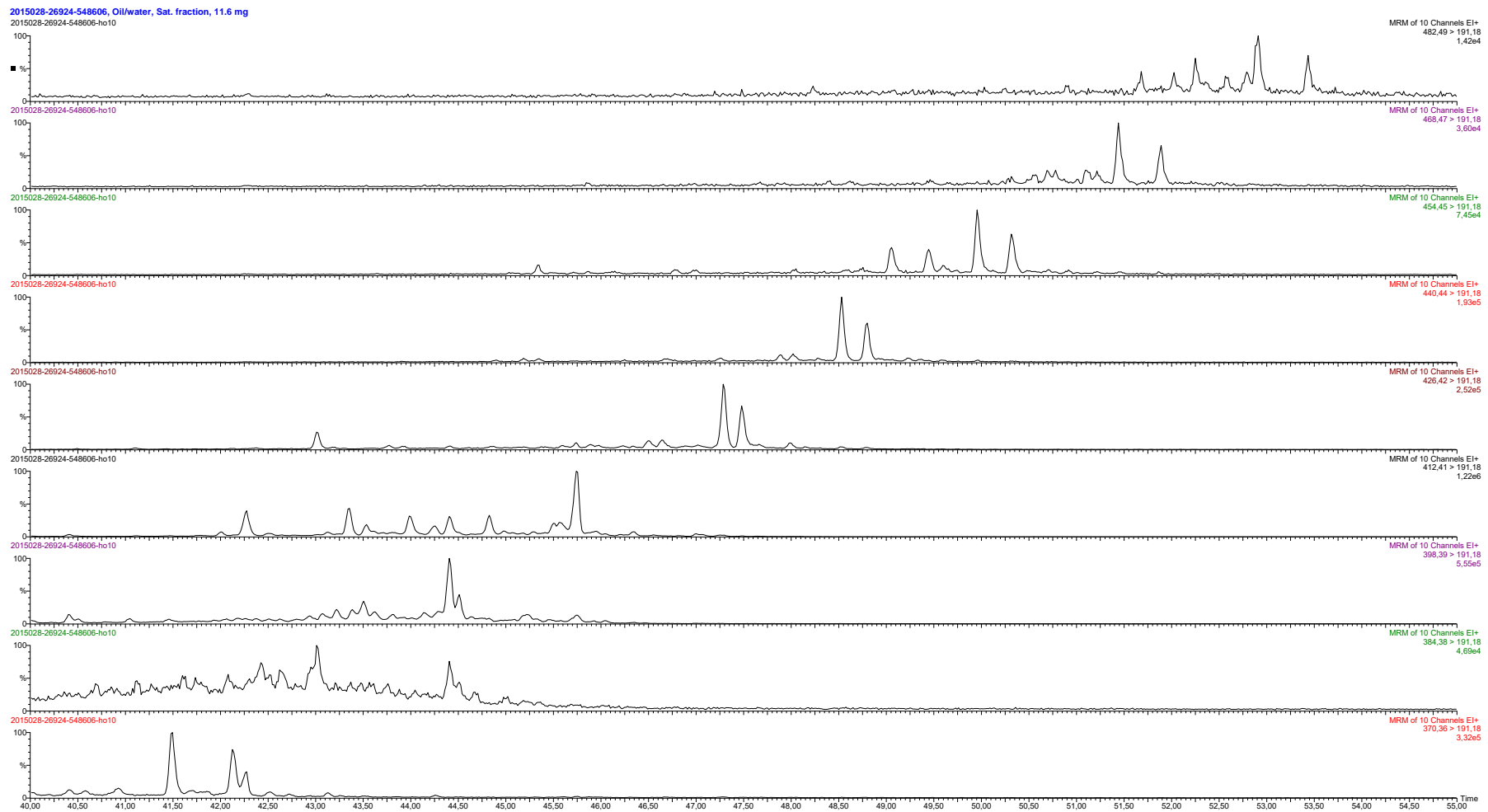
Sample 2015028-26923, GC-MSMS data

[71]



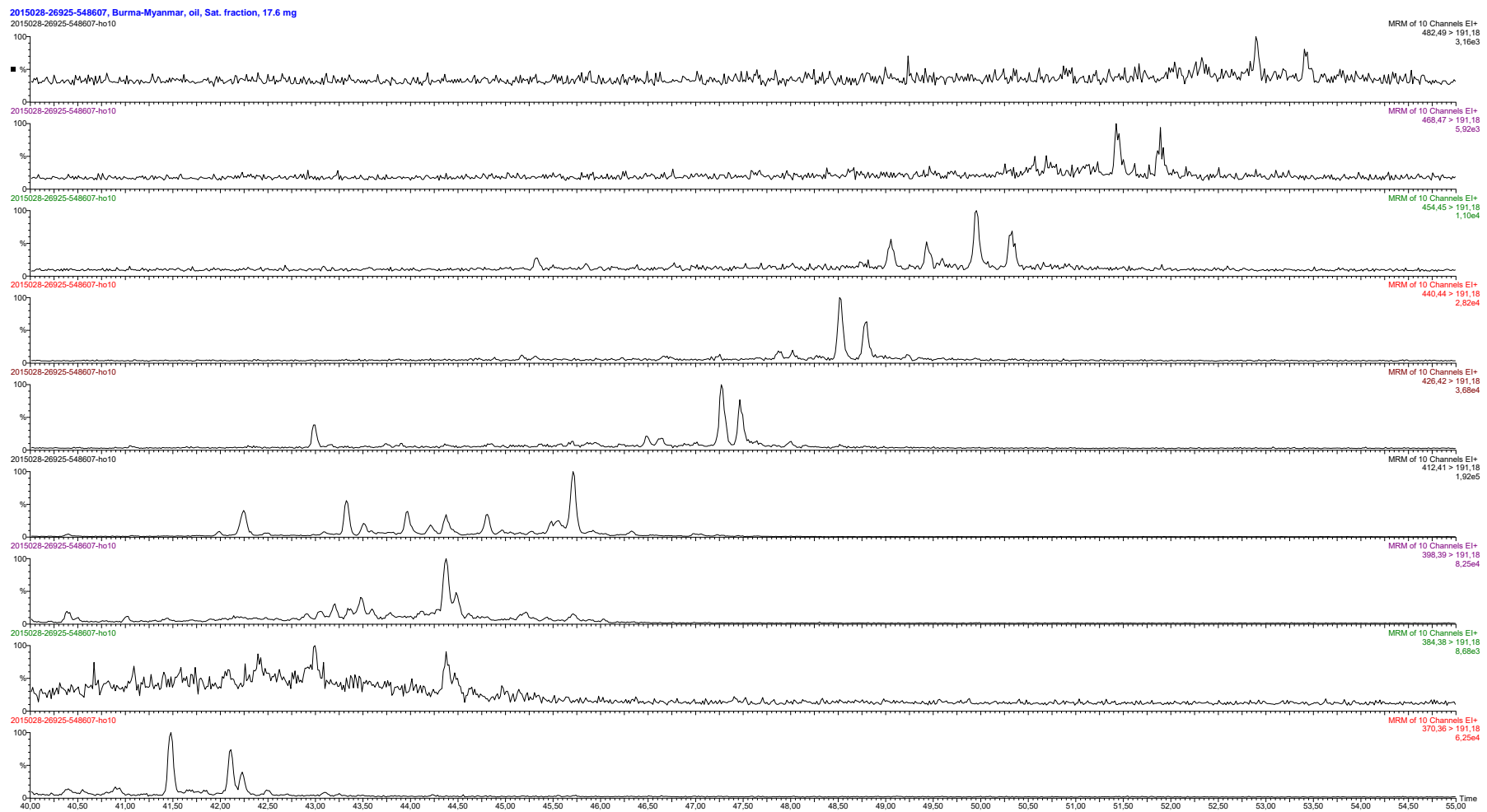
Sample 2015028-26924, GC-MSMS data

[72]



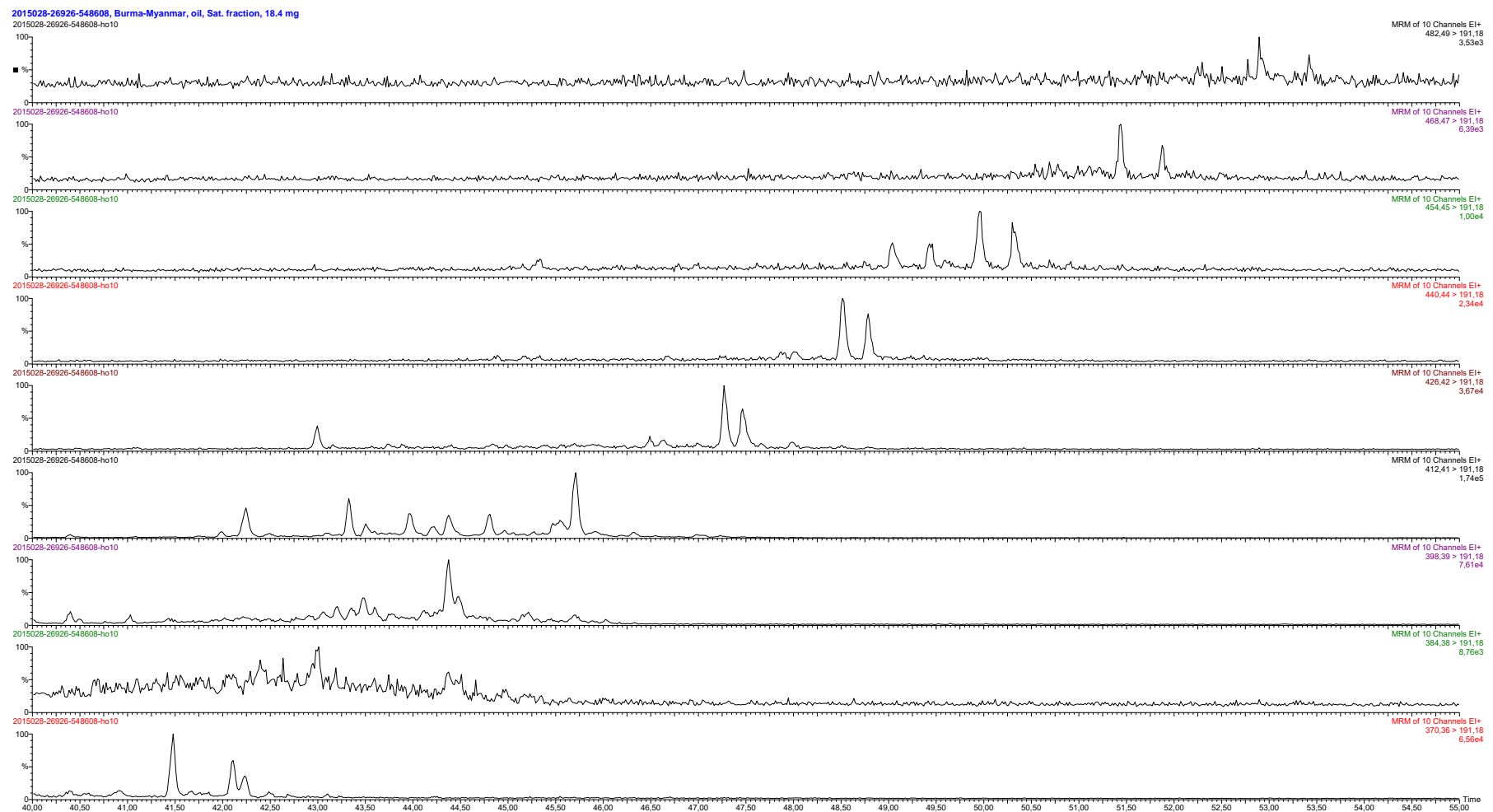
Sample 2015028-26925, GC-MSMS data

[73]



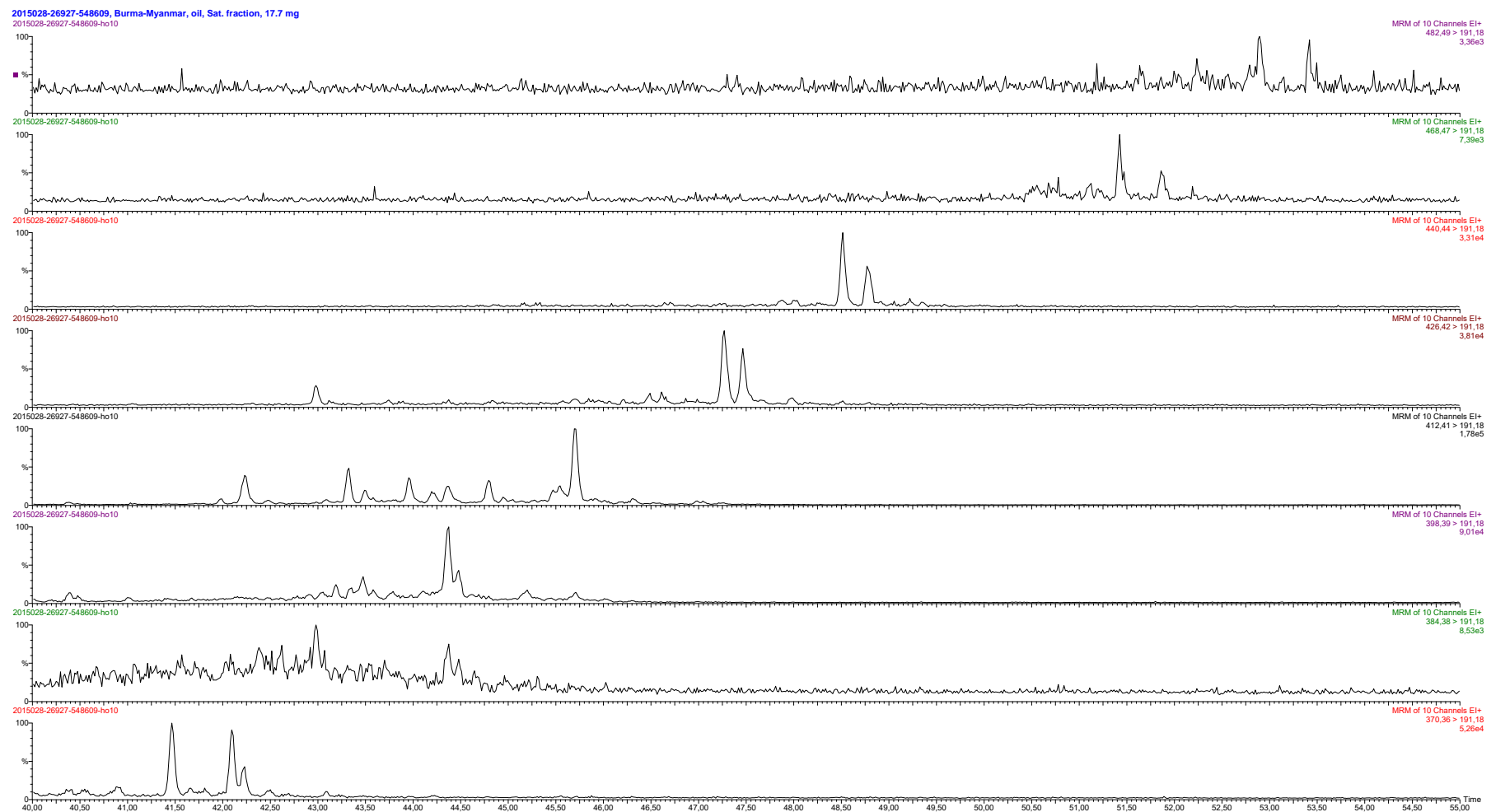
[74]

Sample 2015028-26926, GC-MSMS data



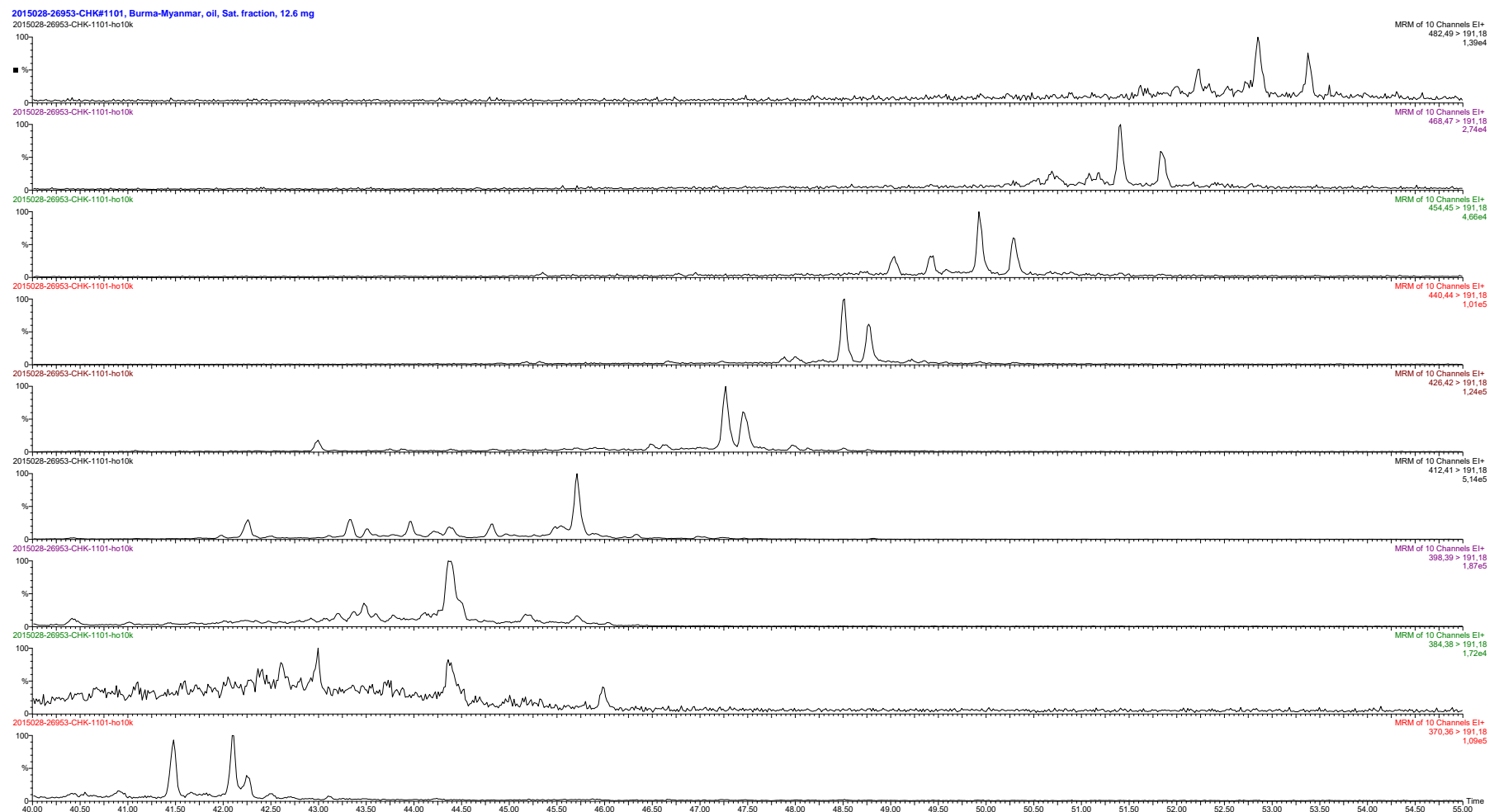
[75]

Sample 2015028-26927, GC-MSMS data



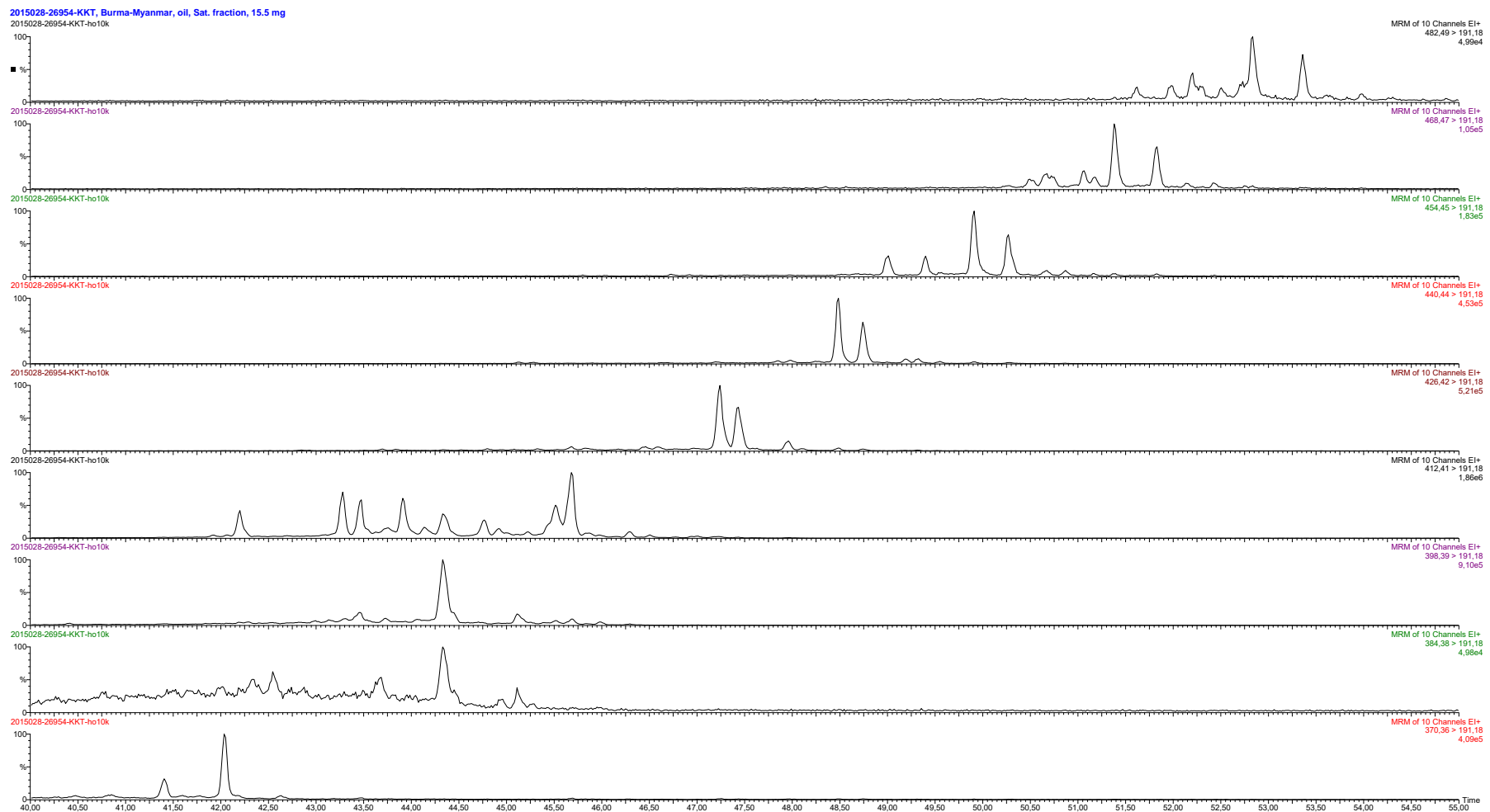
Sample 2015028-26953, GC-MSMS data

[76]

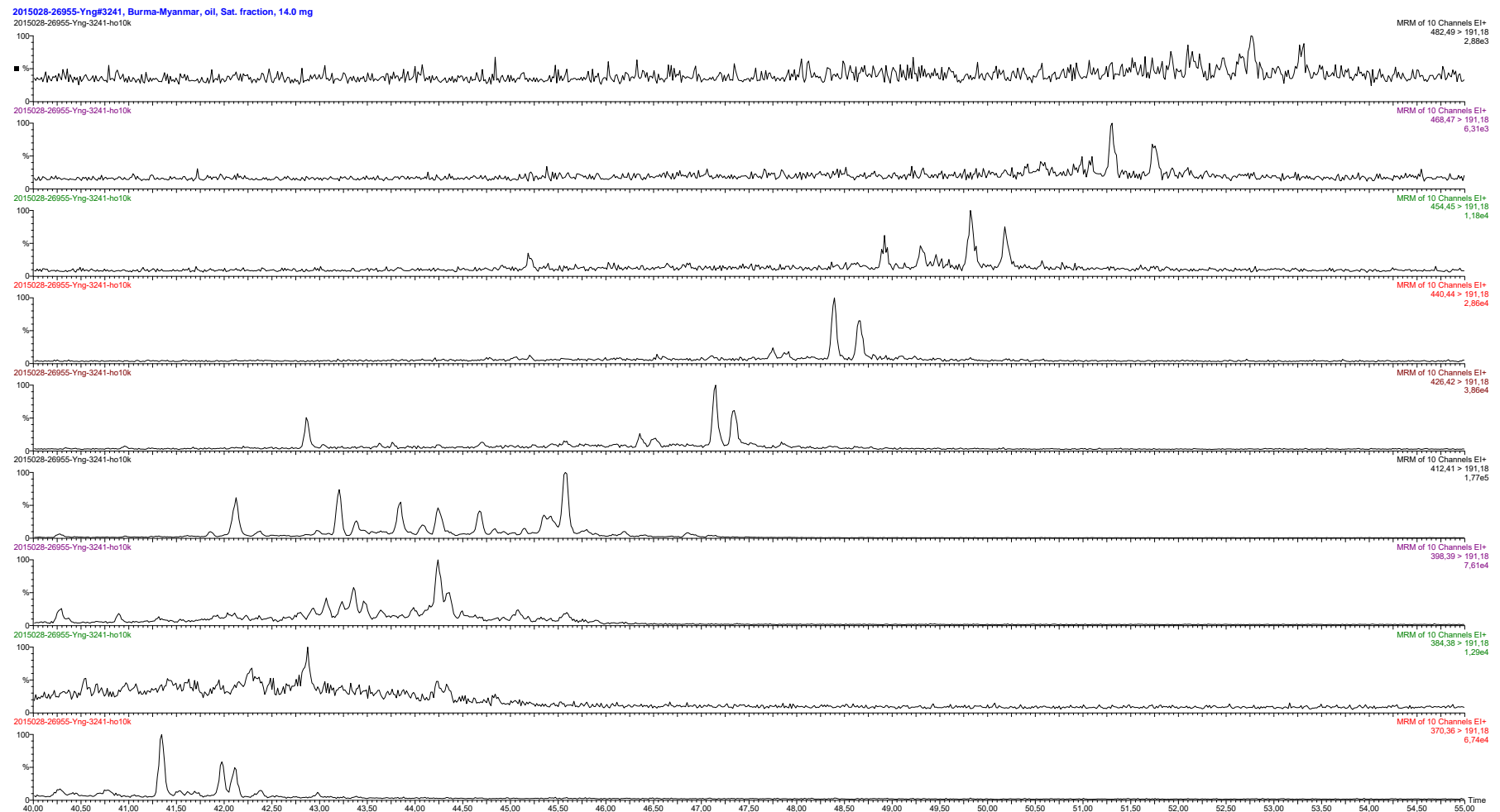


Sample 2015028-26954, GC-MSMS data

[77]

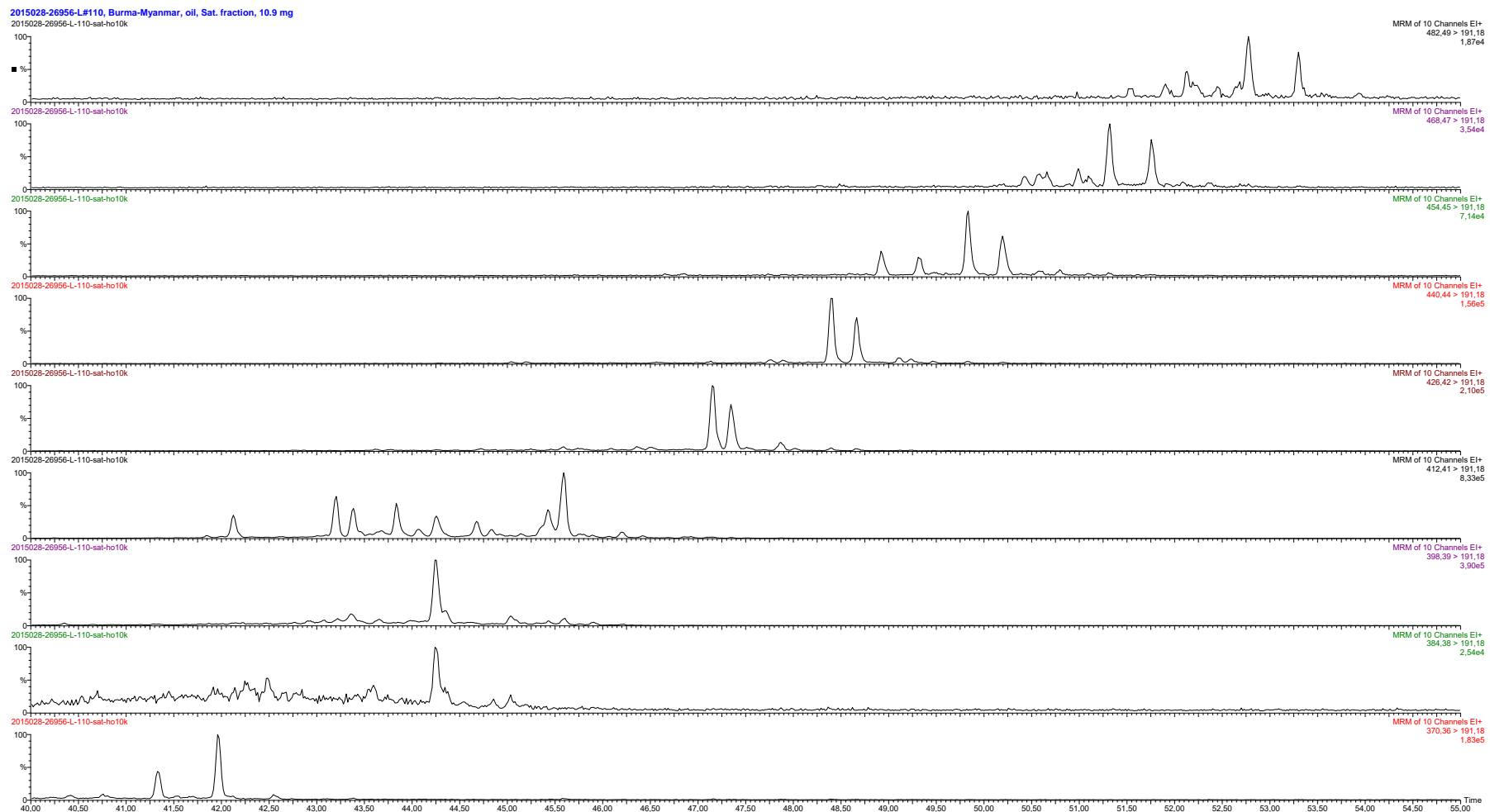


Sample 2015028-26955, GC-MSMS data

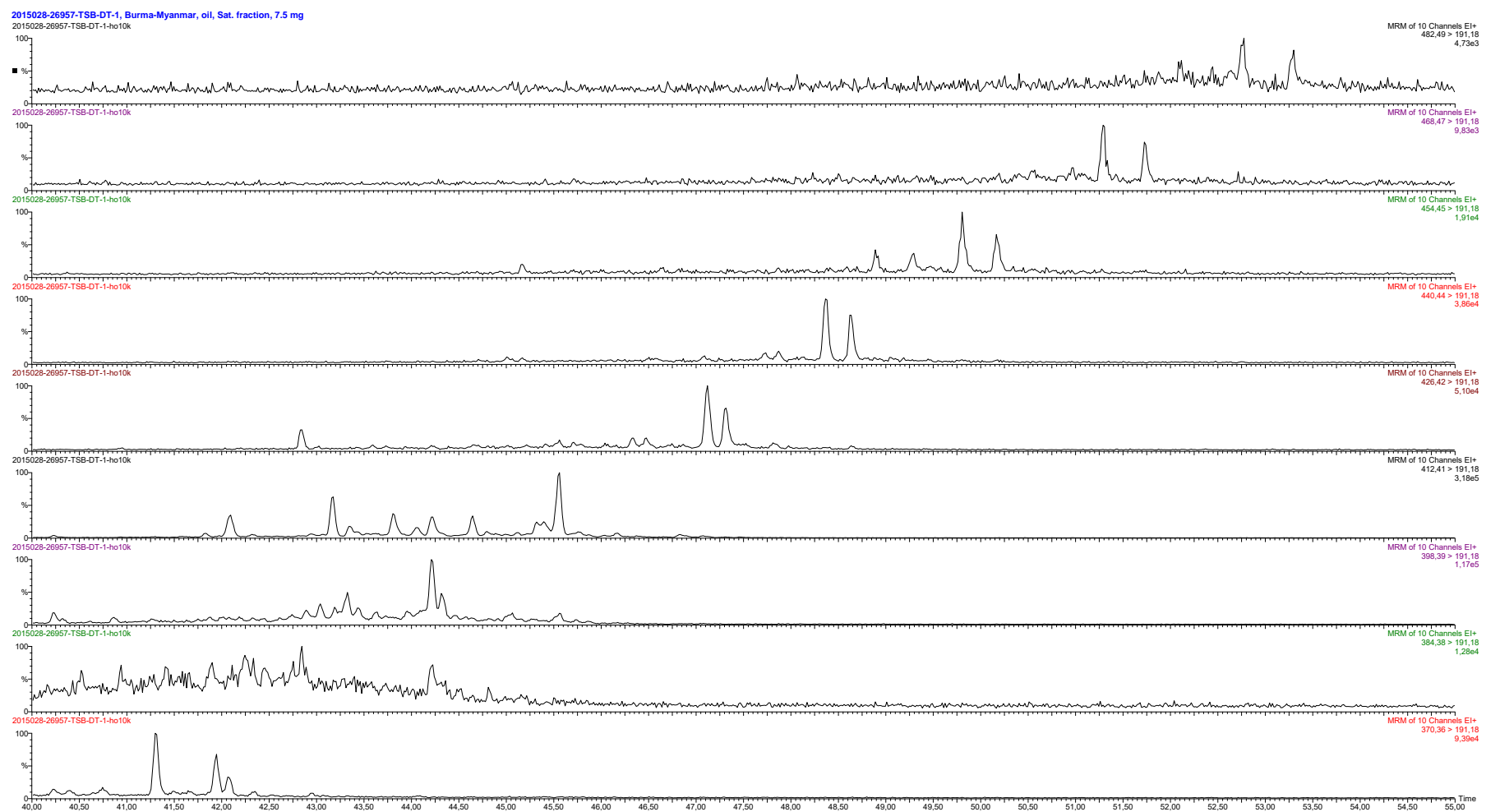


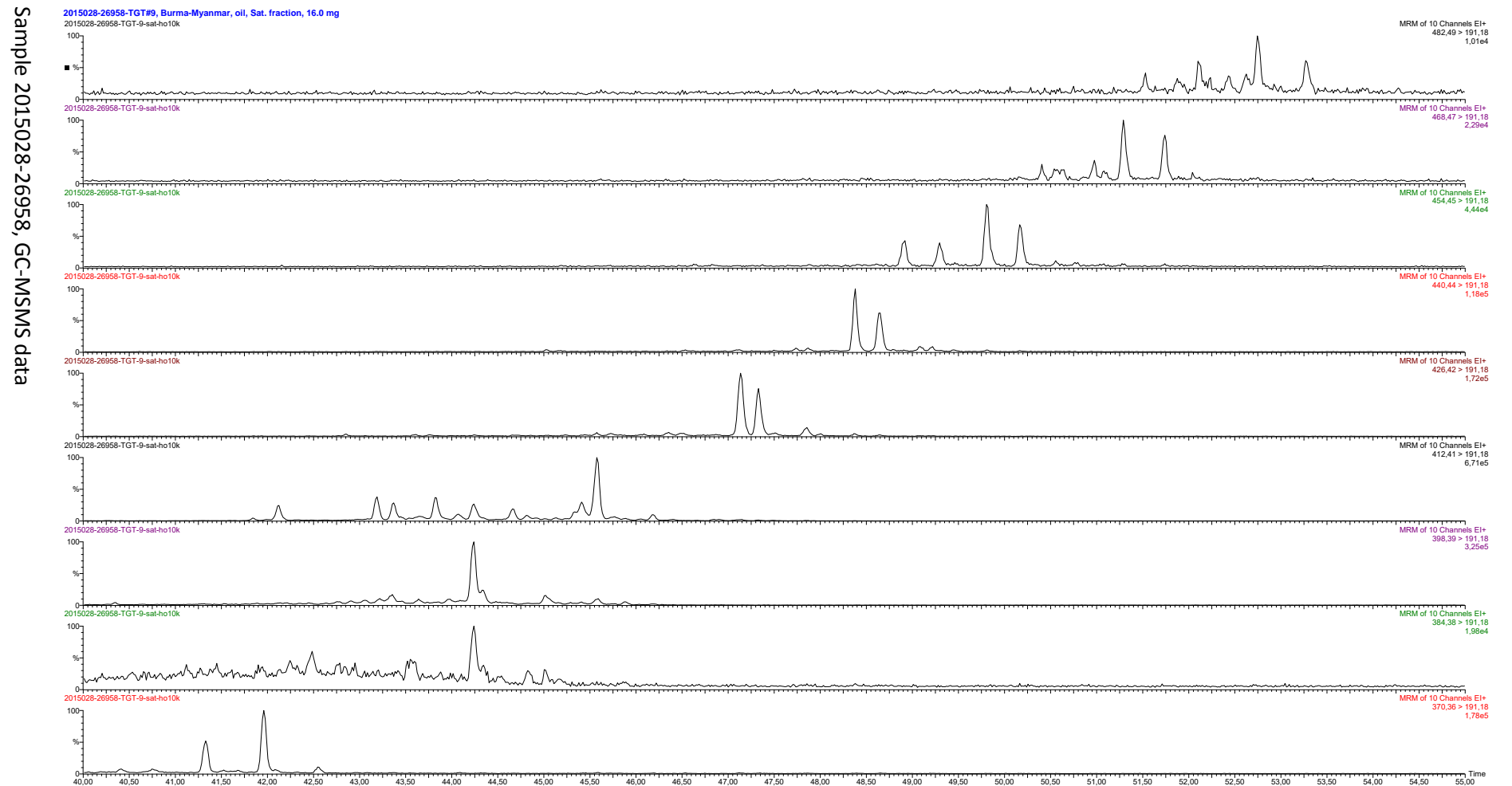
Sample 2015028-26956, GC-MSMS data

[79]



Sample 2015028-26957, GC-MSMS data





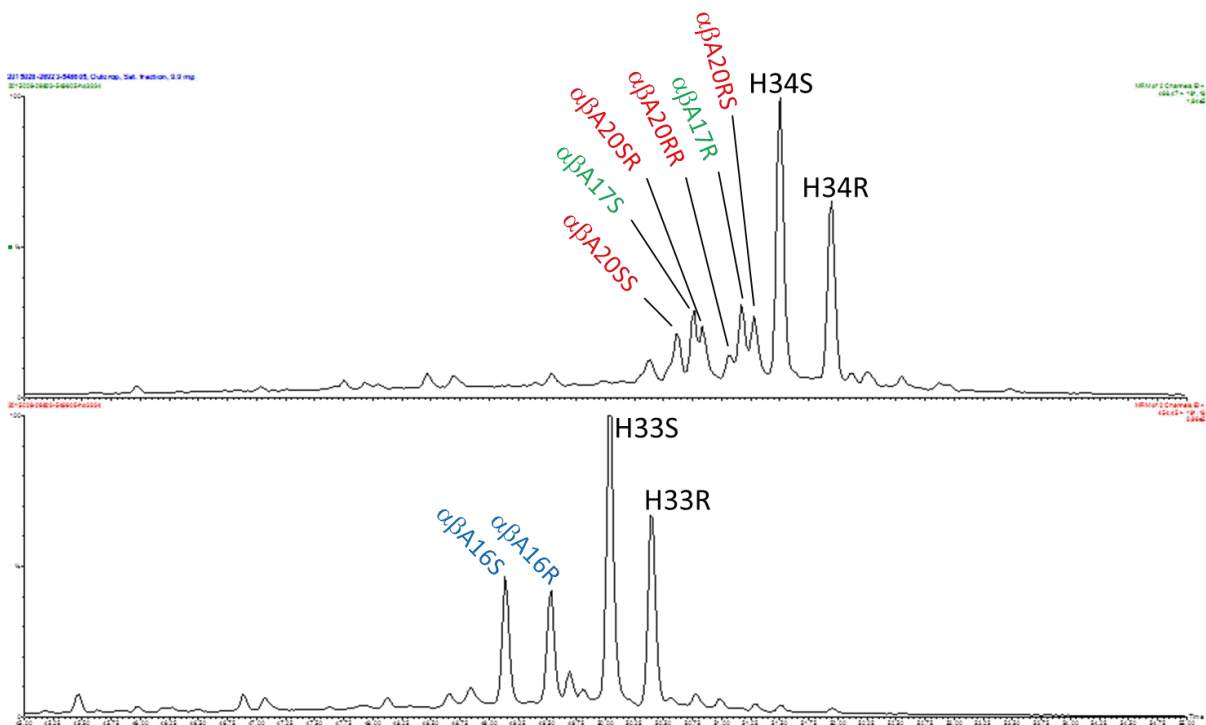
Appendix 4: Isohopanes

GC-MS-MS Parent \Rightarrow Daughter data

C₃₃-C₃₄ isohopanes

m/z 454 \Rightarrow 191

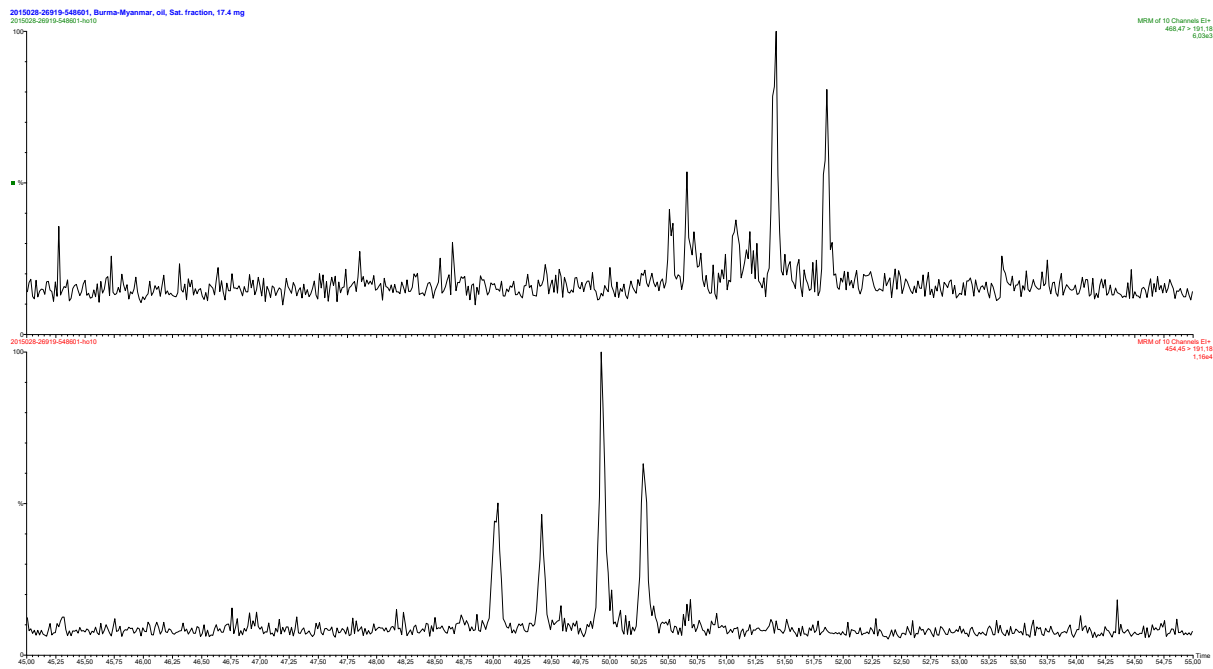
m/z 468 \Rightarrow 191



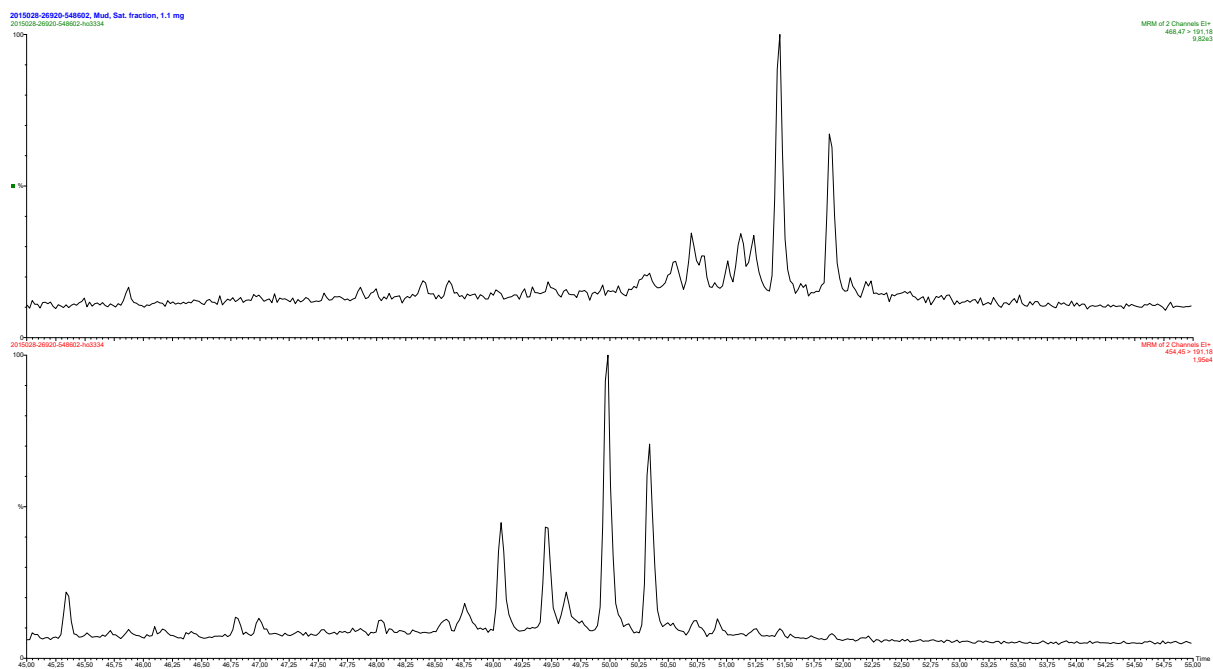
Compound identification key, see Nytoft (2011) for details

Lab. #	Alt. Lab. #	IHR
20150028-26919	548601	0,56
20150028-26920	548602	0,52
20150028-26921	548603	0,59
20150028-26922	548604	n.a.
20150028-26923	548605	0,51
20150028-26924	548606	0,54
20150028-26925	548607	0,51
20150028-26926	548608	0,53
20150028-26927	548609	0,50
20150028-26953	CHK # 1101	0,50
20150028-26954	KKT	0,45
20150028-26955	Yng # 3241	0,58
20150028-26956	L # 110	0,44
20150028-26957	TSB-DT-1	0,50
20150028-26958	TGT # 9	0,52

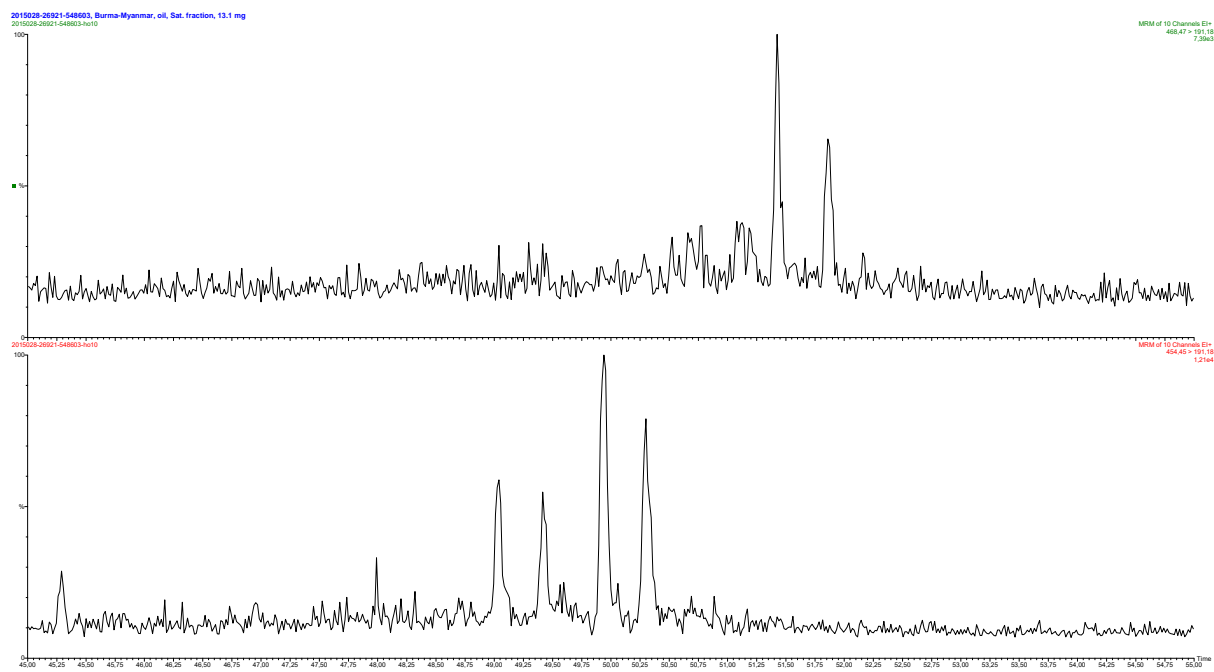
IHR = Isohopane ratio, see Nytoft (2011) for definition



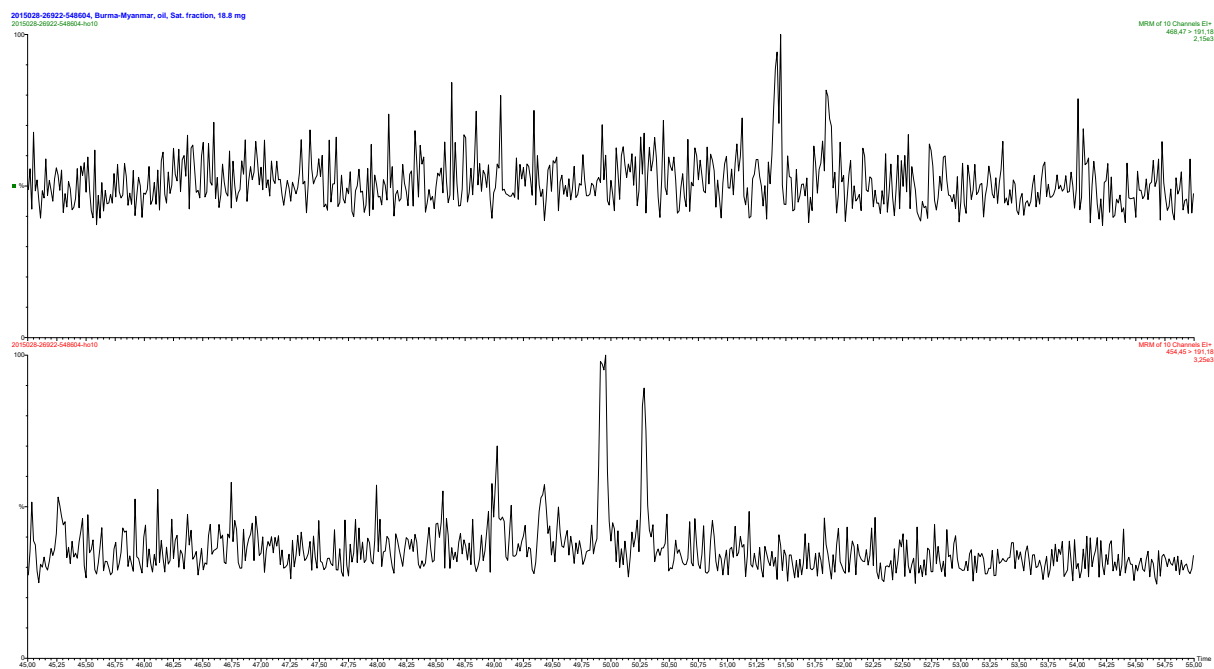
Sample 2015028-26919, GC-MSMS data



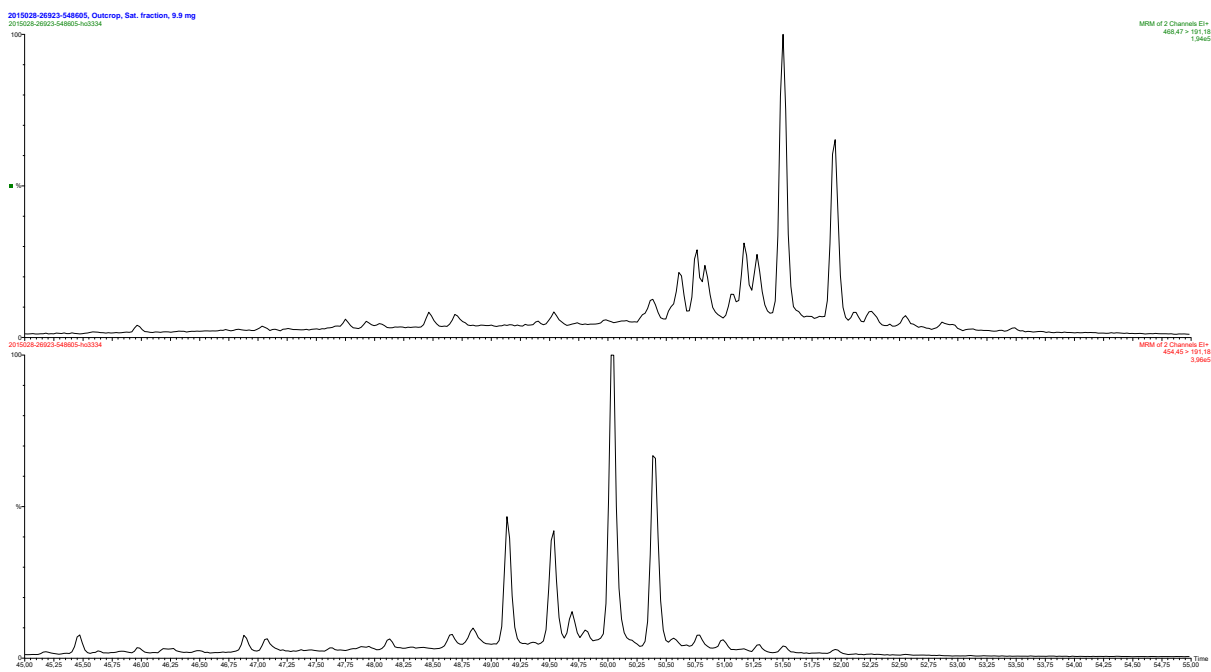
Sample 2015028-26920, GC-MSMS data



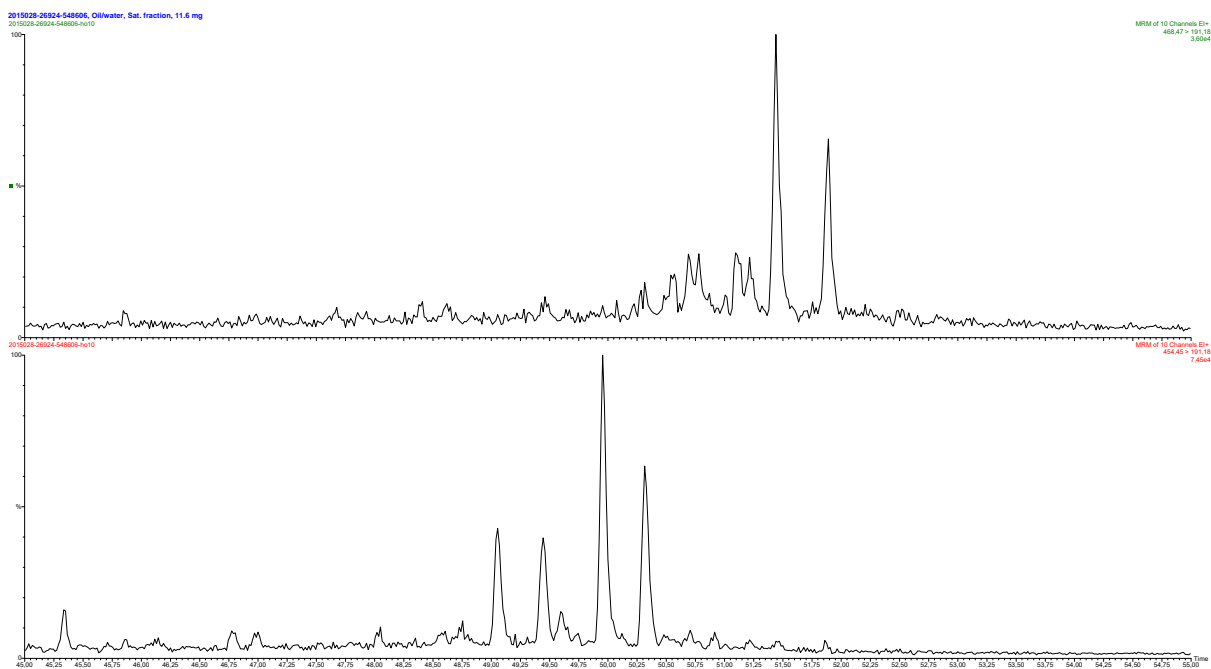
Sample 2015028-26921, GC-MSMS data



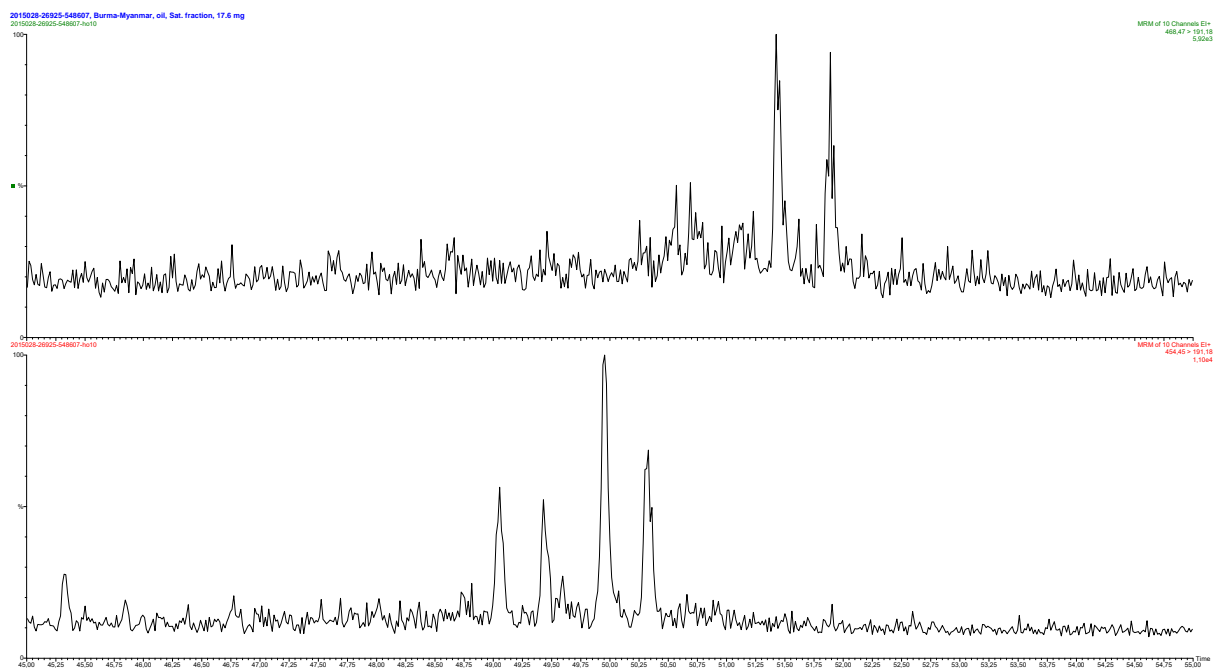
Sample 2015028-26922, GC-MSMS data



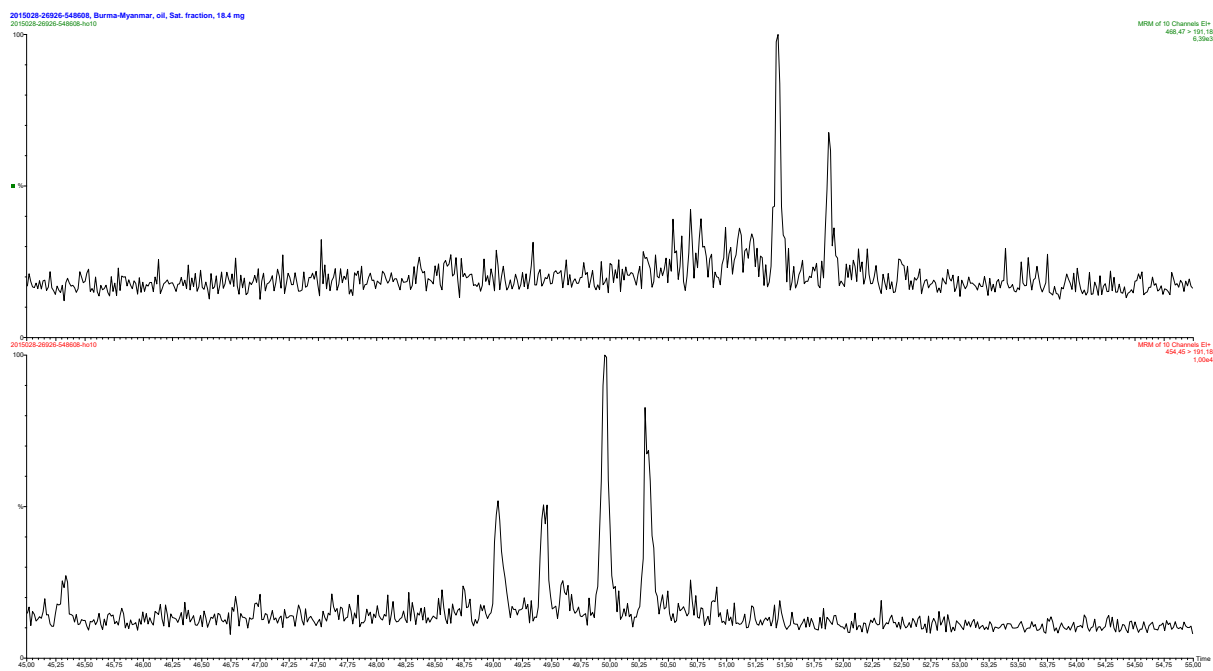
Sample 2015028-26923, GC-MSMS data



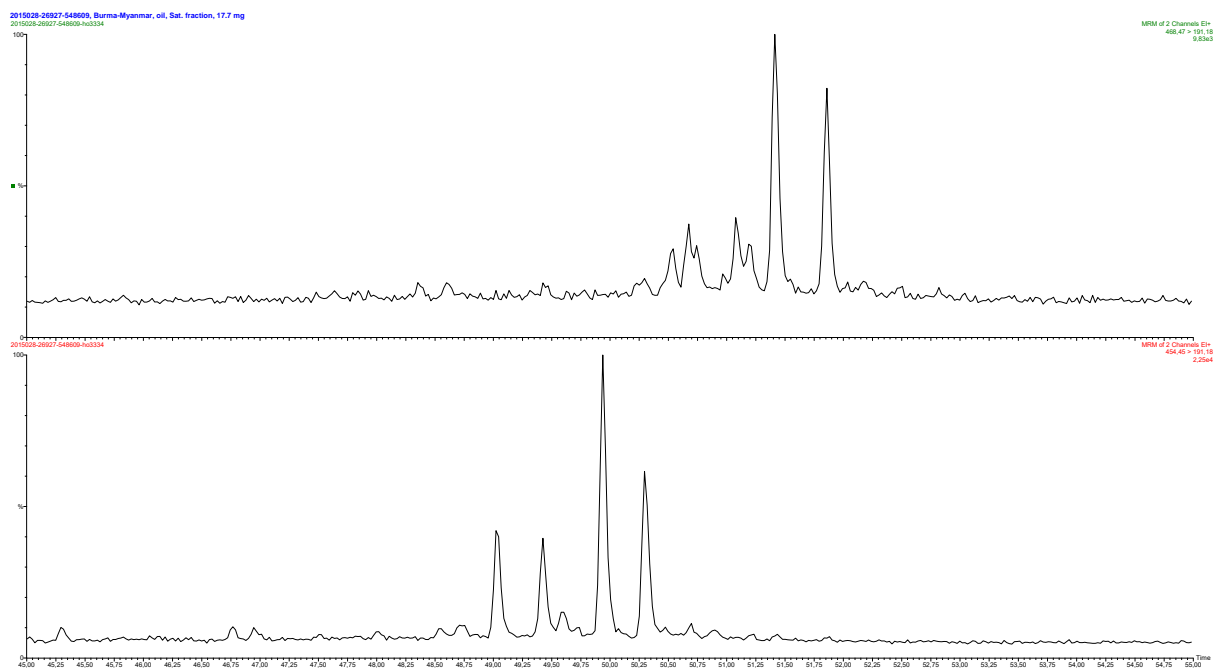
Sample 2015028-26924, GC-MSMS data



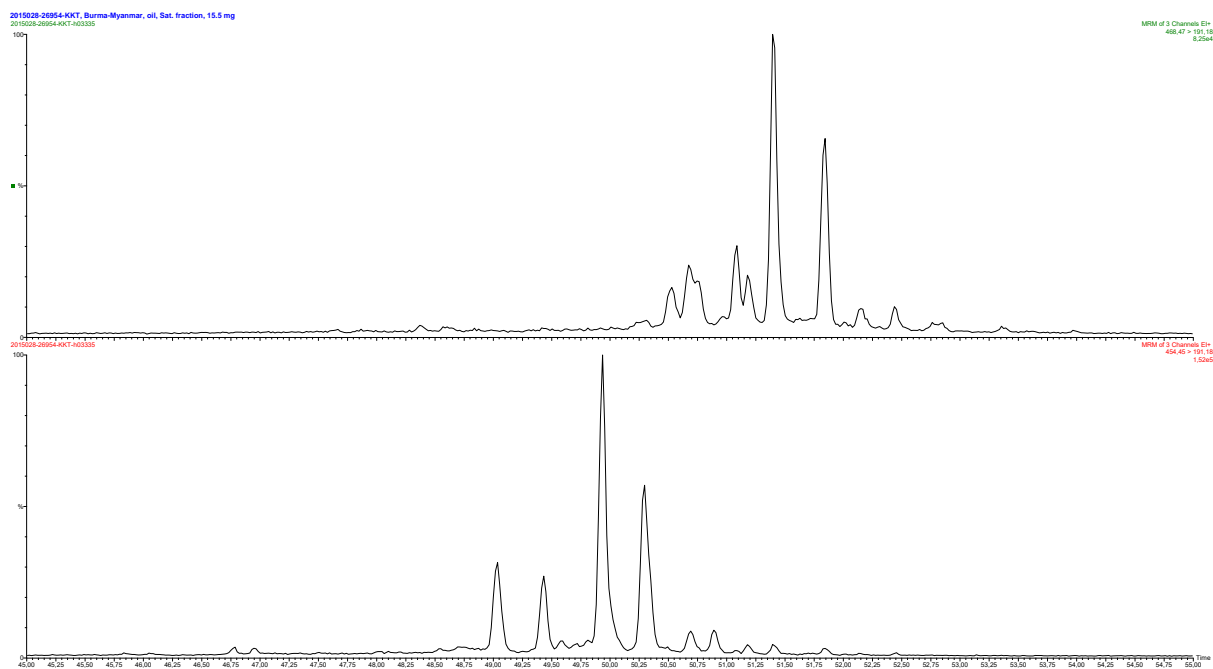
Sample 2015028-26925, GC-MSMS data



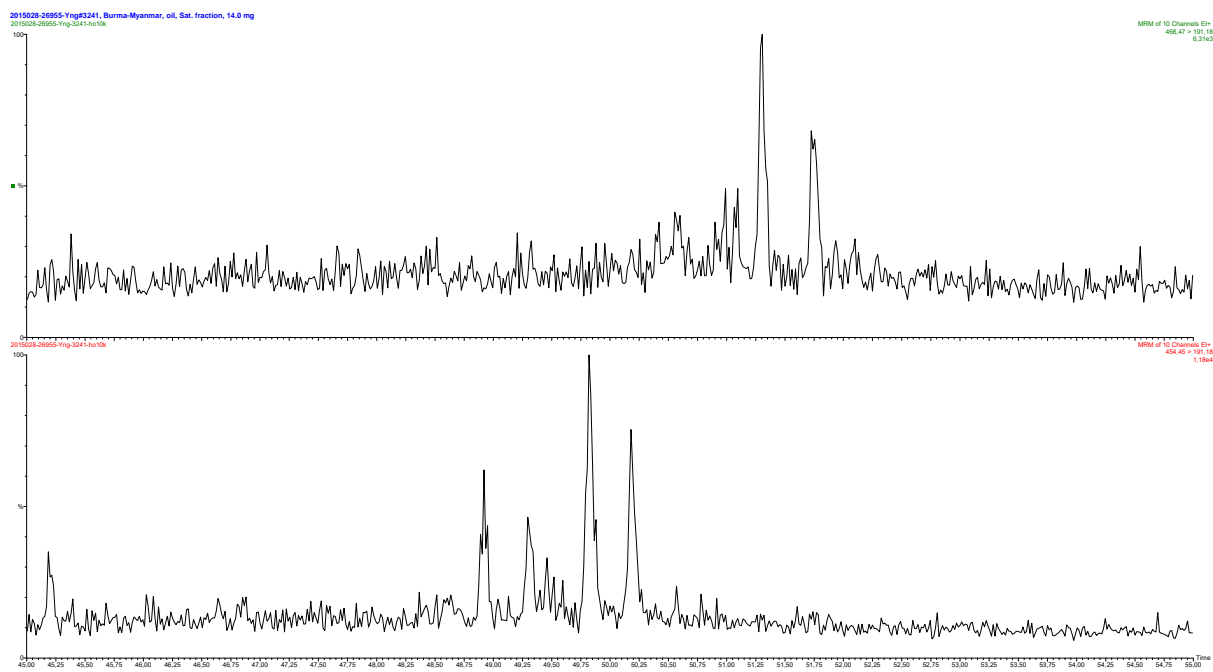
Sample 2015028-26926, GC-MSMS data



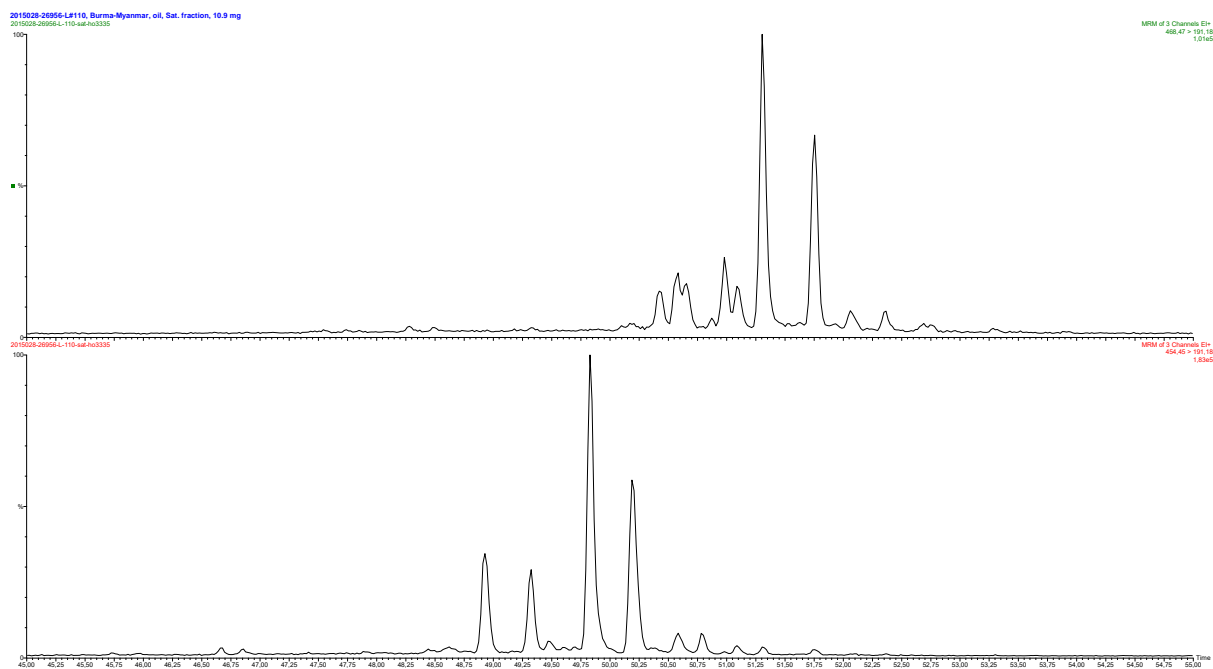
Sample 2015028-26927, GC-MSMS data



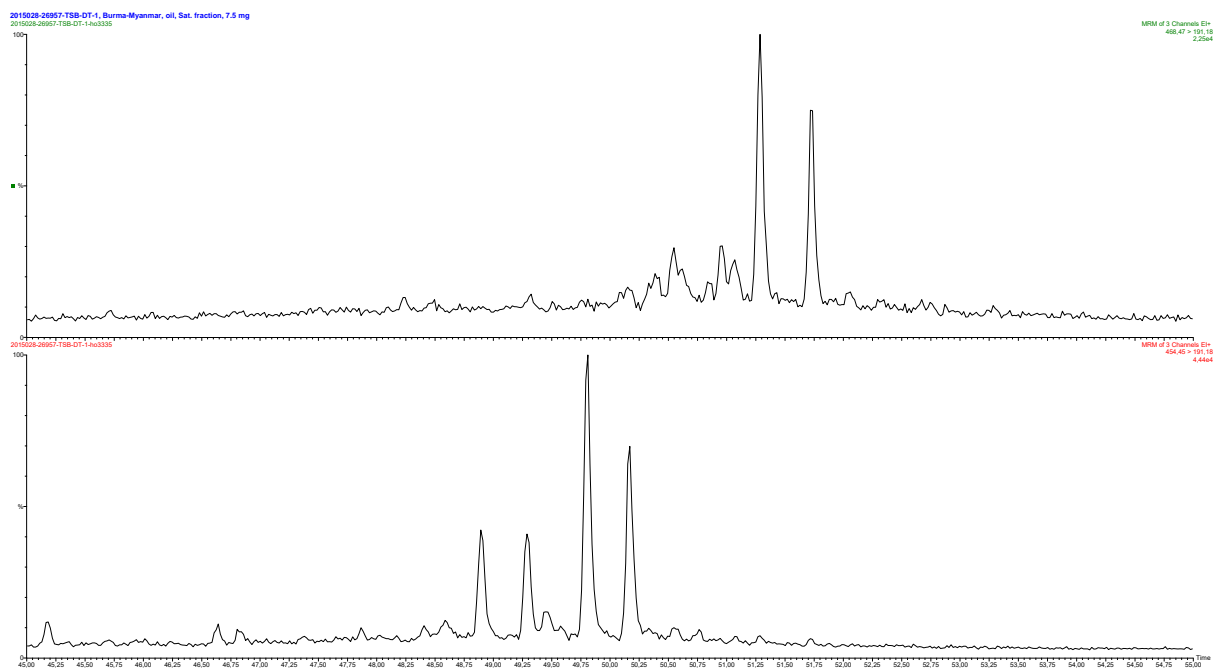
Sample 2015028-26954, GC-MSMS data



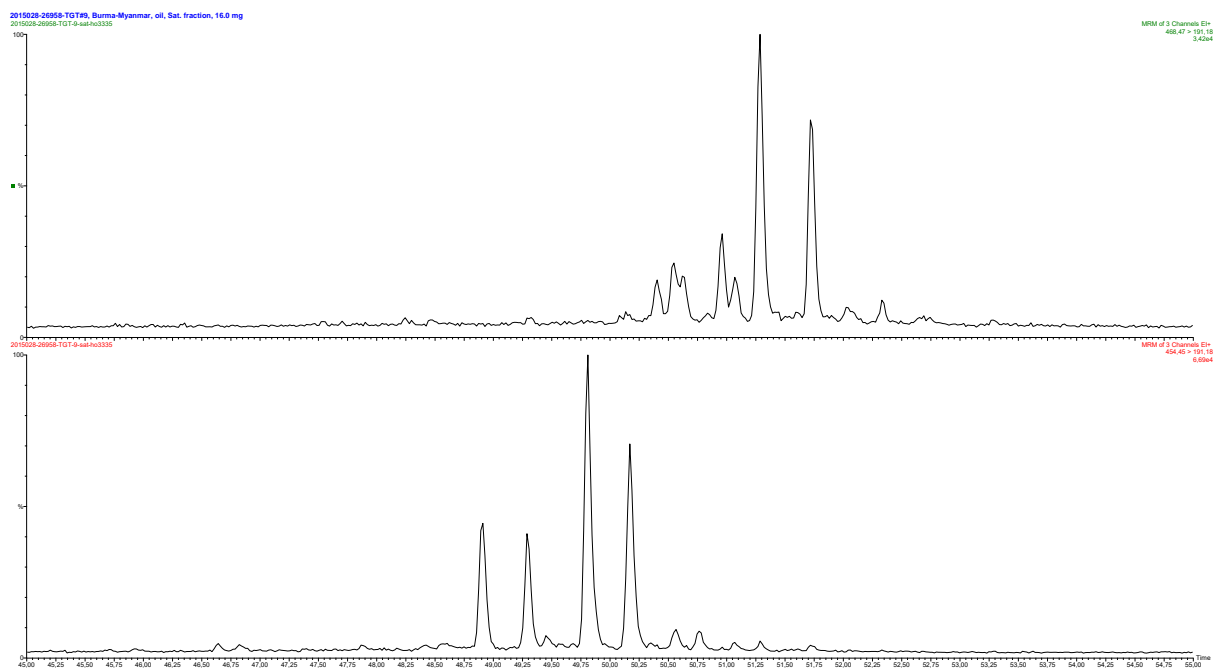
Sample 2015028-26955, GC-MSMS data



Sample 2015028-26956, GC-MSMS data



Sample 2015028-26957, GC-MSMS data



Sample 2015028-26958, GC-MSMS data

Appendix 5: Steranes

GC-MS-MS Parent \Rightarrow Daughter data

C₂₆-C₃₀ steranes

m/z 358 \Rightarrow 217

m/z 372 \Rightarrow 217

m/z 386 \Rightarrow 217

m/z 400 \Rightarrow 217

m/z 414 \Rightarrow 217

Lab. #	Alt. Lab. #	NDR	27%	28%	29%	30%	S27%	S28%	S29%	29S/S+R	$29\beta\beta / (\beta\beta + \alpha\alpha)$	D27 / RS27	D29 / RS29	S27 / S29
20150028-26919	548601	0,28	11,52	23,42	65,05	0,00	11,52	23,42	65,05	0,46	0,52	2,02	1,84	0,18
20150028-26920	548602	0,35	15,05	27,53	57,42	0,00	15,05	27,53	57,42	0,50	0,51	1,56	1,28	0,26
20150028-26921	548603	0,33	13,33	24,39	62,28	0,00	13,33	24,39	62,28	0,54	0,54	1,72	1,26	0,21
20150028-26922	548604	0,27	13,18	25,67	61,15	0,00	13,18	25,67	61,15	0,49	0,58	1,96	1,34	0,22
20150028-26923	548605	0,31	11,03	27,28	61,69	0,00	11,03	27,28	61,69	0,55	0,52	2,14	1,62	0,18
20150028-26924	548606	0,30	11,05	27,08	61,87	0,00	11,05	27,08	61,87	0,55	0,52	2,06	1,54	0,18
20150028-26925	548607	0,42	11,26	24,94	63,80	0,00	11,26	24,94	63,80	0,53	0,57	2,10	1,33	0,18
20150028-26926	548608	0,31	11,46	24,18	64,36	0,00	11,46	24,18	64,36	0,52	0,59	2,35	1,40	0,18
20150028-26927	548609	0,30	9,66	24,00	66,34	0,00	9,66	24,00	66,34	0,52	0,55	2,36	1,49	0,15
20150028-26953	CHK # 1101	0,39	11,19	23,59	65,22	0,00	11,19	23,59	65,22	0,50	0,52	1,73	1,39	0,17
20150028-26954	KKT	0,34	9,19	26,70	64,11	0,00	9,19	26,70	64,11	0,46	0,47	2,77	1,97	0,14
20150028-26955	Yng # 3241	0,33	15,50	26,02	58,49	0,00	15,50	26,02	58,49	0,50	0,51	1,72	1,55	0,26
20150028-26956	L # 110	0,31	10,20	27,10	62,70	0,00	10,20	27,10	62,70	0,48	0,50	2,40	1,79	0,16
20150028-26957	TSB-DT-1	0,32	13,20	27,25	59,55	0,00	13,20	27,25	59,55	0,54	0,52	1,90	1,22	0,22
20150028-26958	TGT # 9	0,35	11,62	26,78	61,60	0,00	11,62	26,78	61,60	0,49	0,55	2,61	1,56	0,19

NDR = nordiacholestanate ratio (Holba et al. 1998)

27%, 28%, 29%, 30% = normalised distribution of C₂₇₋₃₀ total steranes

S27%, S28%, S29% = normalised distribution of C₂₇₋₂₉ total steranes

29 S/S+R = C₂₉ sterane 20S/(20S+20R) isomerisation ratio

29 ββ/(ββ+αα) = C₂₉ sterane αββ/(αββ+ααα) isomerisation ratio

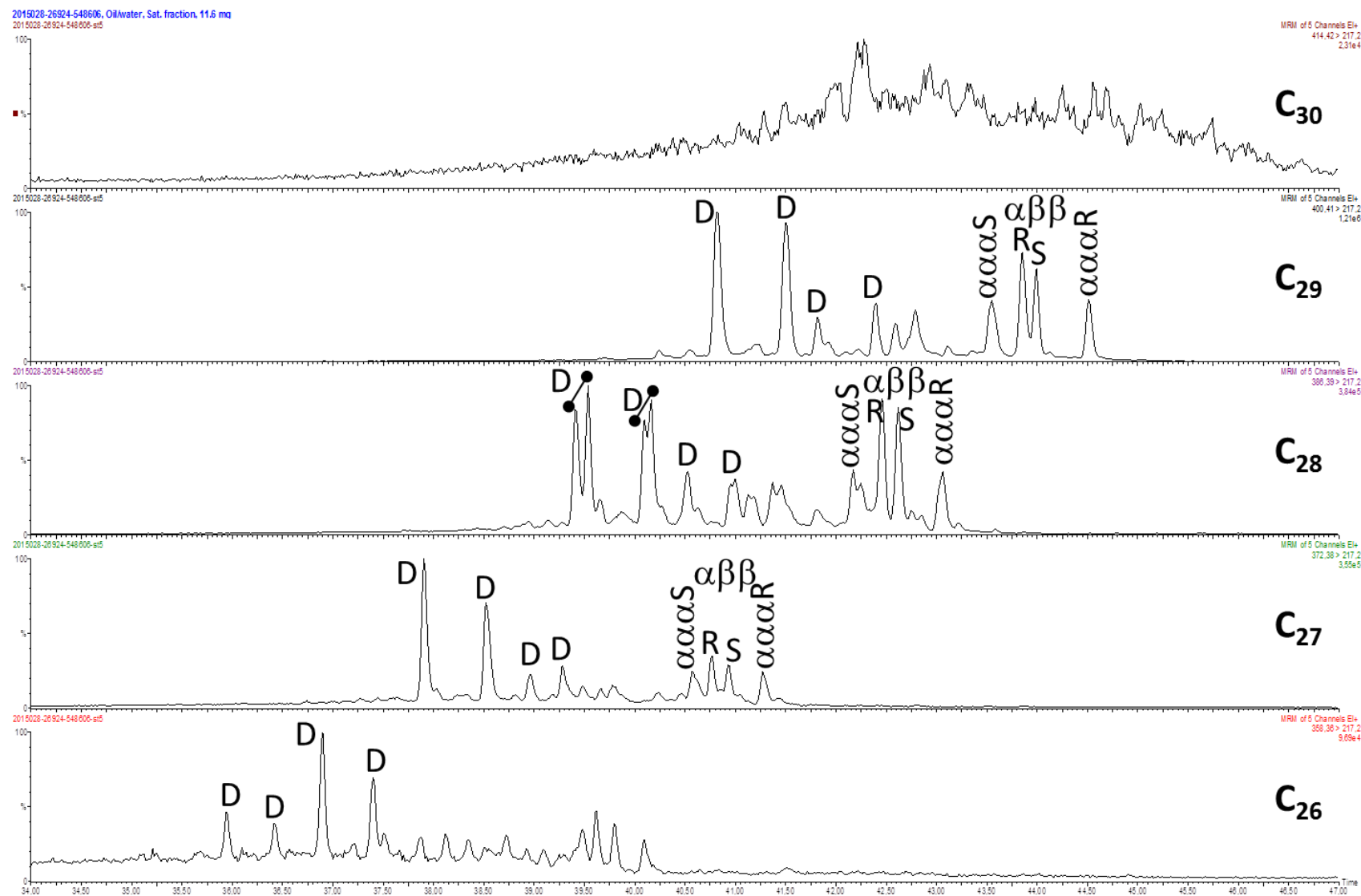
D27/RS27 = Ratio of total C₂₇ diasteranes to total C₂₇ regular steranes

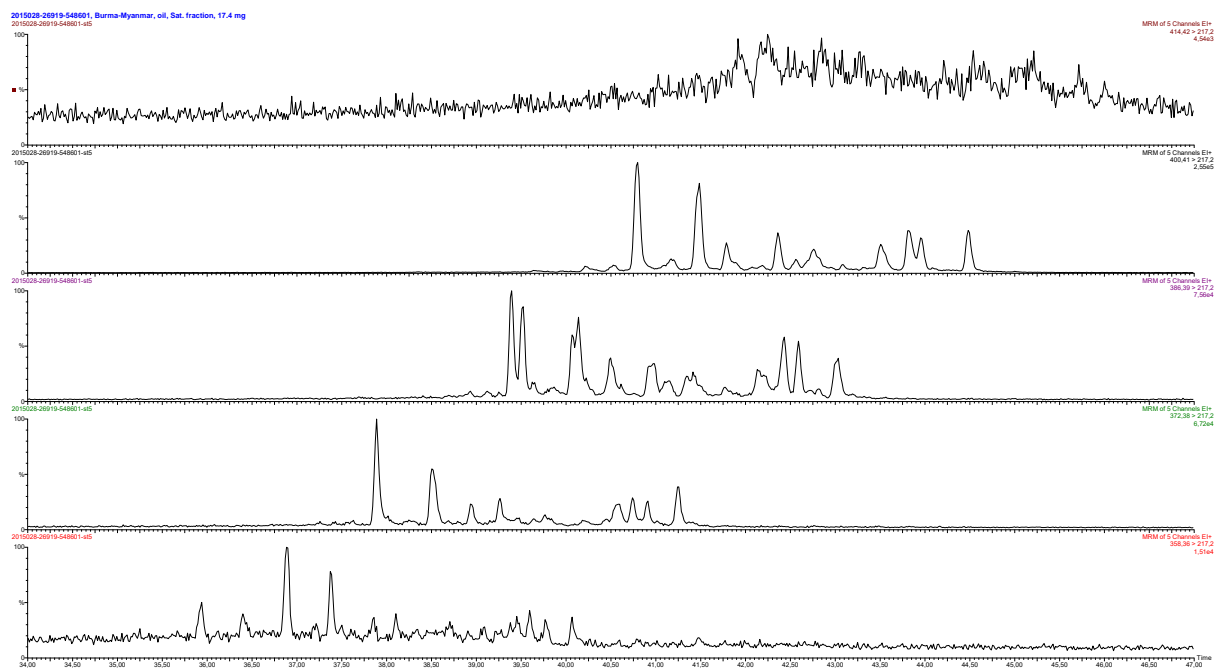
D29/RS29 = Ratio of total C₂₉ diasteranes to total C₂₉ regular steranes

S27/S29 = Ratio of total C₂₇ steranes to total C₂₉ steranes

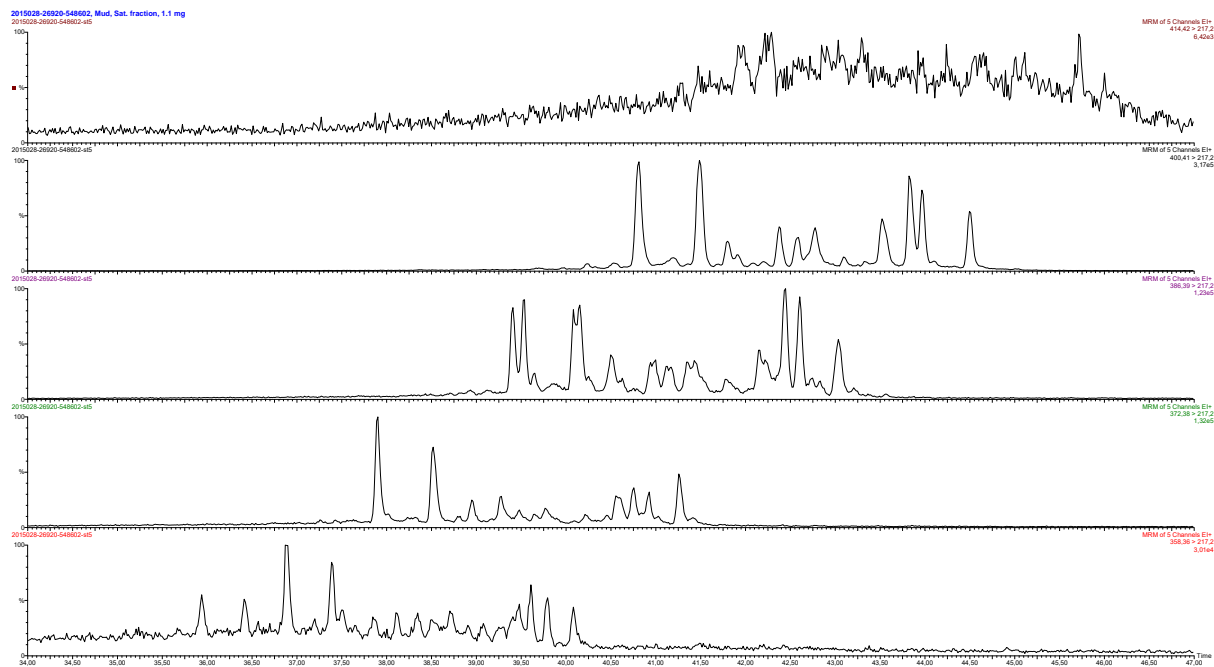
[93]

Compound identification key

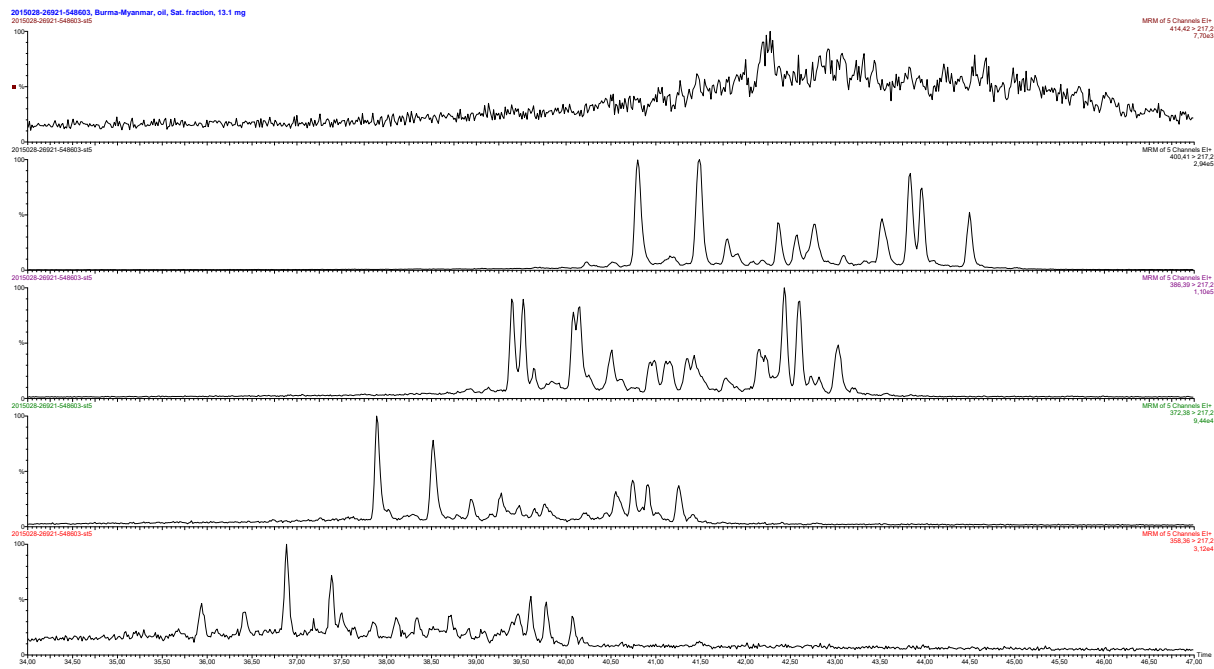




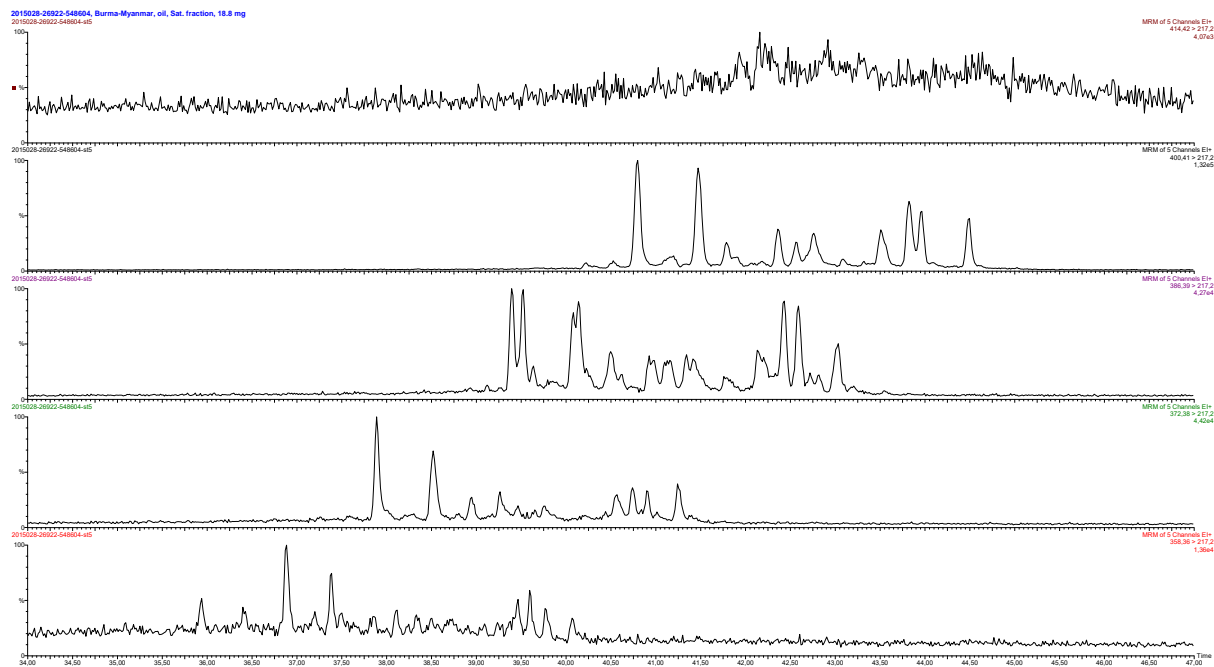
Sample 2015028-26919, GC-MSMS data



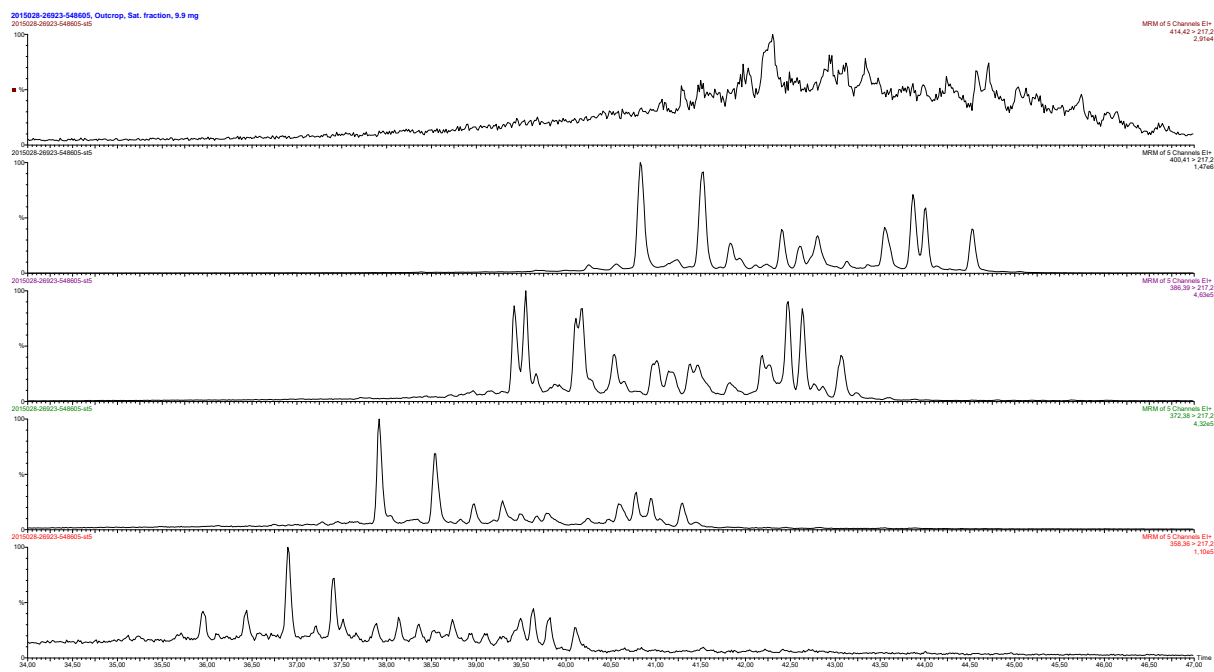
Sample 2015028-26920, GC-MSMS data



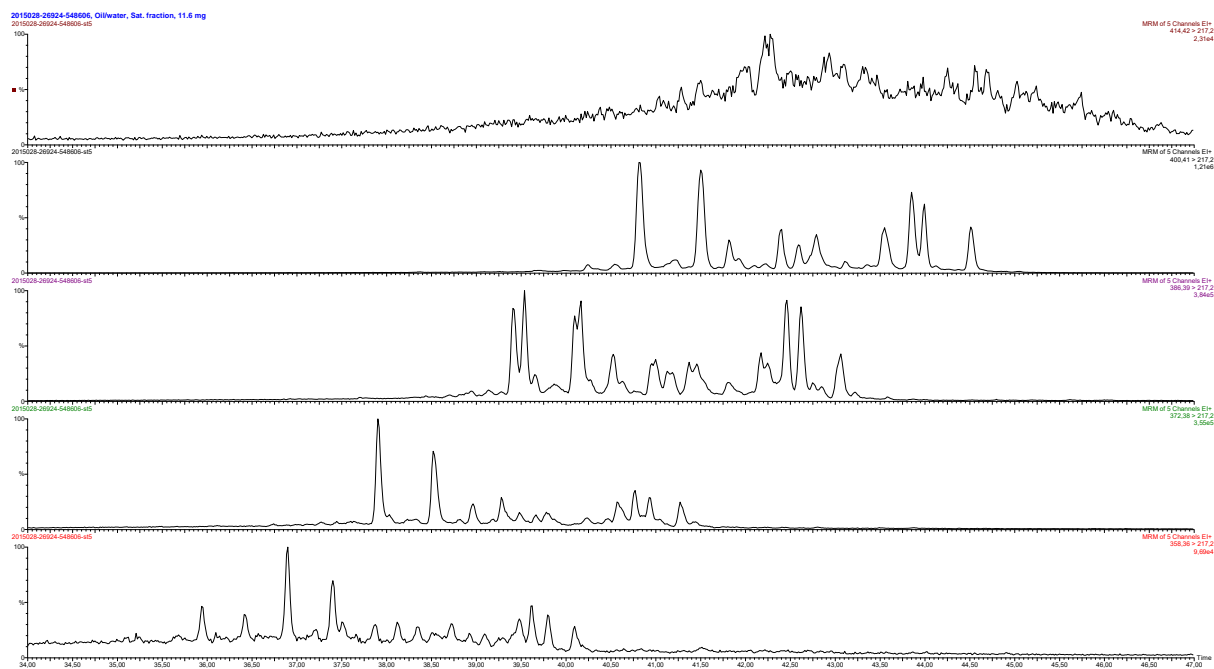
Sample 2015028-26921, GC-MSMS data



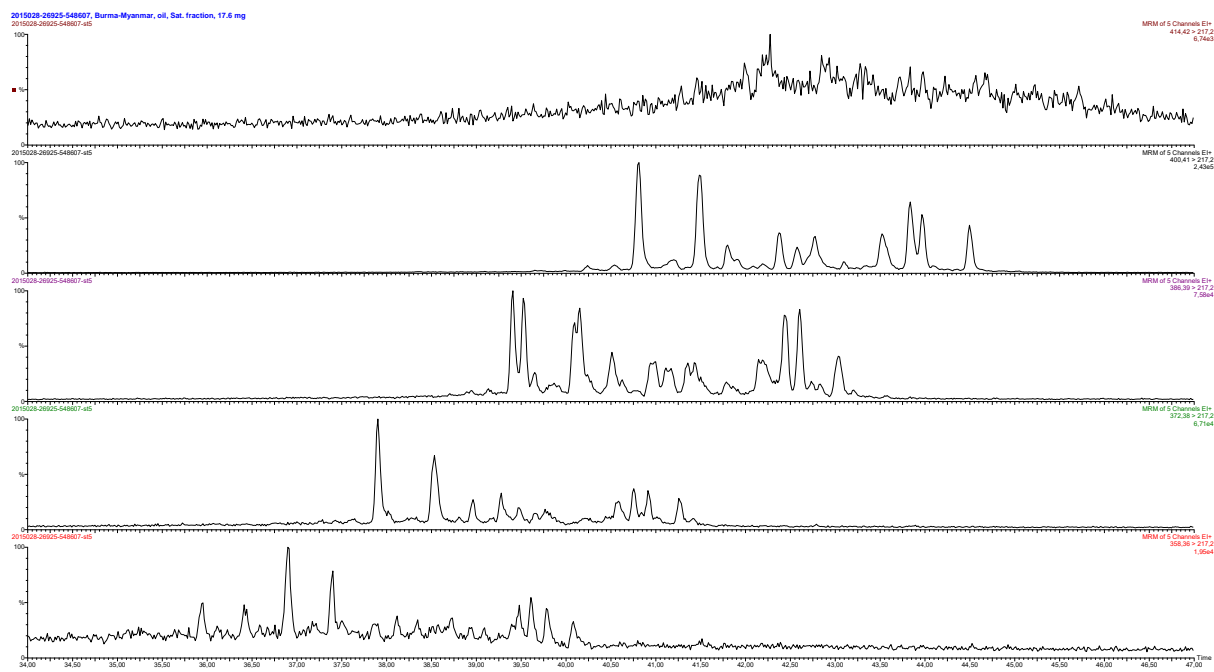
Sample 2015028-26922, GC-MSMS data



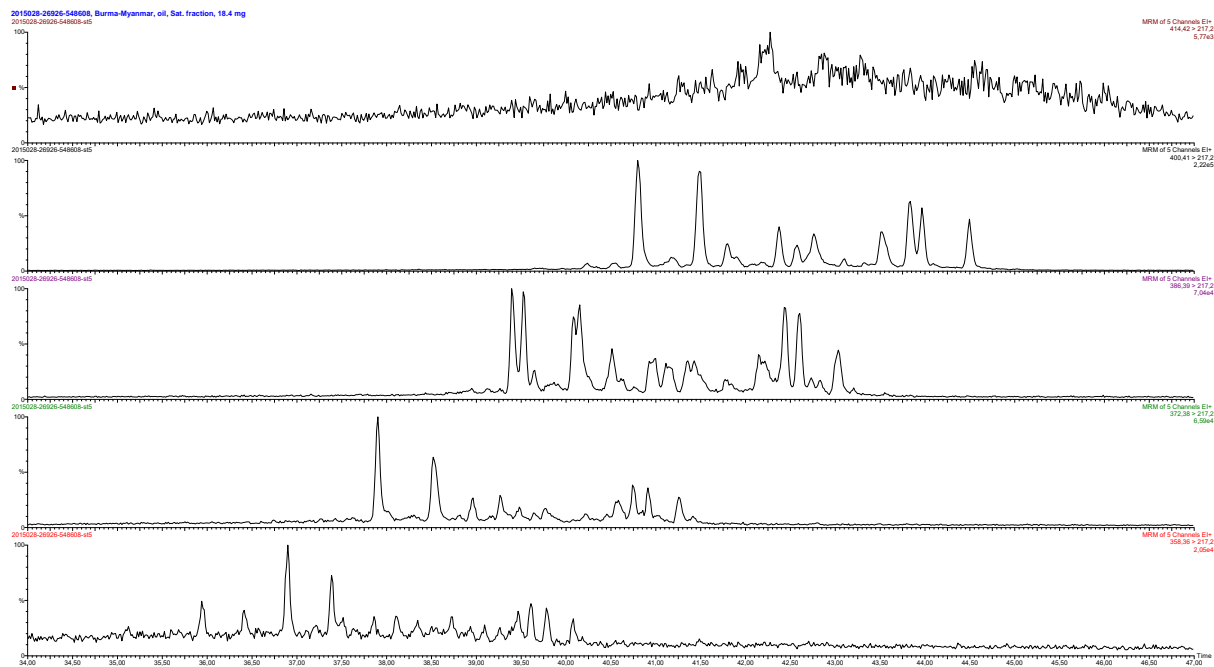
Sample 2015028-26923, GC-MSMS data



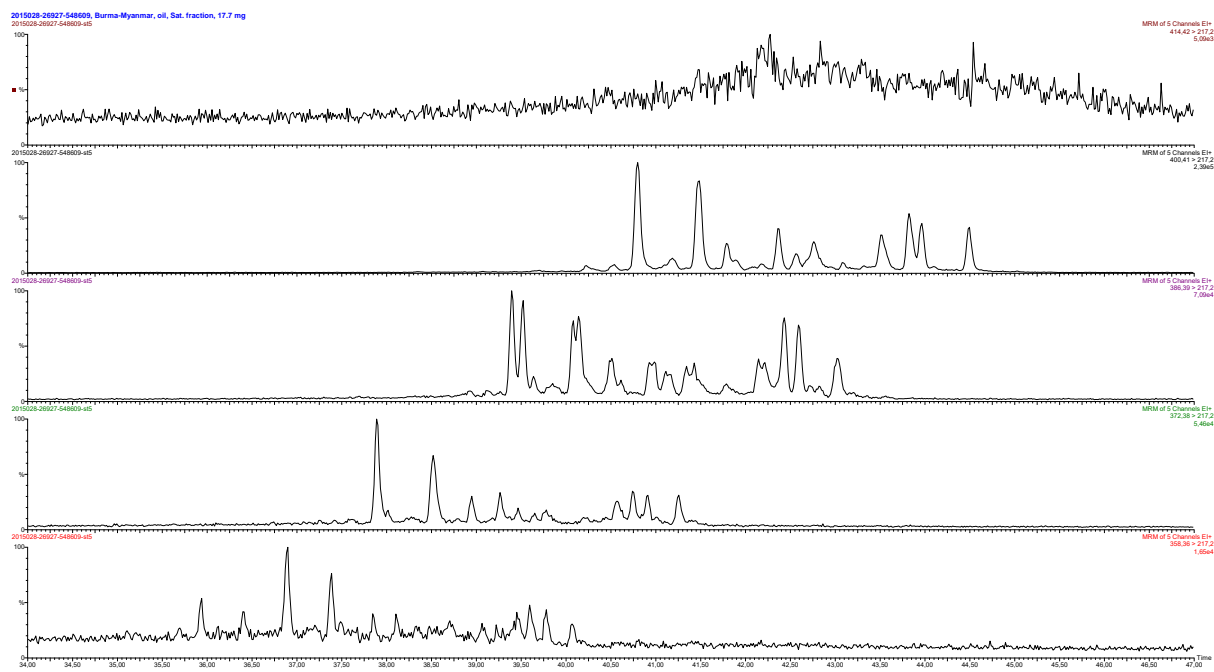
Sample 2015028-26924, GC-MSMS data



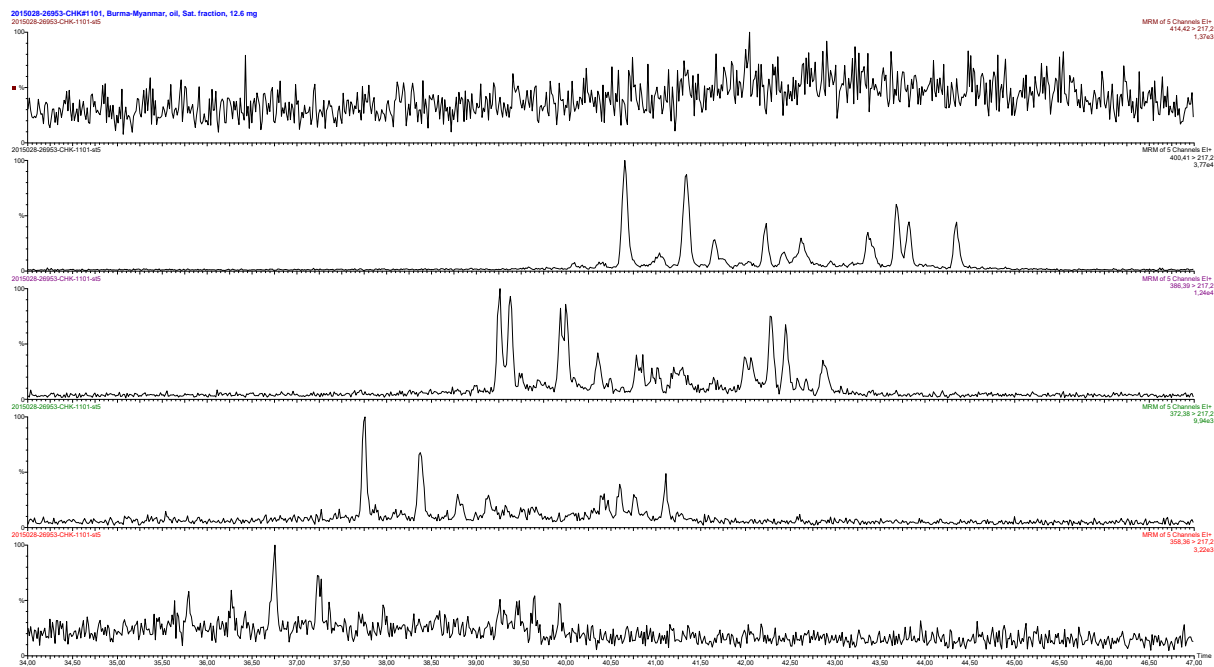
Sample 2015028-26925, GC-MSMS data



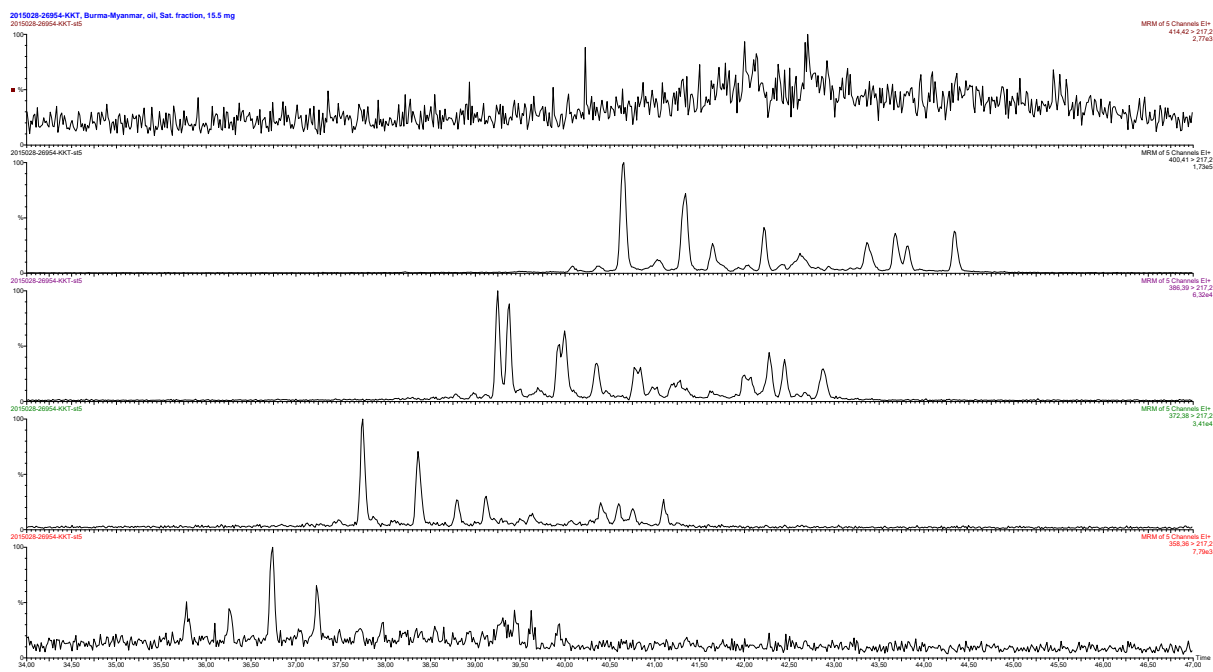
Sample 2015028-26926, GC-MSMS data



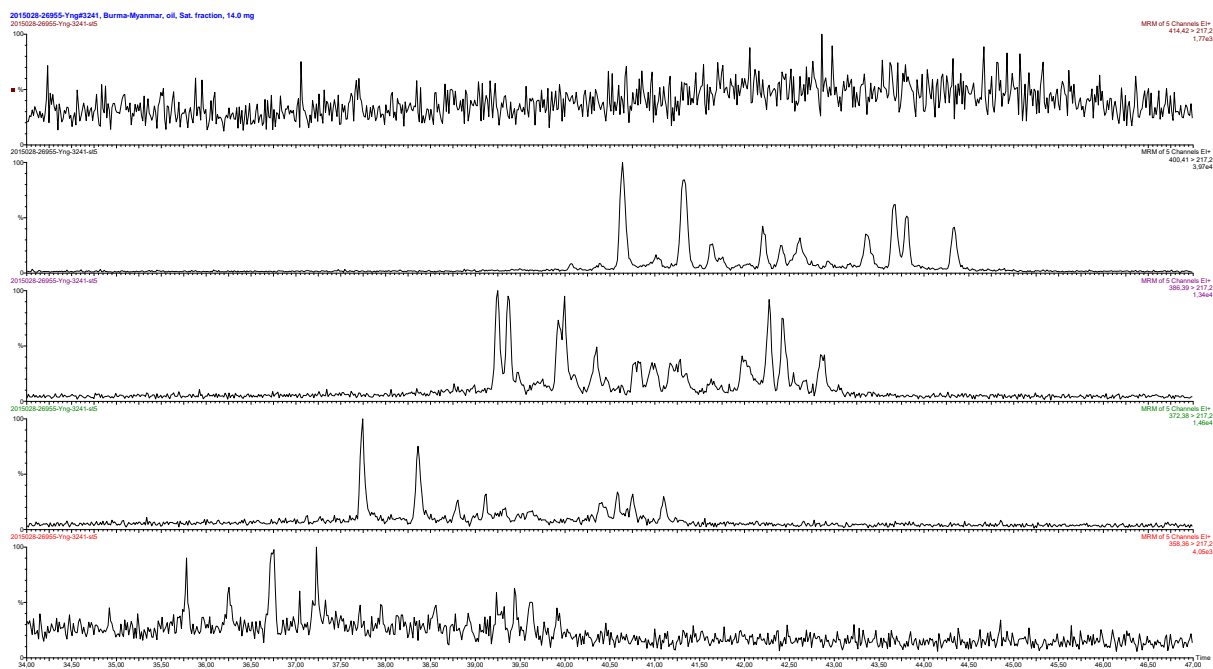
Sample 2015028-26927, GC-MSMS data



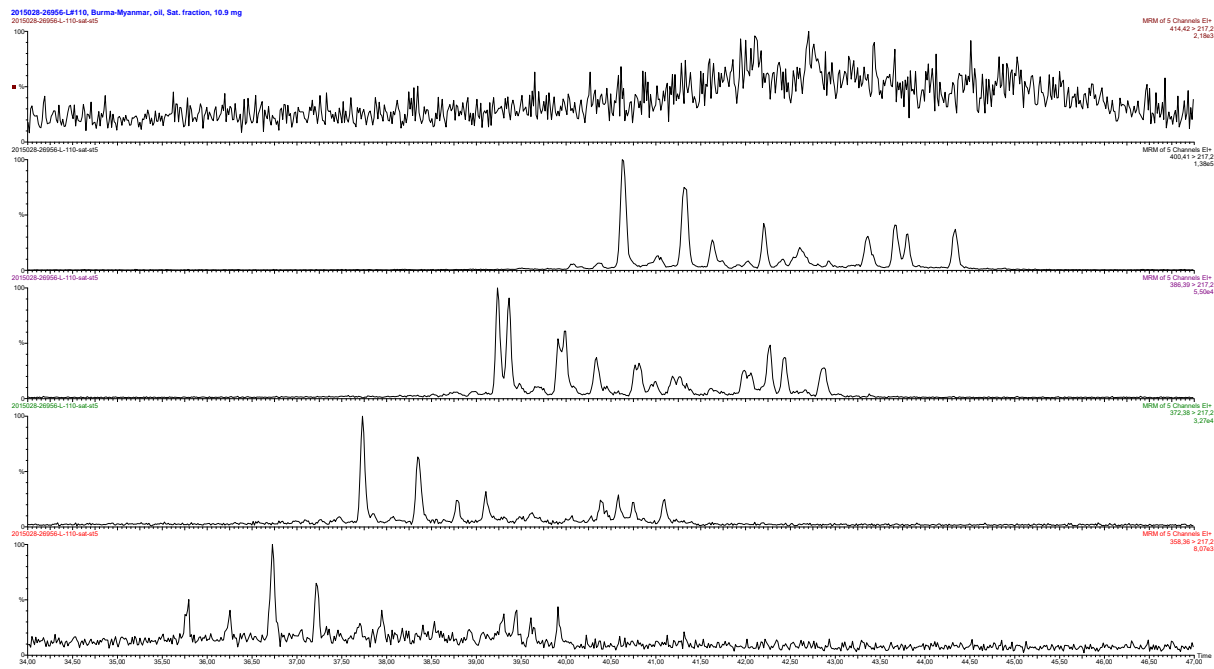
Sample 2015028-26953, GC-MSMS data



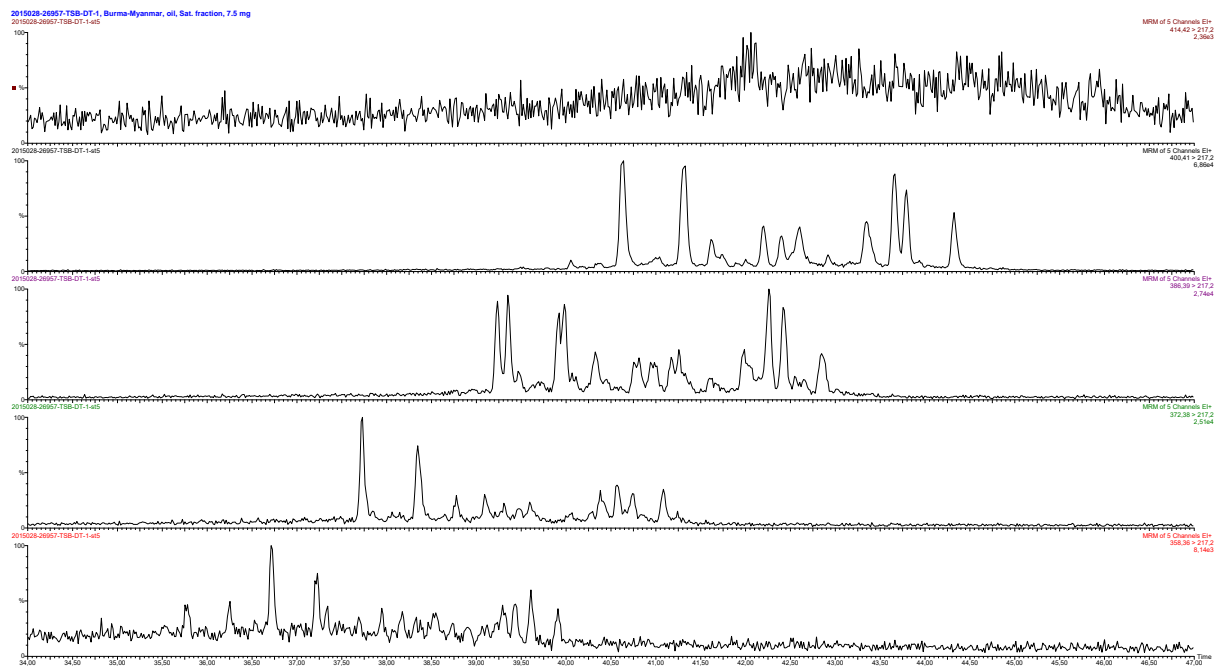
Sample 2015028-26954, GC-MSMS data



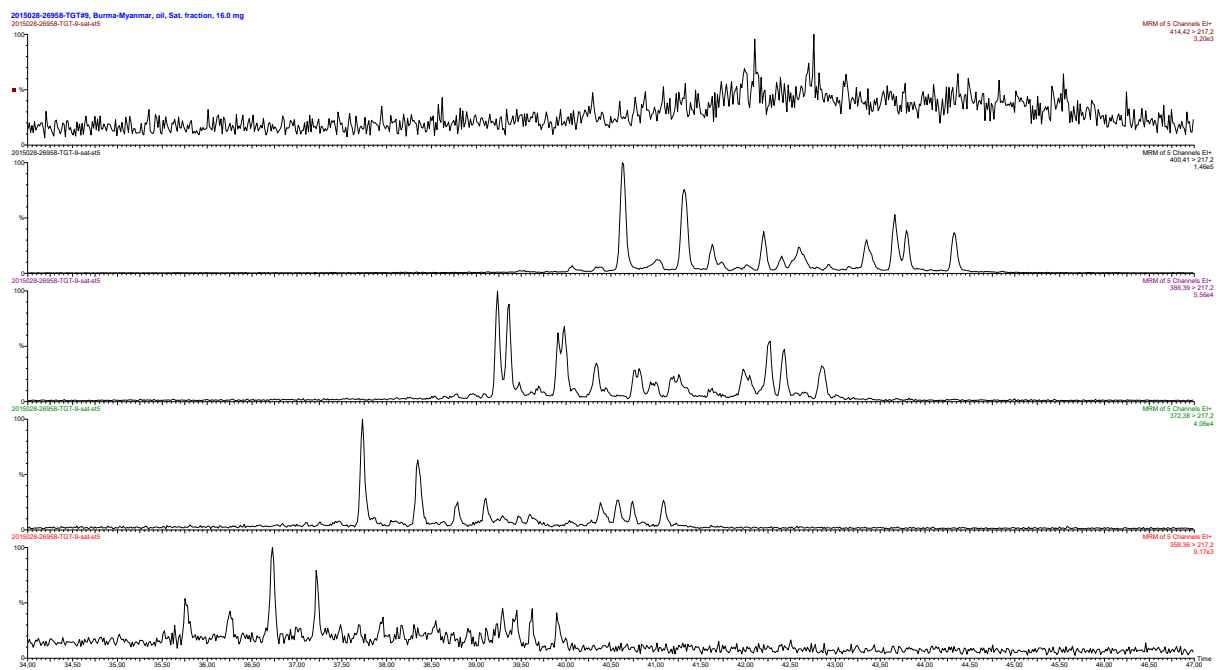
Sample 2015028-26955, GC-MSMS data



Sample 2015028-26956, GC-MSMS data



Sample 2015028-26957, GC-MSMS data



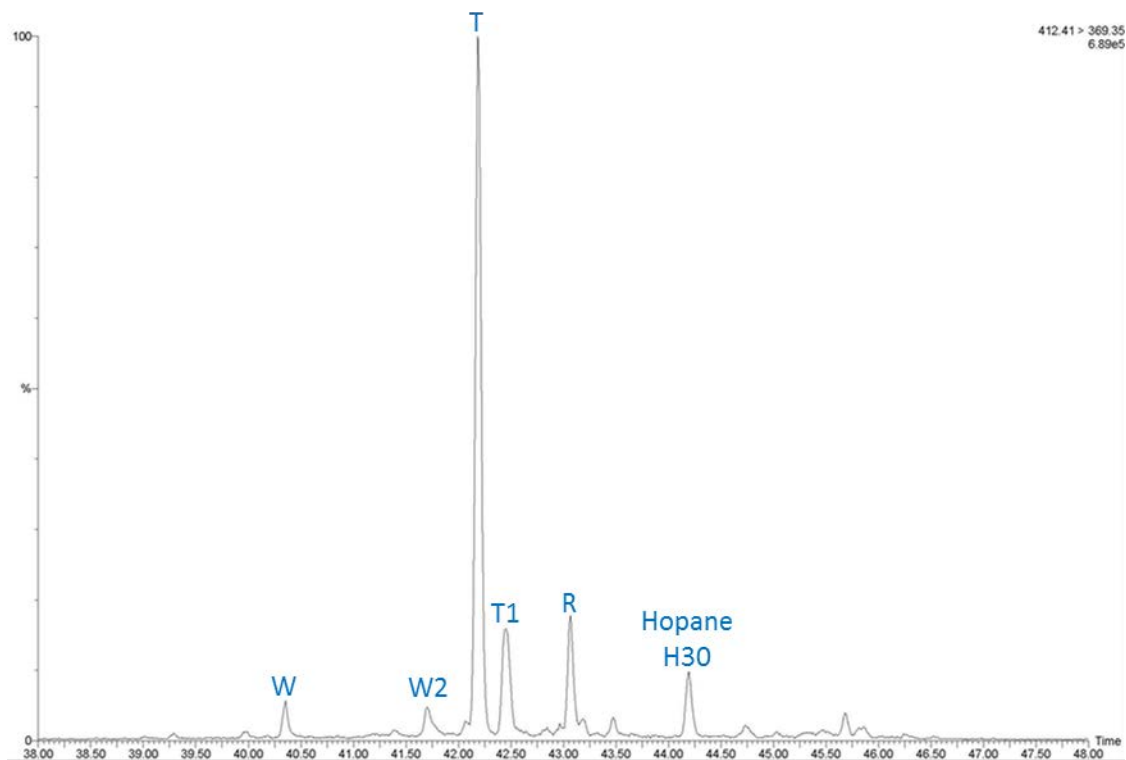
Sample 2015028-26958, GC-MSMS data

Appendix 6: Bicadinanes

GC-MS-MS Parent⇒Daughter data

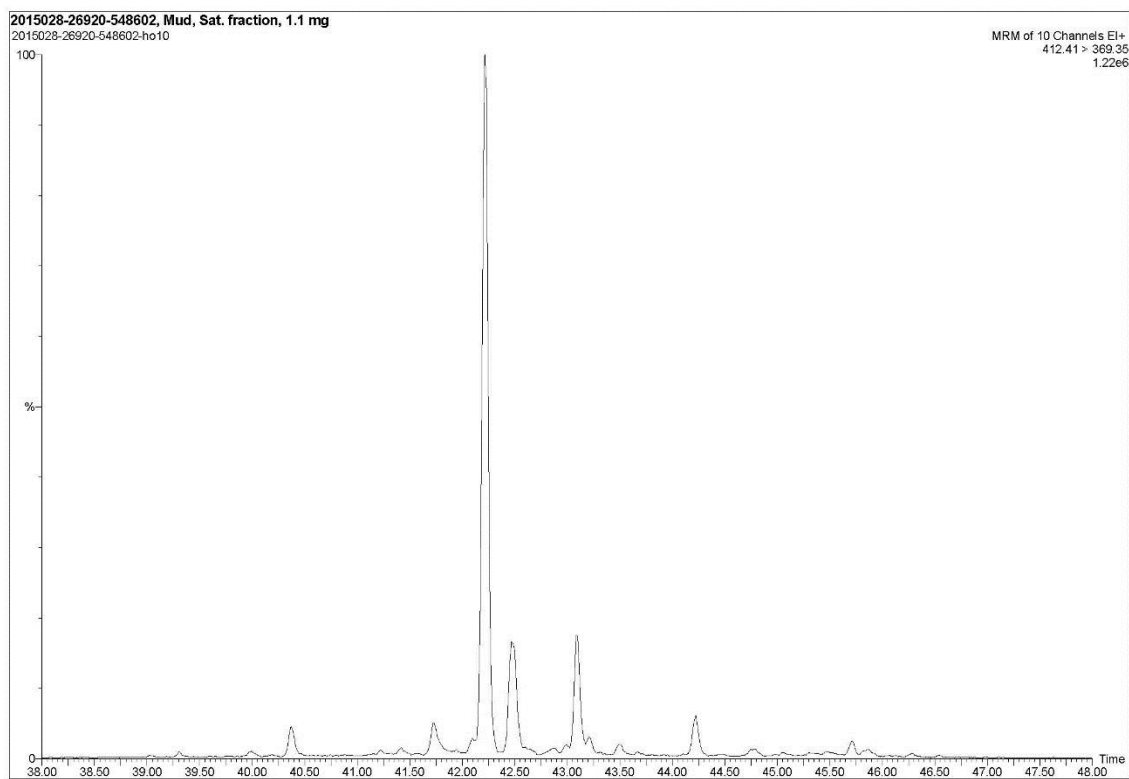
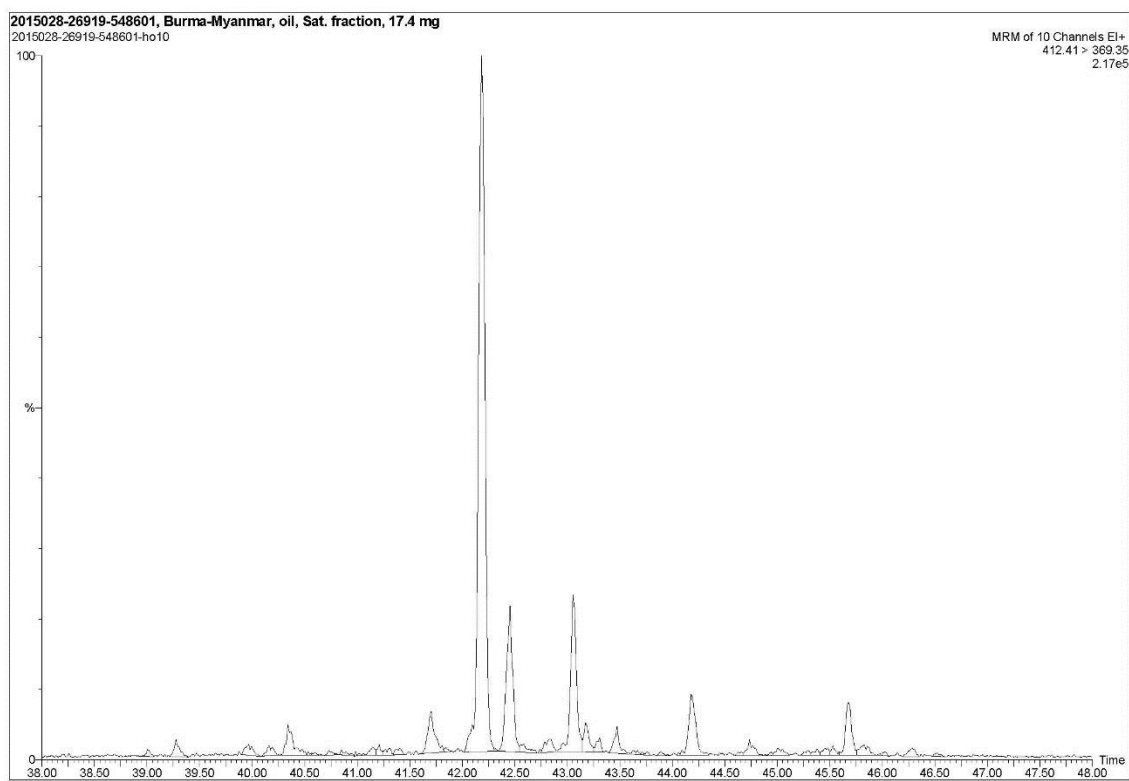
Bicadinanes

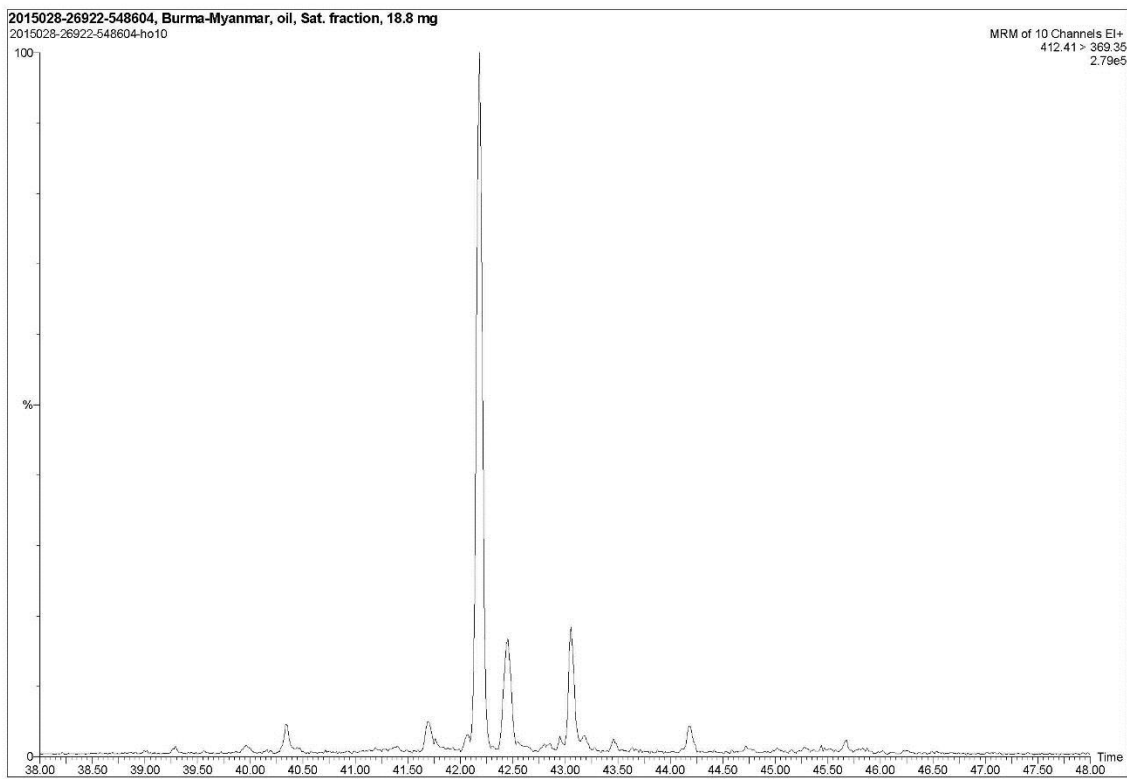
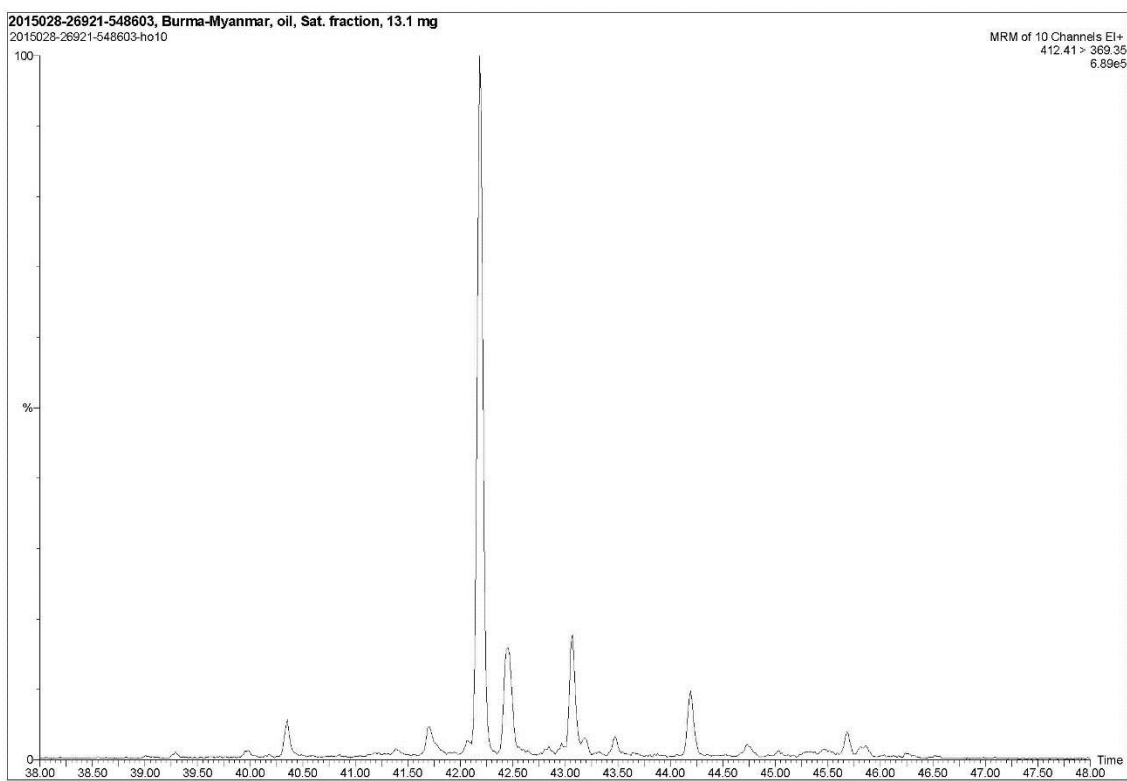
m/z 412⇒369

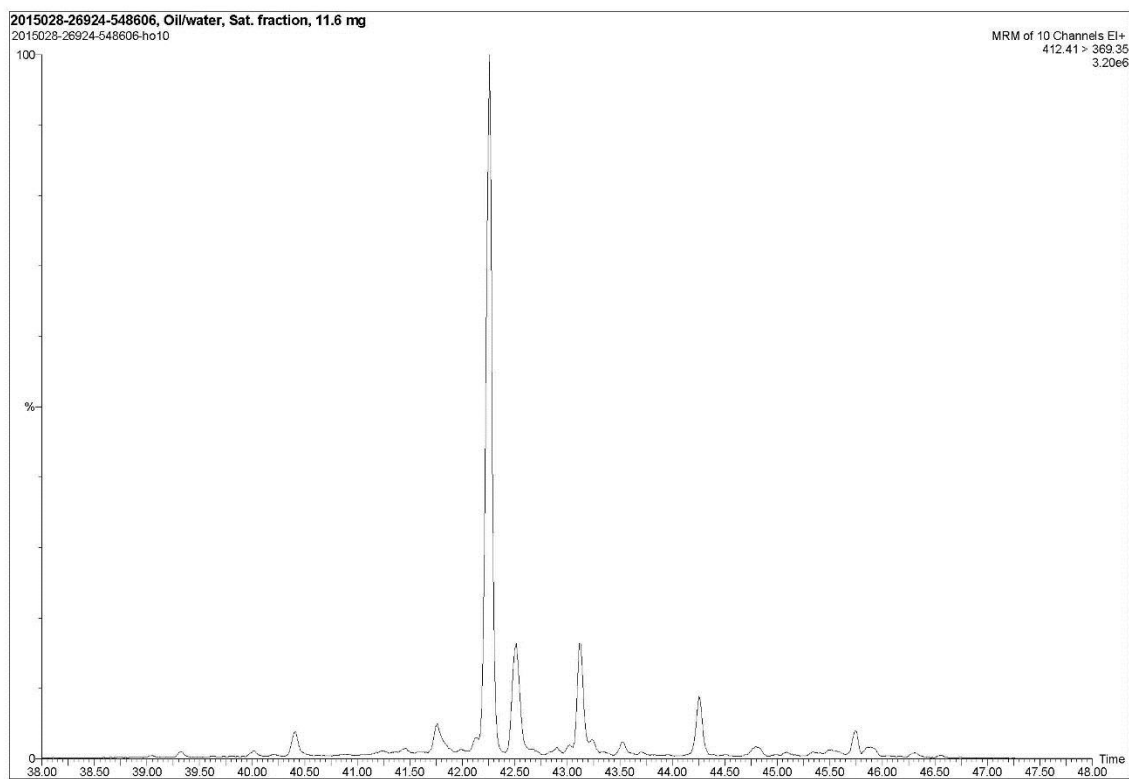
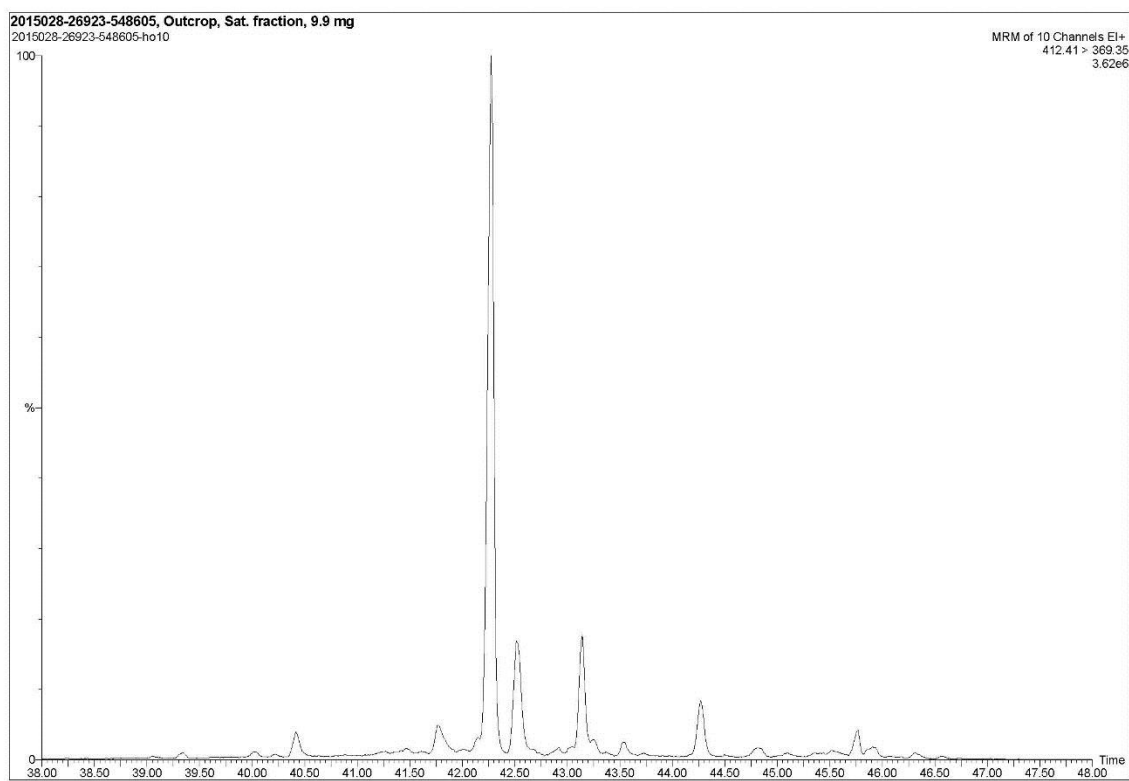


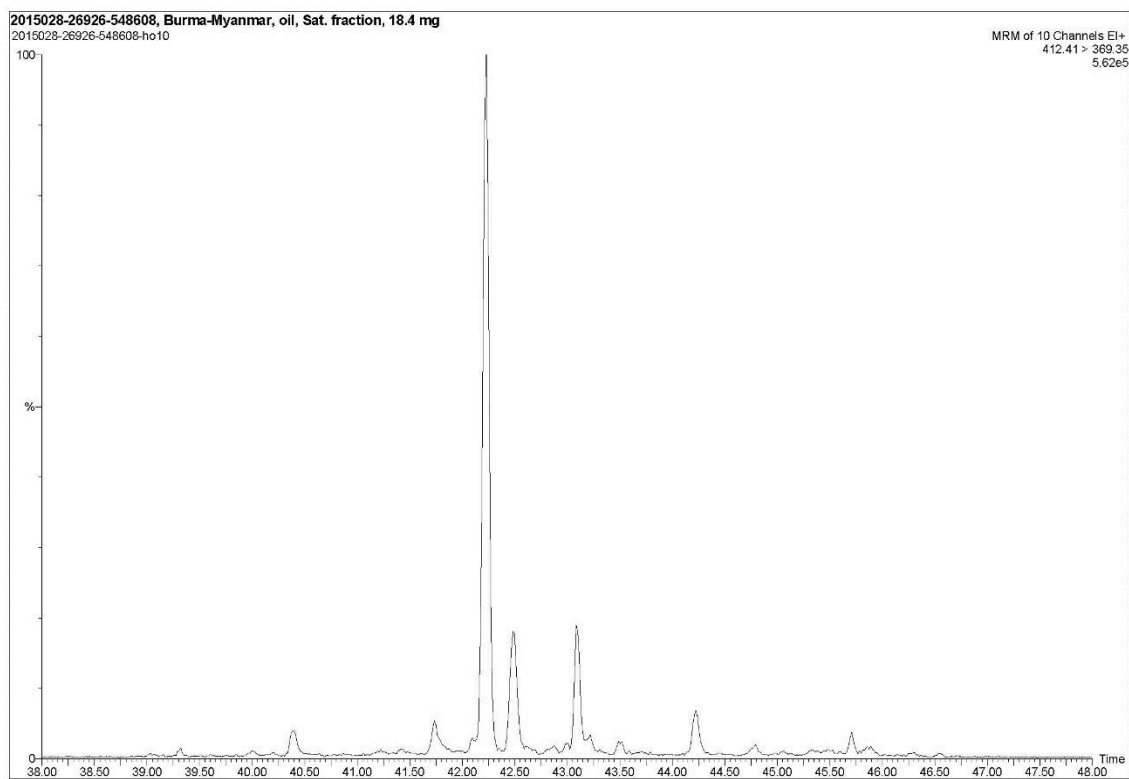
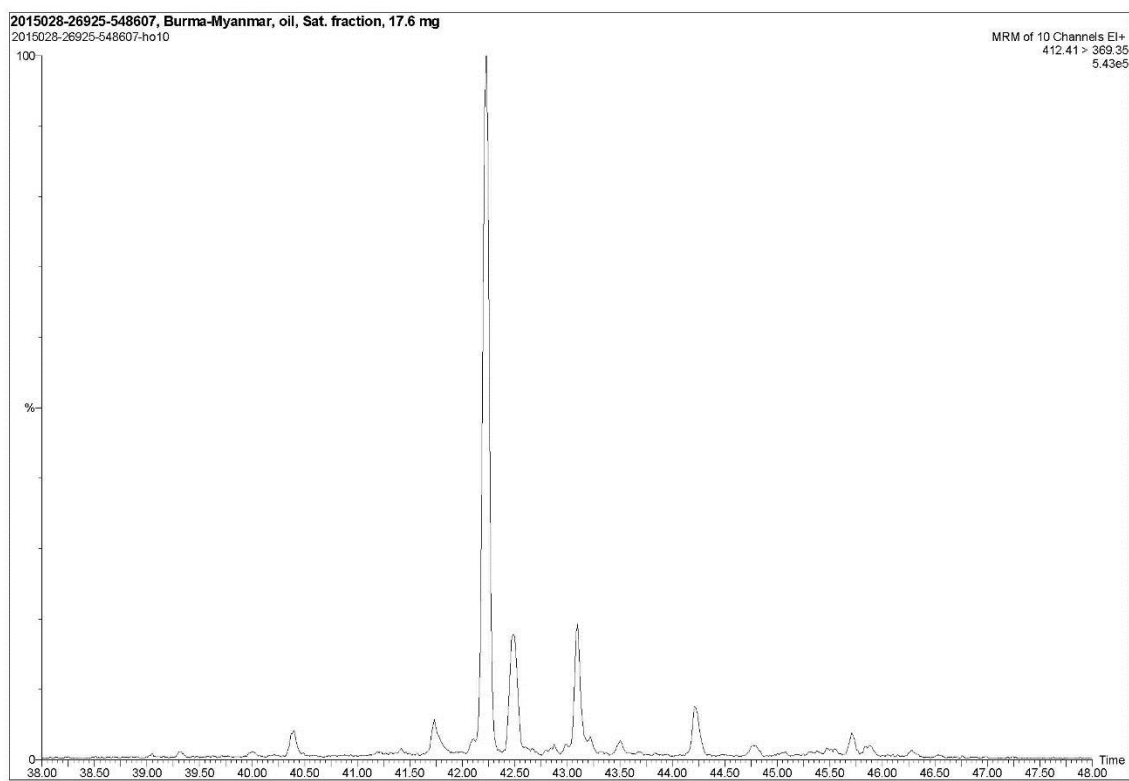
Bicadinane compound identification key

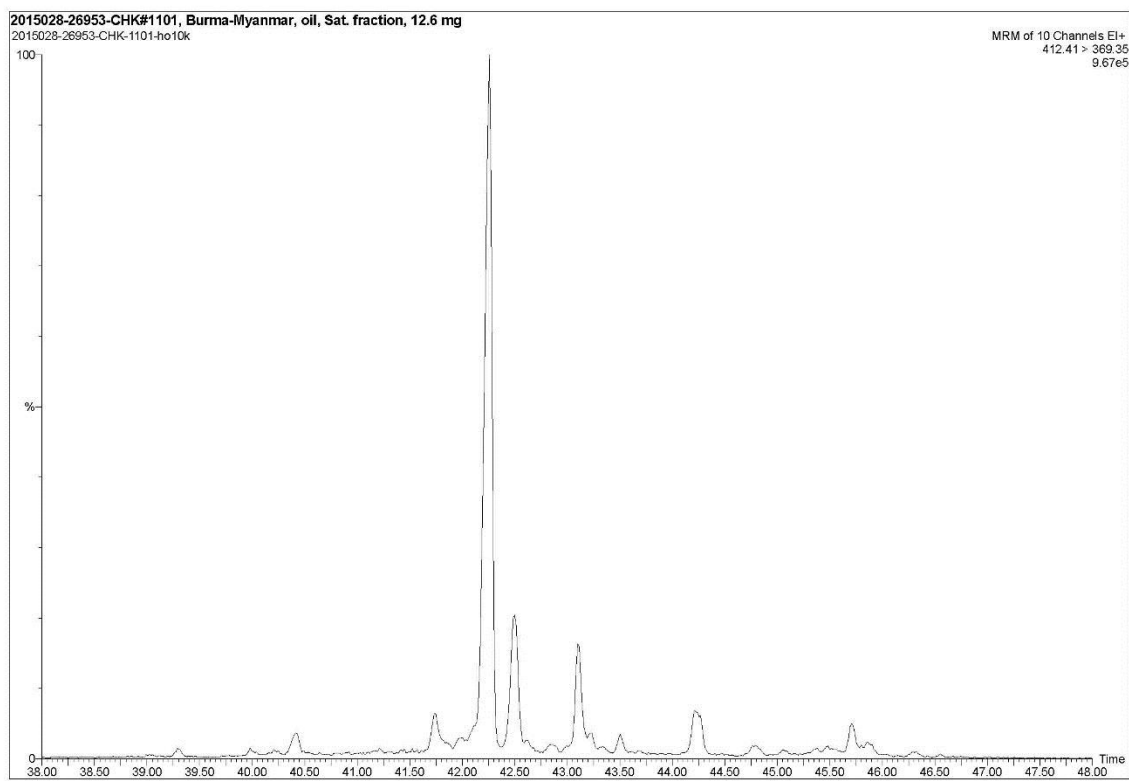
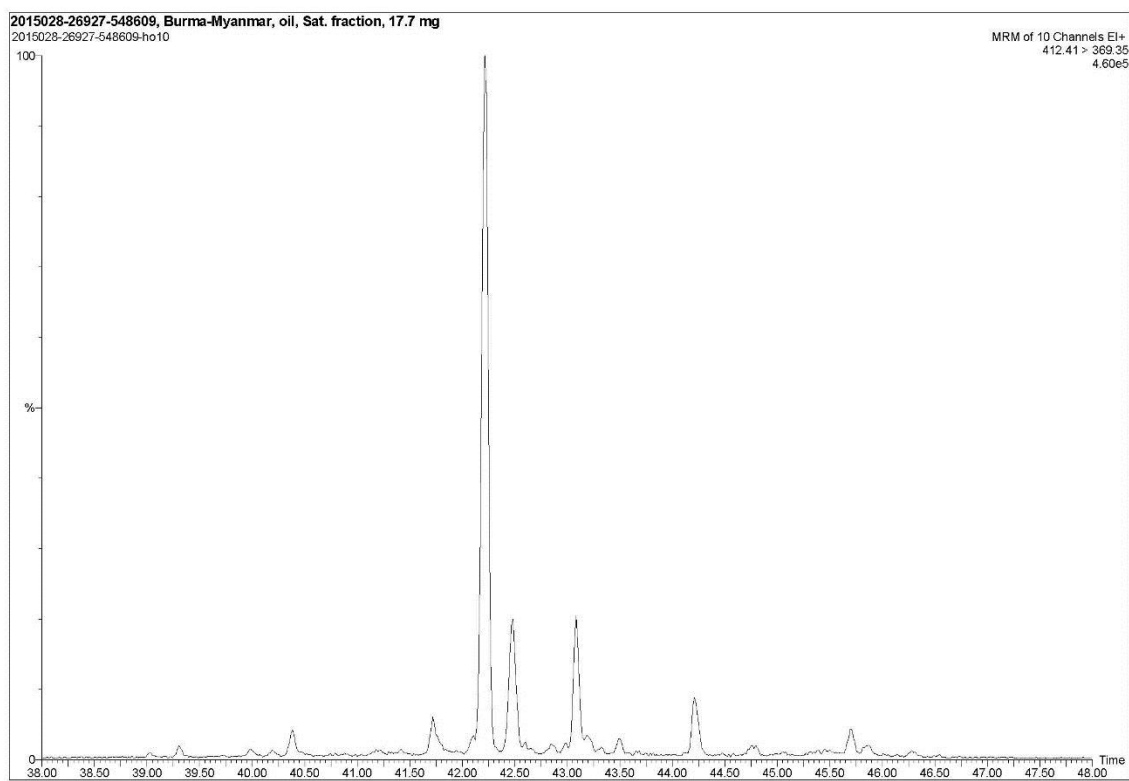
Lab. #	Alt. Lab. #	T/(T+H30)	BMI1
20150028-26919	548601	0,93	2,5
20150028-26920	548602	0,98	2,6
20150028-26921	548603	0,97	2,6
20150028-26922	548604	0,99	2,7
20150028-26923	548605	0,96	2,7
20150028-26924	548606	0,96	2,7
20150028-26925	548607	0,97	2,5
20150028-26926	548608	0,97	2,6
20150028-26927	548609	0,96	2,7
20150028-26953	CHK # 1101	0,96	3,0
20150028-26954	KKT	0,63	3,6
20150028-26955	Yng # 3241	0,83	2,7
20150028-26956	L # 110	0,63	2,8
20150028-26957	TSB-DT-1	0,96	2,7
20150028-26958	TGT # 9	0,73	2,0
T/(T+H30) = ratio of bicadinane T to bicadinane T + hopane			
BMI1 = bicadinane maturation index (Murray et al. 1994)			

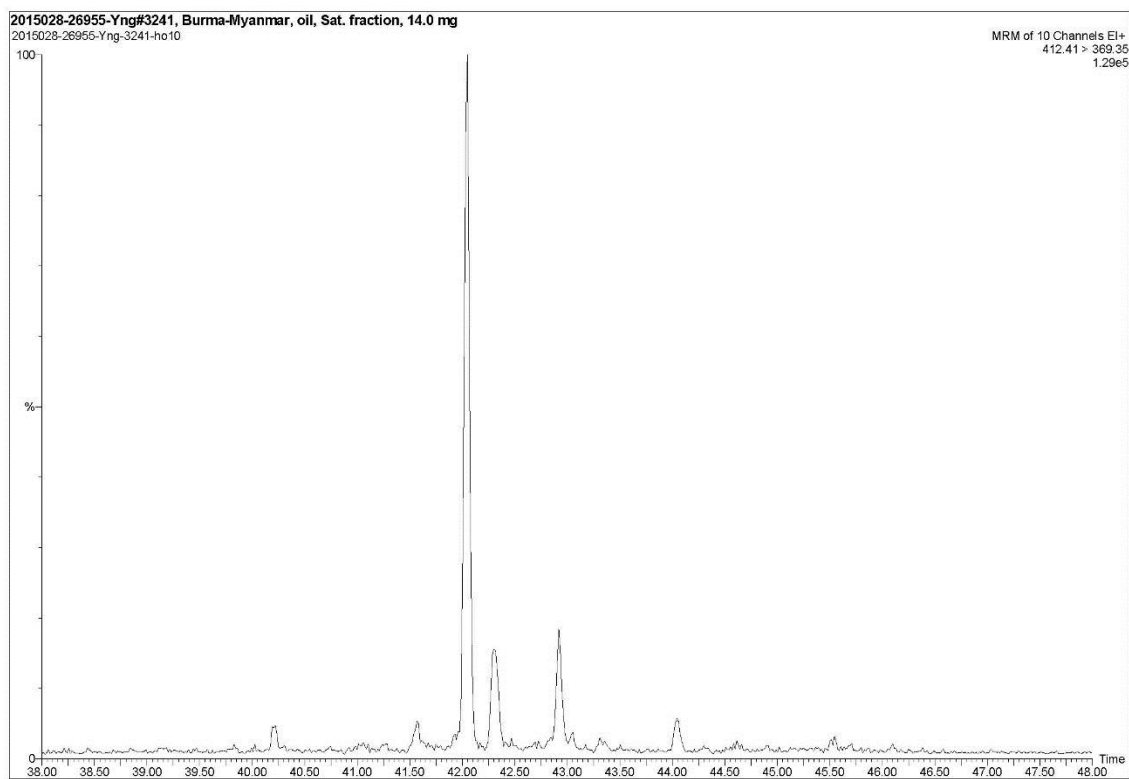
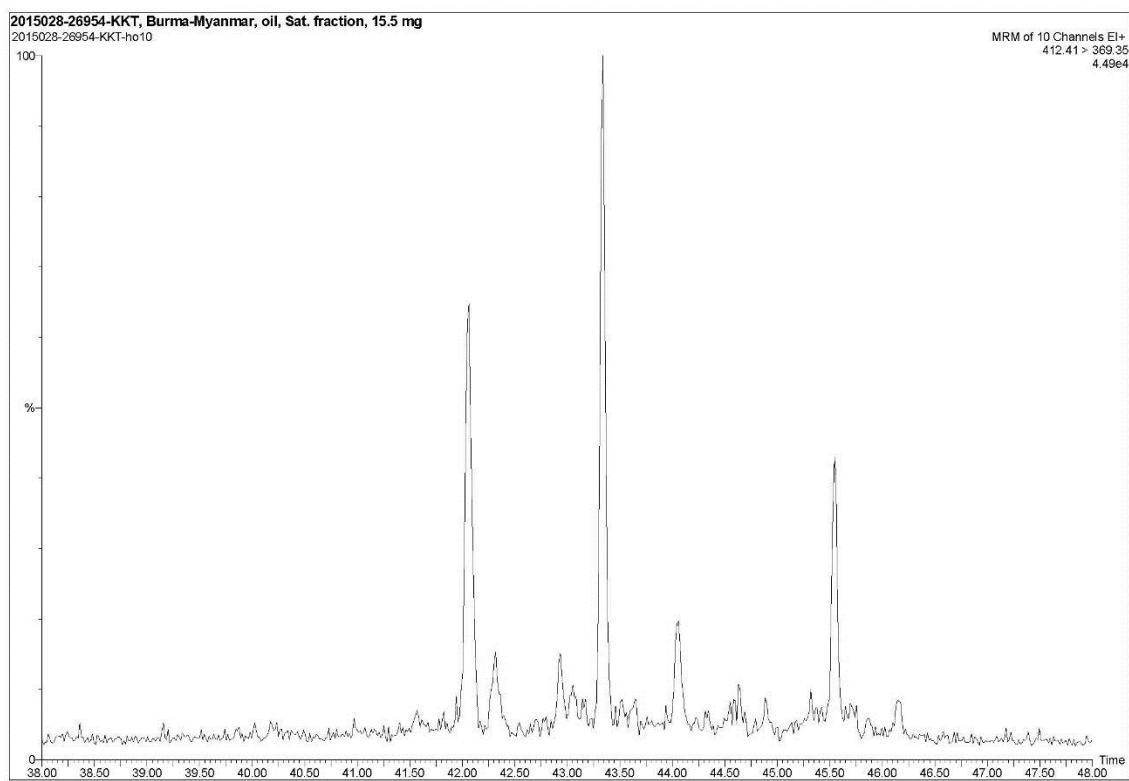


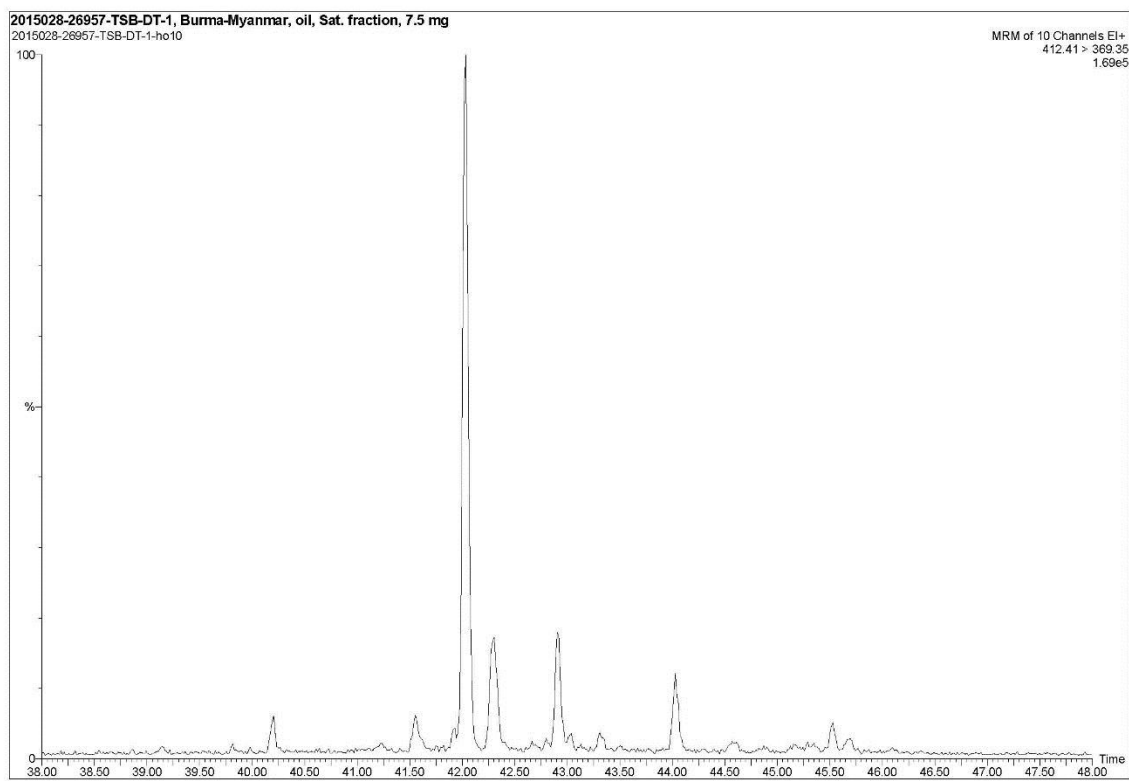
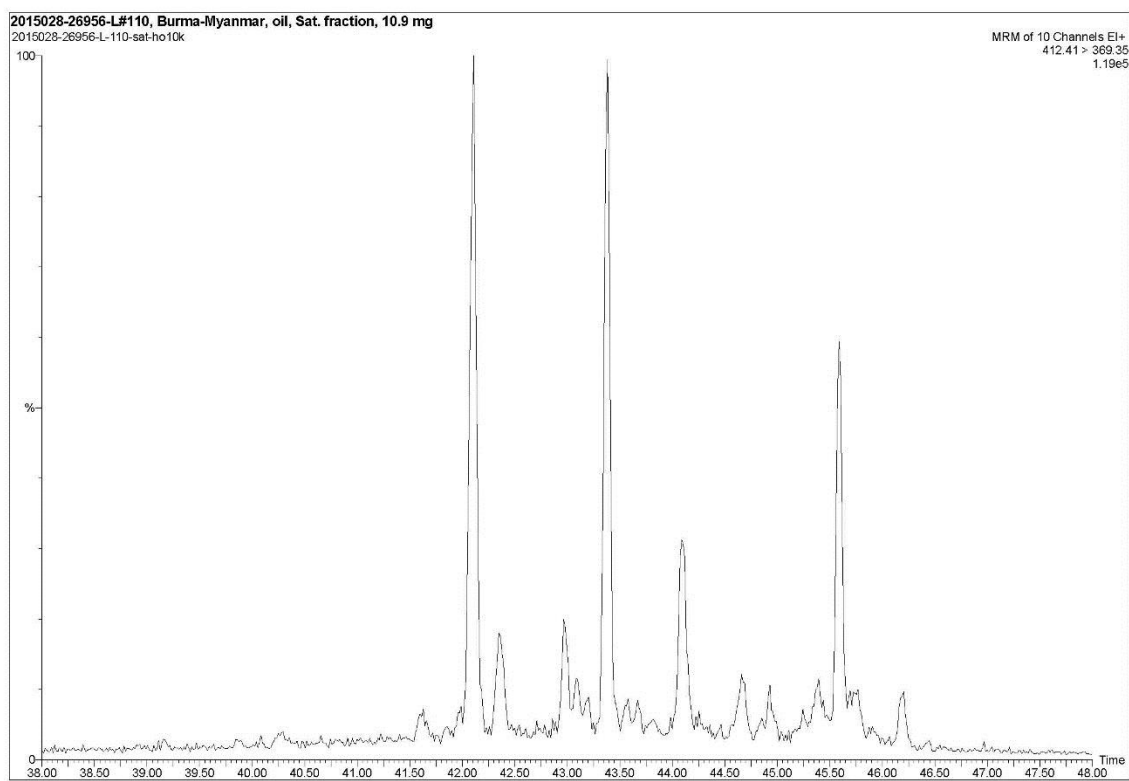












[110]

